

Interrupting two-pore channels 2 (TPC2) and sperm function enhancement

Faroq Ali Kamli

Worcester College

University of Oxford

Supervised by

Prof. John Parrington

Department of Pharmacology

University of Oxford

A thesis submitted for the degree of

Doctor of Philosophy

Trinity Term, 2023

Declaration

I declare that this thesis is entirely my own work, and except where otherwise stated, describes my own research.

Faroq Kamli

Worcester College

Abstract

The proper functioning of sperm is essential for successful fertilization. Various physiological regulators control sperm motility, energy balance, capacitation, and the acrosomal reaction. Intracellular calcium ion (Ca^{2+}) concentration and pH levels play a crucial role in regulating sperm physiology. Two pore channels 2 (TPC2), located on lysosomes, are involved in ion fluxes, and play a vital role in reproductive and embryonic development. This thesis aims to investigate the role of TPC2 as a mediator of sperm function. TPC2 knockout (KO) mice and wild type (WT) mice were used to study the role of TPC2 in sperm physiology. TPC2 KO sperm exhibited significantly increased motility and hyperactivation-related parameters associated with capacitation compared to WT sperm. Additionally, TPC2 KO sperm showed higher ATP content than WT controls. GPD2 protein, involved in tyrosine phosphorylation during sperm capacitation, was found to have significantly higher mRNA transcript levels in TPC2 KO sperm using RT-qPCR analysis. We utilized our model to understand specific molecular changes in TPC2 KO mouse sperm by measuring PPARα, which controls GPD2 activity. TPC2 KO sperm showed a shift towards oxidative phosphorylation, increased mitochondrial activity, and biogenesis. The antioxidant effect of TPC2 was more pronounced than in WT sperm, as indicated by the expression of antioxidant enzymes such as superoxide dismutase 1 and 2 (SOD1, SOD2). PGC1α, involved in mitochondrial biogenesis, was significantly increased in TPC2 KO sperm,

suggesting a potential mechanism underlying the enhancement of sperm function in the absence of TPC2 activity. TPC2 KO sperm undergo capacitation at a faster rate than WT sperm, as evidenced by increased phosphorylation of protein kinase A substrates (PKAs) in TPC2 KO sperm compared to WT. Similar effects were observed in tyrosine phosphorylation and the acrosome reaction. As sperm capacitation is crucial for fertilization, non-capacitated TPC2 KO sperm demonstrated a higher fertility rate than WT sperm in in vitro fertilization (IVF) studies, supporting the notion that interfering with TPC2 activity enhances sperm physiological function. Moreover, TPC2 deficiency led to a more alkaline intracellular pH (pH_i), which activated the CatSper channel and allowed increased influx of Ca2+. Additionally, the alkaline cytosol enhanced the activity of soluble adenylyl cyclase (sAC), leading to sperm capacitation through the activation of the cAMP/PKA signalling pathway, which may contribute to this characteristic. Together this work demonstrates that disturbing the activity of TPC2 improves sperm function and enhances fertilization capability.

Acknowledgment

I would like to express my heartfelt gratitude to all those who have contributed to the completion of my thesis and supported me throughout my academic journey. First and foremost, I would like to express my immense appreciation to my supervisor, Professor John Parrington, for the opportunity and for his unconditional guidance and support and continuous encouragement throughout my research journey. His expertise, and dedication have been instrumental in shaping the direction and quality of my work. I am truly fortunate to have had the opportunity to work under his supervision.

I am indebted to my colleagues for their wonderful companionship and invaluable assistance. Their willingness to share their knowledge and expertise has been an immense source of support. In particular, I would like to express my gratitude to Ala'a, Ali and Xuhui for their generous time and guidance in teaching me advanced research techniques and laboratory skills.

I am indebted to the researcher groups and department teams that have graciously allowed me to utilize their facilities and resources. Specifically, Ming Lei, Daniel Antony, Sridhar Vasudevan, and Angela Russell. I am grateful to the dedicated team at the department, including Graeme Laidler, Hicham Ouallaf, Jimmy Martin and Paula Savin, for their continuous support and assistance. Their expertise, administrative guidance, and willingness to go the extra mile have been invaluable in facilitating the smooth progress of my research.

I would also like to extend my thanks to the Department of Pharmacy and the various research groups within the department for providing me with access to their facilities and resources. The collaborative environment and state-of-the-art equipment have significantly enhanced the scope and depth of my research.

To my dear family, I am forever indebted to you for your unwavering support and encouragement during the challenging times of my DPhil and academic research. Your love, understanding, and belief in my abilities have been a constant source of strength. To my parents, wife, brothers, and sisters, thank you for standing by my side and for always reminding me of the importance of perseverance and determination.

I would also like to extend my thanks to the Department of Pharmacy at Jazan University, Saudi Arabia, and the Saudi Cultural Bureau in London, United Kingdom, for their financial support. Their generosity and belief in my abilities have enabled me to pursue my DPhil and carry out my research, and I am truly grateful for their assistance.

Lastly, I want to thank my friends, Abdullah, Moaad, Mehdi, and Hatem, for their companionship during my time in Oxford. Your friendship and shared experiences have made this journey even more memorable and enjoyable. Thank you for the laughter, support, and camaraderie that have kept me motivated and grounded.

To all those mentioned above and to anyone else who has supported me along this challenging and rewarding path, please accept my deepest gratitude. Your contributions have been instrumental in the successful completion of my thesis, and I am forever grateful for your presence in my life.

Glossary of Abbreviations

AKT	Protein kinase B
AMPK	AMP-activated protein kinase
AR	Acrosome reaction
ATP	Adenosine triphosphate
ATP5a1	ATP synthase
BSA	Bovine serum albumin
CaM	Ca^{2+}-binding protein calmodulin
cAMP	Cyclic adenosine monophosphate
CASA	Computer Automated Sperm Assessment
$CdCl_2$	Cadmium chloride
cDNA	Complementary DNA
DAPI	4’,6-diamidino-2-phenylindole
DCFDA	2’,7’-dichlorofluorescin diacetate
DMSO	Dimethyl sulfoxide
DNA	Deoxyribonucleic acid
ECAR	Extracellular acidification rate
EDTA	Ethylenediaminetetraacetic acid
G3P	Glycerol 3 phosphate
GAPDH	Glyceraldehyde 3-phosphate dehydrogenase
GPD2	Glycerol 3 phosphate dehydrogenase 2

hCG	Chorionic gonadotropin
HTF	Human tubal fluid
pH_i	Intracellular pH
$\Delta\Psi_M$	Mitochondrial membrane potential
mTFA	Mitochondrial transcription factor A
mTOR	Mammalian of rapamycin
NAADP	Nicotinic acid adenine dinucleotide phosphate
NAD	Nicotinamide adenine dinucleotide
NADH	Nicotinamide adenine dinucleotide hydrogen
ND1, ND5	NADH-ubiquinone oxidoreductase chain 1 and 5
OCR	Oxygen consumption rate
PGC1 α	Peroxisome proliferator-activated receptor γ coactivator 1α
PPARs	Peroxisome proliferator-activated receptors
PI (3,5) P_2	Phosphatidylinositol 3,5-bisphosphate
PKA	Protein kinase A
PMSG	Pregnant mare serum gonadotropin
RNA	Ribonucleic acid
ROS	Reactive oxygen species
sAC	Soluble adenylyl cyclase
SDS	Sodium dodecyl sulphate
SDS-PAGE	Sodium dodecyl sulphate–polyacrylamide gel electrophoresis

SOD1	Cytosolic superoxide dismutase
SOD2	Mitochondrial superoxide dismutase
TPCs	Two pore channels
VAP	Average path velocity
VCL	Curvilinear velocity
VSL	Straight line velocity
WT	Wild type
ZP	Zona pellucida

1 Table of Contents

1 Chapter 1 1

Introduction 1

1.1 Male reproduction 2

1.1 Sperm cell structure 2

1.2 Spermatogenesis and maturation 5

1.3 Sperm energy production and metabolism 7

1.4 Capacitation 8

1.5 Acrosome reaction 12

1.6 Fertilization 13

1.7 Two Pore Channels 14

1.8 TPCs in health and disease 16

1.9 TPCs in reproduction 17

1.10 Thesis Aims 18

2 Chapter 2 19

Materials and Methods 19

2.1 Animals 20

2.2 Animal Genotyping 20

2.2.1 DNA extraction 20

2.2.2 Polymerase chain reaction (PCR) 21

2.2.3 Agarose gel electrophoresis 21

2.3 Sperm Analysis 22

2.3.1 Mouse sperm isolation 22

2.3.2 Sperm viability assay 23

2.3.3 Computer Automated Sperm Assessment (CASA) 24

2.3.4 Acrosome reaction assay 24

2.3.5 Reactive oxygen species (ROS) 25

2.3.6 Measurement of changes in the intracellular calcium $[Ca^{2+}]i$ 26

2.3.7 Measurement of the intracellular pH [pH] i 28

2.3.8 Lysotracker assay 30

2.4 Sperm Energy Analysis 31
2.4.1 Measurement of ATP content 31
2.4.2 Measurement of GAPDH activity 32
2.4.3 NAD/NADH assay 32
2.4.4 Energy metabolism phenotype 33
2.4.5 Glycerol 3-Phosphate (G3P) Reduction Assay 34
2.4.6 Oxygen Consumption Rate (OCR) and Extracellular Acidification Rate (ECAR) assessment 34
2.4.7 Mitochondrial membrane potential assay 37
2.5 Sperm Protein Analysis 39
2.5.1 Protein extraction and electrophoresis (SDS-PAGE) 39
2.5.2 Indirect immunofluorescence assay 41
2.6 Testis and Sperm RNA Analysis 43
2.6.1 Testis and sperm RNA extraction and cDNA synthesis 43
2.7 *In Vitro* Fertilization (IVF) 47
2.7.1 Oocyte isolation 47
2.7.2 Sperm collection and oocyte insemination 47
2.8 Data presentation and statistical analysis 48
3 Chapter 3 51
Characterization of Sperm Motility and Metabolism in TPC2 KO Mice Sperm 51
3.1 Introduction 52
3.2 Chapter Aims 55
3.3 Results 56
3.3.1 General characterization of gene expression, viability, and lysosomes in the sperm of WT and TPC2 KO mice 56
3.3.2 TPC2 KO sperm show an enhancement in sperm motility parameters 58
3.3.3 TPC2 KO sperm exhibits increased energy production. 61
3.3.4 Another factor plays a role in the change in motility in TPC2 KO sperm 63
3.3.5 Glycerol 3 phosphate as an energy source that drives ATP production in TPC2 KO sperm via oxidative phosphorylation. 65
3.3.6 Inhibition of TPC2 enhances GPD2 activity. 68
3.3.7 TPC2 KO may enhance GPD2 activity through PPARs. 70
3.4 Discussion 73
3.5 Conclusion 79

4 Chapter 4 81

Potential molecular mechanism for TPC2 KO sperm underlying the metabolism enhancement. 81

4.1 Introduction 82

4.2 Aims of this chapter 86

4.2.1 Results 87

4.2.2 TPC2 KO sperm have enhanced mitochondrial oxidation phosphorylation. 87

4.2.3 The mitochondrial membrane potential is greater in TPC2 KO sperm than in WT sperm. 90

4.2.4 Interfering with TPC2 may enhance cellular protection from oxidative damage. 94

4.2.5 TPC2 KO sperm induces mitochondrial biogenesis and oxidative phosphorylation via activation of the PGC-1α pathway. 98

4.3 Discussion 102

4.4 Conclusion 107

5 Chapter 5 108

Role of TPC2 in sperm capacitation and fertilization enhancement 108

5.1 Introduction 109

5.2 Chapter Aims 111

5.3 Results 112

5.3.1 Loss of TPC2 function makes the sperm intracellular pH more alkaline. 112

5.3.2 TPC2 KO could enhance the activity of CatSper channel. 115

5.3.3 PKA-P activity is increased in the absence of TPC2 activity. 119

5.3.4 TPC2 KO sperm exhibit enhancement of the sperm capacitation and fertilization rate. 123

5.4 Discussion 126

5.5 Conclusion 130

6 Chapter 6 132

General Discussion and Future Directions 132

6.1 General discussion 133

6.2 Overall conclusion 143

7 References: 144

List of Figures

Figure 1-1: Depicts the structure of the human sperm with its two main components, the head and tail.....3

Figure 1-2: Cross sections of the midpiece and tail of human sperm. 4

Figure 1-3: The 9+2 doublet arrangement of the microtubules in the axial filament. 4

Figure 1-4: Stages of spermatogenesis.....6

Figure 1-5: Signalling pathways of sperm capacitation. 11

Figure 2-1The Agilent Seahorse XFe96 extracellular flux analyser plate kit. (Adopted from Gu et. al, 2021). 35

Figure 3-1: Characterization of sperm from WT and TPC2 KO mice. 57

Figure 3-2: Sperm motility and kinetic parameters of WT and TPC2 KO.....60

Figure 3-3: Sperm ATP Content and GAPDH activity of WT and TPC2KO mice. 62

Figure 3-4: The effect of $CdCl_2$ treatment on motility parameter of WT and TPC2KO sperm.....64

Figure 3-5: The metabolism rete of G3P and gene expression of GPD2 in WT and TPC2KO sperm. ...67

Figure 3-6: The effect of Naringenin treatment on the GDP2 activity of the sperm in WT and TPC2 KO mice.....69

Figure 3-7: The effect of PPARα agonist and antagonist on GPD2 activity. 72

Figure 4-1: The metabolism pattern and mRNA marker of mitochondrial activity of WT and TPC2 KO sperm. 88

Figure 4-2: The mitochondrial membrane potential of WT and TPC2 KO sperm.....93

Figure 4-3: ROS generation in the sperm of WT and TPC2 KO mice.....97

Figure 4-4: TPC2 KO sperm enhances the mitochondrial activity. 100

Figure 4-5: The effect of TPC2 inhibitor on the proteins involved in the mitochondrial function on WT and TPC2 KO sperm. 101

Figure 5-1: TPC2 effects on the intracellular pH. 114

Figure 5-2: Ca^{2+} response to progesterone and ionomycin in the sperm of WT and TPC2 KO sperm. 117

Figure 5-3: Ca^{2+} response to CatSper inhibitor of WT and TPC2 KO sperm. 118

Figure 5-4: p-PKA activity in the WT and TPC2 KO sperm. 121

Figure 5-5: Tyrosine phosphorylated protein in WT and TPC2 KO sperm. 122

Figure 5-6: Acrosome reaction of WT and TPC2 KO sperm. 124

Figure 5-7: Fertility rate of non-capacitated WT and TPC2 KO sperm. 125

List of Tables

Table 1 : Primers used in PCR reactions to genotype the mice. 22

Table 2: Preparation of Potassium Phosphate Buffer (50 mM) and final pH obtained. 30

Table 3: Template mixture of cDNA synthesis from testis and sperm RNA. 44

Table 4: Composition of one reaction mixture used for RT-qPCR. 46

Table 5: list of primers used for RT-qPCR. 49

Table 6: Fertility rate of non-capacitated WT and TPC2 KO sperm. 125

Chapter 1

Introduction

1.1 Male reproduction

Sperm are the male origin gametes, a unique cell type that is produced during the spermatogenesis process which takes place in the testis. The duration of spermatogenesis varies among mammalian species; in humans, it takes around 70 days while in mice it takes around 35 days. Spermatogenesis begins at puberty and continues throughout the male's life (Bronson, 2011).

1.1 Sperm cell structure

Sperm have a highly specialized shape that is fundamental for delivering the paternal DNA to the oocyte. The sperm is divided into two parts: the head and the tail (Figure 1-1) (Pacey and Williams, 2018). The paternal genome is contained in the head, as is the acrosome, which contains essential enzymes such as hyaluronidase and acrosin, which are involved in the penetration of the zona pellucida, allowing fertilization to occur (Yoshinaga and Toshimori, 2003). The tail of the sperm is divided into four pieces; the connecting piece, the midpiece, the principal piece, and the end piece. The connecting piece links the head with the tail and serves as the disassembly site for the head during fertilization (Lehti and Sironen, 2017). The midpiece region primarily contains the neck of the sperm and the anterior part of the sperm tail. In this region the flagellum axial filament is surrounded by the mitochondria which are

fundamental for adenosine triphosphate (ATP) production (Piomboni et al., 2012). The principal and end pieces are the extension of the axial filament of the midpiece but do not contain the mitochondria and are surrounded by the cytoplasm and the cellular membrane. The tail propels the sperm towards the oocyte for fertilization. The axial filaments that extend from the neck to the end of the tail form the motor portion of the sperm called the axoneme. This is composed of a 9+2 arrangement of the microtubule doublets that extend throughout the length of the tail regions and have inner and outer dynein arms that extend from each of the outer nine doublets (Mortimer, 2018; Turner, 2005) (Figures 1-2 and 1.3). These dynein arms are thought to be responsible for the sperm flagellum's propulsive force (Inaba, 2003; Turner, 2005).

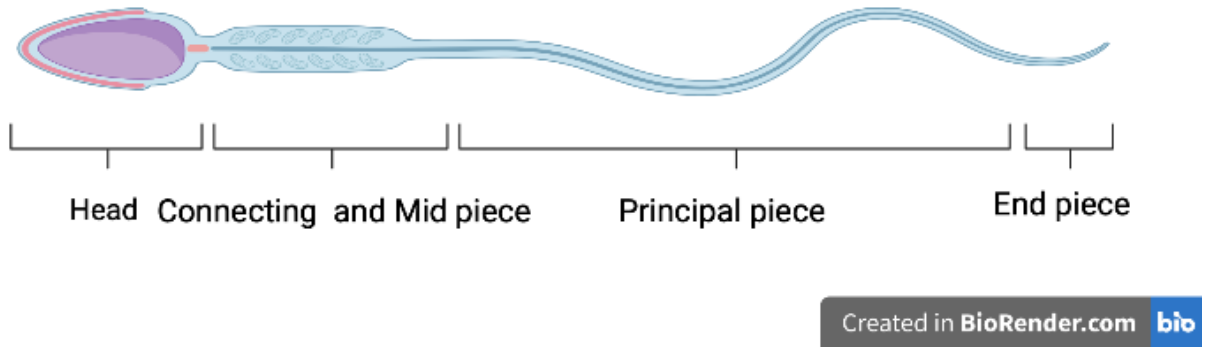


Figure 1-1: Depicts the structure of the human sperm with its two main components, the head and tail. The head contains the nucleus and the acrosome. The tail has four regions: the connecting piece, midpiece, principal, and tail pieces. The connecting piece links the head with the tail. The midpiece, or 'neck,' is made up of the mitochondria, which provide the energy for the sperm's motility and are surrounded by the axial filament, which protrudes across the whole tail. The principal and end pieces are the extension of the midpiece which moves the sperm toward the oocyte.

Created via BioRender website Scientific Image and Illustration Software | BioRender https://www.biorender.com Accessed 16, Jan 2023.

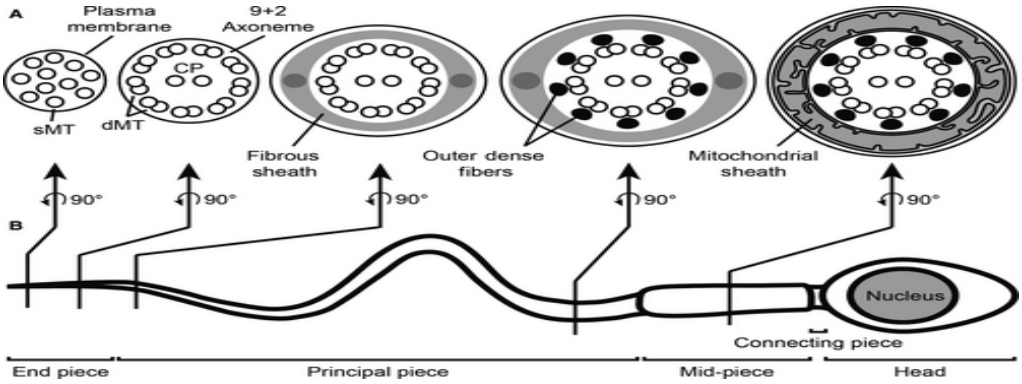


Figure 1-2: Cross sections of the midpiece and tail of human sperm.

The axial filament, which extends through the midpiece and tail, is composed of 9+2 doublet microtubules surrounded by a fibrous sheath. To provide energy for movement, mitochondria are wrapped around the axial filament in the midpiece. Adapted from Zabeo et al., 2019.

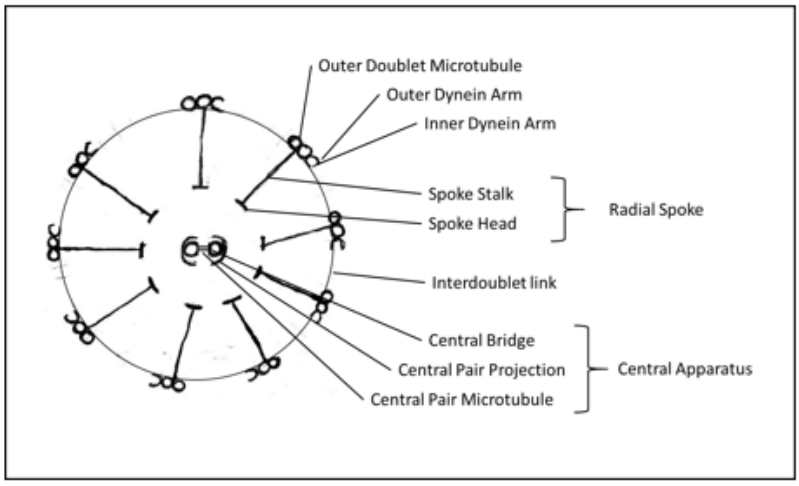


Figure 1-3: The 9+2 doublet arrangement of the microtubules in the axial filament.

Adapted from Pacey and Williams, 2018.

1.2 Spermatogenesis and maturation

Spermatogenesis is the complex process of sperm cell development in the male reproductive system. It involves a series of tightly regulated events that occur within the seminiferous tubules of the testes, leading to the production of mature spermatozoa (Sutovsky and Manandhar, 2006) (Figure 1-4). The first stage of spermatogenesis involves the mitotic division of spermatogonia as a preliminary for subsequent meiosis. There are two types of spermatogonial cells called A and B. Type A cells can be either formed by the self-renewal of the population of sperm stem cells or predestined differentiation to form type B spermatogonia and subsequently the primary spermatocytes (Waheeb and Hofmann, 2011). The primary spermatocyte progresses through meiosis I and this leads to the haploid secondary spermatocyte which then undergoes the second meiotic division, and this leads to the formation of the haploid round spermatid (Wistuba et al., 2007). In the next phase the round spermatids drastically change their shape and content. The shape transforms from a round shape to the spindle shape and form that is the typical shape of sperm. The nucleus and the acrosome are in the head, the energy source is provided via mitochondria at the midpiece, while the flagellum makes possible the capacity for movement in the female tract. The final stage of spermatogenesis is marked by the release of the elongated sperm into the lumen of the seminiferous tubule

and subsequently the sperm continues its journey of development in the male reproductive tract (Pacey and Williams, 2018).

However, at this stage the sperm are still immotile and must undergo an additional process of maturation to gain the ability for movement. The maturation process, which occurs in the epididymis, is responsible for sperm storage and transportation. The sperm modifications in the epididymis include activation of signalling pathways in the sperm, modification of lipids and proteins on the surface of the sperm, and acquisition of some proteins in order to make the sperm able to move in the female tract and fertilize the oocyte (Eddy et al., 1985; Gervasi and Visconti, 2017; James et al., 2020).

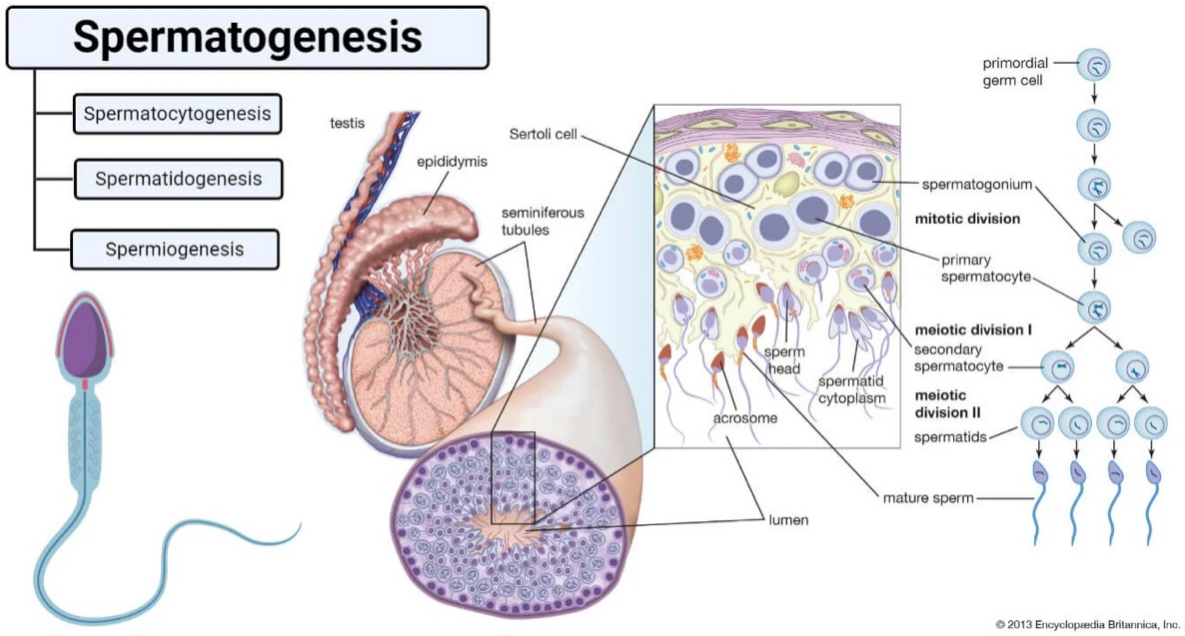


Figure 1-4: Stages of spermatogenesis.

(Adapted from The Biology Notes, Spermatogenesis- Definition, Stages and Process with figure available at https://thebiologynotes.com/spermatogenesis/ published on 04 Feb 2023. Accessed on 10 Mar 2023.

1.3 Sperm energy production and metabolism

After ejaculation, the sperm utilises the nutrient molecules present in the seminal fluid and female reproductive tract to generate energy. Sperm are like other types of cells, in that they rely on the transfer of energy in the form of ATP to fuel the various biological processes. There are many physiological processes in the sperm that require ATP to accomplish that function. ATP is essential for the flagellar movement; more specifically it is required for the phosphorylation and dephosphorylation of the dynein arms and the sliding of the dynein arms against the microtubule doublets that generates the flagellar waveform (Lindemann and Lesich, 2010). Additionally, ATP is necessary for ion transport across the plasma membrane, mediated by channels such as the Na^+ K^+-ATPase channel, which plays a role in fertility (Jimenez et al., 2011). Moreover, ATP is involved in signalling pathways such as those of cAMP production and protein phosphorylation that have a fundamental role in sperm physiology (Visconti, 2012).

The two primary metabolic pathways for energy production in the sperm are oxidative phosphorylation and glycolysis. Oxidative phosphorylation occurs in the mitochondria in which the ATP is produced by the electron transport chain and ATP synthase in the inner mitochondrial membrane (Piomboni et al., 2012).

It is much more efficient than glycolysis as it can generate around 30 ATP molecules from every one oxidized molecule of glucose. In the sperm, glycolysis takes place in the head and flagellum since these regions have a lack of the respiratory oxidative enzymes. Glycolysis involves the hydrolysis of the glucose molecule in which two molecules of ATP are produced (du Plessis et al., 2015). However, it remains a topic of debate regarding which of these pathways plays the most significant role in sperm energy production.

1.4 Capacitation

Freshly ejaculated sperm are not capable of fertilizing the oocyte and must spend a period of time in the female reproductive tract to acquire fertilization ability (Chang, 1951, Austin, 1951). They undergo highly complex physiological and biochemical modifications known as sperm capacitation (Yanagimachi, 1994). These modifications include hyperactivated motility, the acrosome reaction, membrane remodelling due to cholesterol efflux, an increase in the intracellular pH, and alteration in the intracellular concentrations of $Ca^{2+}$and HCO_3^- that can regulate the activity of cAMP and eventually lead to activation of protein phosphorylation and protein kinase A (Travis and Kopf, 2002; Baldi et al., 2000).

The most fundamental factors that play a crucial role in sperm capacitation are Ca^{2+}, HCO_3^-, and membrane phospholipid modification. Modification of the

$[Ca^{2+}]_i$ is a key biochemical event that occurs during sperm capacitation. The potential mechanistic role of Ca^{2+} in the capacitation process is mainly through activation of sAC which enhances the production of cAMP which then activates PKA and tyrosine phosphorylation leading to capacitation being initiated (Signorelli et al., 2012). Ca^{2+} also induces capacitation via the Ca^{2+}-binding protein calmodulin (CaM) which is distributed in the sperm head and the flagellum and has a crucial role in sperm function (Jones et al., 1980). Si and Olds-Clarke, (2000) found that CaM is involved in sperm capacitation and the acrosome reaction and in modulating the cAMP downstream pathway that plays a key role in sperm capacitation.

Sperm are like somatic cells in that they can either obtain Ca^{2+} from the extracellular medium or from intracellular Ca^{2+} stores. Extracellular Ca^{2+} is one of the necessary constituents for *in vitro* sperm capacitation (Baldi et al., 2000). There are several channels for extracellular Ca^{2+} influx localized at the plasma membrane that could participate in the capacitation process. They include the canonical transient receptor potential vanilloid (TRPV), voltage-gated Ca^{2+} channels (VGCCs), store-operated Ca^{2+} channels (SOCCs), and the sperm-specific CatSper channel (Kumar et al, 2016; Albrizio et al, 2015; Darszon et al., 2012;

Sun et al., 2017). It has been reported that TRPV and CatSper have an essential role in sperm capacitation (Nowicka-Bauer and Szymczak-Cendlak, 2021).

Intracellular Ca^{2+} release from the stores is also crucial for the regulation of the physiological processes of the sperm. Since the sperm does not have an endoplasmic reticulum (ER), numerous structures are considered as intracellular stores such as the acrosome and the redundant nuclear envelope (RNE), that are regulated by the inositol trisphosphate receptor (IP_3R), ryanodine receptor (RYR), and SERCA2 ATPase that are localized on the acrosome, and SPCA1 that is localized on the membrane of the RNE (Costello et al., 2009; Correia et al., 2015; Lawson et al., 2007; Harper et al., 2005).

Bicarbonate (HCO_3^-) is an indispensable factor in sperm capacitation. HCO_3^- can regulate the pH_i and it activates the CatSper channel that allows Ca^{2+} influx and increases $[Ca^{2+}]_i$ (Santi et al., 1998; Nishigaki et al., 2014). It has been suggested that transport of HCO_3^- affects sperm motility through alkalinization of the sperm pH_i (Sun et al., 2017). Additionally, it has been reported that HCO_3^- activates the sAC which enhances the endogenous level of cAMP which plays a role in PKA and tyrosine phosphorylated protein activation and consequently activates sperm capacitation (Hereng et al., 2014).

Cholesterol efflux from the sperm plasma membrane modulates the lipid composition of the membrane that occurs during capacitation. The mobility of cholesterol from the plasma membrane is enhanced in the presence of albumin and high density lipoprotein (HDL) (Aitken and Nixon, 2013). Once cholesterol is transferred from the cellular membrane, it enhances the polarization and fluidity of the plasma membrane that facilitates the permeability of the extracellular ions such as Ca^{2+} and HCO_3^- through the membrane and induces sperm capacitation (Visconti and Kopf, 1998).

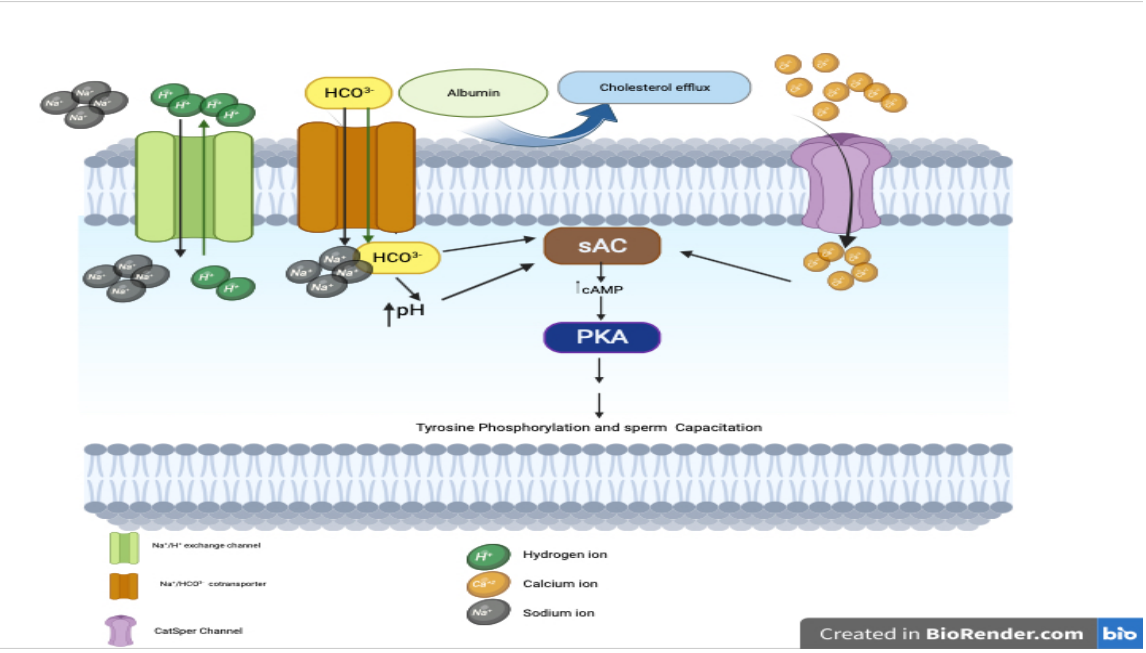


Figure 1-5: Signalling pathways of sperm capacitation.

Increase in pHi and Ca^{2+} through influx of HCO_3^- via activation of the Na^+/ HCO_3^- cotransporter (NBC), Na^+/H^+ exchanger (NHE), and CatSper channels. These might stimulate adenylyl cyclase sAC and increase cAMP levels. cAMP improves the activity of PKA. Cholesterol efflux in addition enhances the fluidity of the membrane that facilitates and increases HCO_3^- and Ca^{2+} influx. Subsequently, it activates PKA, which leads to increases in protein tyrosine phosphorylation, hyperactivated motility and the acrosome reaction.

Created via BioRender website Scientific Image and Illustration Software | BioRender https://www.biorender.com Accessed 27, Jan 2023.

1.5 Acrosome reaction

The final phase prior to fertilization that occurs in the sperm is the acrosome reaction (AR). The acrosome is derived from the Golgi apparatus and is located in the head of the sperm. It contains the hydrolytic enzymes that help to lyse the cumulus cells and aid penetration of the zona pellucida (ZP) which is essential for interaction of the sperm and oocyte (Berruti and Paiardi, 2011). The AR involves the fusion of the plasma membrane with the outer membrane of the acrosome at multiple sites of the sperm that leads to release of the enzymes and proteins and exposes the equatorial segment that contains the IZUMO1 protein which is crucial for sperm-oocyte fusion (Ramalho-Santos et al., 2002). Experimentally, the AR has been induced following the exposure of the sperm to the follicular fluid that contains hormones such as progesterone (Serrano and Garcia-Suarez, 2001). Additionally, when the sperm crosses the cumulus-oocyte complex, it undergoes the AR since the former produces progesterone (Yamashita et al., 2003). It has been suggested that the AR is induced via progesterone as this activates the CatSper channel and triggers Ca^{2+} influx (Roldan et al., 1994; Sumigama et al., 2015). It has been reported that the ZP is capable of inducing the AR which is crucial for sperm-oocyte binding (Florman and Storey, 1982; Baker, 1996).

1.6 Fertilization

In humans, the journey of the sperm is a complex process that starts when the sperm is deposited directly into the female reproductive tract. The sperm must then navigate through the female reproductive tract before reaching the ampulla, where the oocyte is located (Coy et al., 2012). During this journey, the sperm undergoes biochemical and physiological modifications that are essential for it to accomplish the fertilization process. These changes include sperm capacitation, hyperactivated motility, and the acrosome reaction. The oocyte is surrounded by a layer of cumulous cells. Once the sperm passes through the cumulous layer, it binds to the zona pellucida receptors, triggering the acrosome reaction (Wassarman, 1999). This reaction allows the sperm to penetrate the zona pellucida and enter the oocyte, where the sperm's contents, which includes the paternal genome, centrioles, and various RNAs, enter the ooplasm. The fertilizing sperm also activates the oocyte, which enables the latter to exit its meiotic arrest (Jones, 2005). These events are influenced by factors including hormones, pH, ions, reactive oxygen species (ROS), and Ca^{2+}, and are controlled by many signalling pathways. Any disruption or disfunction of the processes of sperm activation such as capacitation, hyperactivation, and the acrosome reaction, can result in infertility, which may require assisted reproductive technology to increase the chances of having a biological child.

1.7 Two Pore Channels

Two pore channels (TPCs; gene name TPCN) are members of the voltage gated cationic channel (VGCCs) superfamily. They contain two dimers of six-transmembrane (6 TM) domains and a pore region that allows the ion fluxes (Lin-Moshier et al., 2014). These ionic channels are mainly expressed and located in the acidic organelle vesicles of the endo-lysosomal system (of animals) and vacuoles (of plants) (Marchant and Patel, 2015). Three isoforms of this channel, TPC1, TPC2, and TPC3, exist in animals. The first two isoforms are expressed in humans and mice while in addition TPC3 is expressed in a variety of animals including rabbits and chickens. Plants possess only a single TPC1 isoform (Hedrich et al., 2018).

It has been suggested that TPCs are the molecular targets for the second messenger nicotinic acid adenine dinucleotide phosphate (NAADP) which mobilizes intracellular Ca^{2+} in mammalian cells (Brailoiu et al., 2009; Calcraft et al., 2009; Zong et al., 2009; Soares et al., 2007). Several studies conducted on TPC1 and TPC2 via manipulation of their expression support TPCs being NAADP targets. Recently, some studies have suggested that NAADP acts indirectly to activate TPCs. Using photolabeling and co-immunoprecipitation approaches,

they identified an NAADP binding protein that is smaller than TPCs but interacts with the latter (Lin-Moshier et al., 2012; Ruas et al., 2015).

Against the evidence that NAADP is the regulator of Ca^{2+} release via TPCs, some recent studies have generated controversy over the mechanism of activation of TPCs and ion permeability. It has been reported that an endolysosome specific phosphoinositide called phosphatidylinositol 3,5-bisphosphate PI (3,5) P_2 activates and regulates TPCs which are highly selective channels for sodium (Na^+) ion fluxes with little Ca^{2+} ion permeability (Wang et al., 2012). Similarly, Cang et al., (2014) noted that the currents of TPC1 were activated via PI (3,5) P_2 through a highly permeable Na^+ channel. TPCs are not only permeable for Ca^{2+} or Na^+. It has also been suggested that TPC1 is a proton permeable channel that is highly selective for the H^+ ion and can be either activated directly via NAADP or via Ca^{2+} released from TPC2 (Pitt, et al., 2016). In a recent review, Morgan et al., (2022) suggest that TPCs are permeable for Ca^{2+}, Na^+, and H^+ with conservation in the TPC activator ligand. To summarise, abundant evidence reveals that NAADP and PI (3,5) P_2 can act as TPC activators while the ion selectivity remains unclear. Therefore, each activator has the potential to exhibit selectivity towards a particular ion permeability that could lead to diverse and potentially contrasting effects on cellular function.

1.8 TPCs in health and disease

TPCs have been the subject of extensive research and linked to a variety of physiological processes and diseases. For example, cellular differentiation requires functional TPCs. Thus, during the differentiation of skeletal muscle cells, this has been observed (Aley et al., 2010). TPC2 has also been studied in the zebrafish and it has been suggested that TPCs signalling is involved in zebrafish myogenesis (Kelu et al., 2019). In addition, TPCs' role in osteoclastogenesis has been studied and its overexpression shown to promote this process (Notomi et al., 2021). Moreover, NAADP-induced Ca^{2+} signalling and TPC2 were demonstrated to be essential for vascular endothelial growth factor (VEGF) induced angiogenesis, a process that is essential for tumour progression (Favia et al., 2014). Trufanov et al. (2019) demonstrated that TPC1 is involved in the elevation of Ca^{2+} required for the contraction of rat aortic smooth muscle cells in response to norepinephrine. Several studies using TPC knockout (KO) mice support the role of TPC1 and TPC2 in various physiological processes. These include brown adipose tissue thermogenesis, intracellular trafficking, immunity, neo-angiogenesis, cellular energy metabolism, and cancer hallmarks such as proliferation, metastasis, and abnormal cellular energy metabolism (Lear et al., 2015; Favia et al., 2014; Müller et al., 2021; Cang et al., 2013).

1.9 TPCs in reproduction

The roles of TPCs in sperm biology and fertility have been investigated. It has been demonstrated that in sea urchins the sperm NAADP plays a fundamental role during the fertilization process in which the NAADP levels are increased remarkably (Churchill at al., 2003). Billington et al., (2002) found that NAADP concentration of sea urchin sperm is considerably higher than that of oocyte speculating that NAADP receptors could be activated at higher concentration. During the fertilization of sea urchin eggs, the luminal pH of the acidic stores increases to become more alkalinized upon the release of the Ca^{2+} resulting from the effect of NAADP which could be through the activation of TPCs (Morgan and Galione, 2007). These findings suggested that transfer of NAADP which mediates the Ca^{2+} via TPCs from the spermatozoa to the oocyte may have a crucial role in fertilization.

When sperm interacts with eggs, Ca^{2+} level increases that stimulates phospholipase and NAADP triggering acrosomal Ca^{2+} release (Vasudevan et al., 2010). Notably, the exogenous permeable NAADP form (NAADP-AM) is capable to increase the intracellular [Ca^{2+}] of sea urchin sperm even in the absence of the extracellular Ca^{2+} as the NAADP can be produced in the human sperm (Sánchez-Tusie et al., 2014). Arndt et al., (2014) showed that TPC1 is required for the sperm acrosome reaction which plays a fundamental role in the process

of fertilization. More recently, it has been revealed that TPC1 contributes to acrosomal Ca^{2+} release regulated by acrosomal pH, where alkalinization of the acrosome induces acrosomal Ca^{2+} release through TPC1 (Oliver et al., 2023). These findings provide the pivotal role of the acidic stores in the fertility.

1.10 Thesis Aims

TPCs, which are ion permeable channels, have been associated with and contribute to several physiological processes including intracellular trafficking, immunity, neo-angiogenesis, and cellular energy metabolism. In the context of sperm, which are solely dedicated to fertilizing the oocyte, their physiological functions can be modulated via ion channels. Therefore, this thesis aims to explore the role of TPC2 in sperm function and its impact on fertility. The following objectives have been investigated.

1- To characterise the motility and metabolism of the sperm of WT and TPC2 KO mice and identify potential related molecular regulatory proteins.

2- To study the mitochondrial activity and biogenesis of WT and TPC2 KO sperm and understand the role of TPC2 in regulating mitochondrial activity.

3- Cellular pH regulation is a crucial aspect of sperm physiological processes such as sperm motility, capacitation, the acrosome reaction, and fertilization. An important goal is to investigate the effect of loss of TPC2 activity on the cellular pH and its impact on sperm capacitation and fertilization.

Chapter 2

Materials and Methods

2.1 Animals

TPC2 knock out (homozygous Tpcn2YHD437) (mutant allele nomenclature: $Tpcn2^{Gt\ (YHD437)Byg}$) mice were used that have been established previously by the Parrington and Galione groups (Department of Pharmacology, University of Oxford). $Tpcn2^{-/-}$ mice were developed from an embryonic stem (ES) cells (YHD437) containing a gene trap mutation as described by Calcraft et al., (2009). These animals carry this insertional mutation in the *Tpcn2* gene between exons 1 and 2. As the control we used wild type (WT), strain matched (C57BL/6) mice. Animals were housed in individual ventilated cages and always had free access to food and water and were maintained on a 12 hour light/dark cycle with a controlled temperature and humidity environment. All experiments and procedures were approved by the local ethical review committee of the University of Oxford in accordance with UK Home Office under the Animal Scientific Procedures Act 1986.

2.2 Animal Genotyping

2.2.1 DNA extraction

The animal ear was clipped and used for DNA extraction and genotyping for the TPC2 gene. 100 μl of digestion buffer (25 mM NaOH diluted on the day from 10 M, and 200 μM EDTA pH 8) was added to the tissue in 1.5 ml Eppendorf tube

and incubated at 95^{O}C for 1 hour. The tube was mixed once after 30 min of incubation by vortex mixer for 10 sec. Following the incubation, 100 μl of 40 mM Tris-HCl pH 5 was added to neutralize the solution, then the sample was stored at -20^{O}C until use.

2.2.2 Polymerase chain reaction (PCR)

Three PCR primers (Table 2.2) were used to assess the presence of the WT or mutant TPC2 allele. 1 μl of DNA template was added to the reaction mixture with a final volume of 20 μl. The reaction mixture was composed of 8.7 μl nuclease-free H_2O, 0.1 μl of 200 μM of each primer, and 10 μl of DreamTaq Green PCR Master Mix (Thermo Scientific™, K1081). The cycling parameters were programmed on the PCR machine (Eppendorf Master cycler gradient, Germany) as follows: initial denaturation at 94^{O}C for 5 min; then, 30 cycles of denaturation at 94^{O}C for 15 sec, annealing at 56^{O}C for 30 sec and extension at 72^{O}C for 1 min. Finally, there was one cycle at 72^{O}C for 6 min for final extension and storage of the sample was at -20^{O}C until use.

2.2.3 Agarose gel electrophoresis

The gel was formed by mixing 1.5 g of agarose (Sigma, A9539) in 100 ml of 1 x TAE buffer (Thermo scientific, B49) and dissolved by heating the solution in the microwave for 2 min. 3 μl of ethidium bromide (Promega, H5041) was added to

the mixture to a final concentration of approximately 0.2-0.5 μg/ml. The solution was poured into the gel tray and the comb was placed at the top edge of the tray. The gel was allowed to solidify, and the PCR reaction samples were loaded and run on the gel for electrophoresis at 100 mV for 30 min. UV light was used to visualise the DNA fragments (bands). The ladder (GeneRuler 1 kb DNA Ladder, Thermo Scientific SM0311) was loaded in the first lane and used to infer the molecular size of sample DNA.

Table 1 : Primers used in PCR reactions to genotype the mice.

Allele	Sense primer (5'-3')	Antisense primer (5'-3')
WT	CTT CGG AGC CTT CTT TCC TT	CTG TCC CTG ACG AGT GGT TT
TPC2 YHD 437	GTC GGG GCT GGC TTA ACT ATC G	

2.3 Sperm Analysis

2.3.1 Mouse sperm isolation

Sperm were collected from the cauda epididymis and vas deferens of adult male (>8 weeks old) mice in pre warmed M2 medium or Human Tubal Fluid media (HTF) containing 4 mg/ml bovine serum albumin by piercing the cauda epididymis with a 27-gauge needle and incubating at 37^{o}C under 5% CO_2 for 15 min to let the sperm swim out of the epididymis. The sperm were then washed

in PBS by centrifugation at 2400 rpm for 5 min. The supernatant was discarded, and the sperm pellets resuspended in the suitable medium for further analysis.

2.3.2 Sperm viability assay

Eosin Y (Sigma, E 4009, USA) and nigrosine (Sigma, 43925, India) were used to evaluate the sperm viability. Eosin stains the dead sperm heads with a pink colour while the live sperm head appears white. Nigrosine solution enhances the contrast between the sperm head and background which makes the sperm assessment easier. This assay is done after the sperm isolation as described in Björndahl et al. (2004). 100 μl of the sperm suspension was loaded onto a microscopic slide (Thermo Scientific, 2951-001) and mixed well with 2 volumes of 1 % eosin in dd H_2O for 15 sec. After homogenising the mixture, 300 μl of 10 % aqueous nigrosine was added to the sample drop and mixed well. A drop of the mixture equal to 100 μl was smeared onto the slide and air dried. A bright field microscope was used to observe the sperm using a 40 X objective lens to evaluate the sperm viability. The dead cells were stained with a dark pink or red head whereas the live cells have either white or faint pink heads. More than 200 cells were counted, and the sperm viability was calculated by the percentage of live sperm relative to the total number of sperm.

2.3.3 Computer Automated Sperm Assessment (CASA)

Sperm were collected as described above but incubated in pre warmed phosphate buffer saline PBS free of Ca^{2+} and nutrient molecules for 30 min at 37^{o}C with 5% CO_2. 30 µl of the sperm suspension was loaded into a prewarmed Leja slide chamber (Microm, SC100-01-02-A-CE) on an Olympus CX41 microscope. Sperm motility and hyperactivation parameters were assessed via CASA with software HTM-CEROS (version 12.3, Hamilton Throne) recording at least 200 mouse sperm per slide for each group. The image acquisition settings were 60 frames per second, the minimum contrast (50), the minimum cell size (5 pixels), the VAP cut-off (5µm/s), and the cell intensity (90). Total sperm motility (MOT), progressive motility (PRO), curvilinear velocity (VCL), straight line velocity (VSL), and average path velocity (VAP) were measured.

2.3.4 Acrosome reaction assay

Sperm were collected and washed in PBS by centrifuging at 2400 rpm for 5 min. 2 x 10^6 sperm were suspended in M2 medium and incubated in 5% CO2 at 37^{o}C. The samples were divided into two groups at a sperm density of 6 x 10^6 and loaded into a 96 well plate at 1 x 10^6 sperm per well. The first group was treated with 10 µM A23187 ionophore, where the second group was only treated with DMSO (Sigma, 41639) as a control group. Sperm were collected at different time

point and pipetted onto poly lysine coated slides (Polysine ™ Adhesion Microscope Slides, Fisher Scientific, 10219280, USA) and air dried. The sperm were fixed using 1:1 of absolute ethanol and acetone on ice for 10 min and washed 3 times by dipping in PBS for 10 sec and then air dried. For the acrosome staining lectin PNA Alexa fluor 594 conjugated (Invitrogen, L32459) was used and incubated for 30 min in the dark. The slides were washed 3 times in PBS and then mounted using ProLong™ Diamond Antifade Mountant with DAPI (Invitrogen, P36966). The coverslip was added, and the slides were sealed using nail polish for assessment. The acrosomal status were assessed using a Life technology EVOS FL Auto Cell Imaging System fluorescent microscope. The unreacted acrosome has an intact acrosome (red fluorescence) whereas the reacted one has no probe present. The percentage of sperm with a reacted acrosome were calculated as a percentage of total numbers.

2.3.5 Reactive oxygen species (ROS)

ROS generation in the sperm was performed using cell permeant reagent 2',7'-dichlorofluorescin diacetate DCFDA / H_2DCFDA Cellular ROS Assay Kit (Abcam, ab113851). H_2DCFDA is a cell permeable probe the deacylated by cellular esterases to form H_2DCF that oxidized by cellular ROS into a highly fluorescent DCF. Sperm were collected as before and washed in PBS via centrifugation and

incubated in 5% CO_2 at 37^{o}C. The samples were divided into 2 groups for each animal and loaded into 24 well plates. The first group was treated with 80 µM naringenin (Santa Cruz, sc-219338, USA) while the control group was treated with only DMSO. DCFDA / H_2DCFDA was diluted in the manufacturer's buffer assay to make a 20 mM stock solution and diluted again in the M2 medium for a working concentration at 10 µM and the sperm were incubated in this for 30 min in 5% CO2 at 37^{o}C. The sperm were then collected in a 1.5 ml Eppendorf tube and washed twice at least by centrifugation at 2400 rpm for 5 min to remove the excess of DCFDA / H_2DCFDA reagent. The sample were suspended in fresh M2 medium and 100 µl volume of the suspension was loaded into a 96 well plate at a sperm density of 1 x 10^6 per well. The fluorescence intensity was measured immediately using a fluorescent microplate reader (FLUOstar Omega, BMG LABTECH) at excitation 485 nm and emission at 535 nm in the end point mode in the presence of media.

2.3.6 Measurement of changes in the intracellular calcium [Ca^{2+}]i

Changes in the intracellular Ca^{2+} were measured on 96 well plates in a fluorescence plate reader (Fluostar Omega, BMG Labtech, Germany) at 36°C. Sperm were collected and washed as described in 2.3.1. The samples were divided into two groups, with one treated with 80 µM naringenin and the other

only with DMSO as a control group. Sperm were loaded with the fluorescent Ca^{+2} indicator fluo 4-AM (Invitogen, F14201) in a final concentration of 5 µM and in the presence of Pluronic F127 (0.1% w/v), (Sigma, P2443) and incubated for 30 min at 37°C in a 5% CO_2 incubator. After the incubation, sperm were washed at least 2 times in a pre warmed PBS at 2400rpm for 5 min at room temperature then loaded into a 96 well plate at a density of 1 x 10^6 sperm per well. Fluorescence was excited at 480 nm and the fluorescence emission was recorded at 520 nm with bottom optics. The fluorescence intensity was recorded before and after injection of 20 µM progesterone (Sigma, USA, P3972) and 10 µM A23187 ionophore (Sigma, C7522) whereas in the inhibition of Catsper experiment the sperm were incubated in 1 µM NNC 55-0396 (Cambridge Bioscience, CAY17216 USA) for 5 min before the injection of solutions. Changes in the fluorescence intensity of Fluo 4-AM are represented as $\Delta F/F_0$, reflecting the fluorescence change after the injection (ΔF) as a proportion to the mean of at least 5 readings of basal fluorescence (F_0) before the application of progesterone and NNC 55-0396. The solutions were injected manually into the wells using a single pipette.

2.3.7 Measurement of the intracellular pH [pH] i

2.3.7.1 Loading the fluorescent reagent (SNARF 5AM)

The sperm intracellular pH measurement was performed as previously described in Seksek et al., 1991, and Chávez et al., 2020. Sperm were collected and washed in PBS then resuspended in M2 medium in 24 well plates and incubated in 5% CO_2 at 37^{o}C. The sperm were treated with 80 µM naringenin for 30 min while the control was treated only with DMSO. SNARF-5F 5-(and-6)-carboxylic acid, acetoxymethyl ester, acetate (Invitrogen, S-23923) was the pH indicator fluorophore that was used to measure the intracellular sperm pH. SNARF-5F AM was diluted in M2 medium and loaded onto the sperm at a final concentration of 10 µM and incubated for 30 min. After the incubation, the sperm were collected in a 1.5 ml Eppendorf tube and washed in PBS for 3 times by centrifugation at 2400 rpm for 1 min each at RT to remove the extracellular dye and the pellet resuspended in M2 medium at room temperature until use.

2.3.7.2 Intracellular pH Calibration

To obtain the intracellular sperm pH, we performed an *in vivo* pH calibration for sperm. Following the fluorescent probe washing sperm were resuspended in the calibration medium containing 120 mM KCl, 25 mM HEPES and 1 mM $MgCl_2$ at different extracellular pHs (pH_e) of 6.0, 6.5, 7.0, 7.5, and 8.0 that were adjusted by addition of KOH (BDH Laboratory Supplies, 102104V) using a Five Easy pH

meter (Mettler Toledo). Approximately, 1 x 10^6 sperm were loaded into a 96 well plate. 10 µM of Nigericin (Enzo Life Sciences, BML-CA421-0005) was added to the calibrated sperm and the sample was incubated in the dark at room temperature for 10 to 15 min. Nigericin addition allowed an exchange of K^+ for H^+ which resulted in a rapid equilibration of external and internal pH. The fluorescence was measured in the end point mode and acquired at an excitation wavelength of 580 nm and emission at 640 nm a using fluorescent microplate reader (FLUOstar Omega, BMG Labtech).

2.3.7.3 Intracellular pH Imaging

After removing the excess dye, the calibrated sperm and the samples were immobilized on a microscope slide coated with 0.5 mg/ml concanavalin A from *Canavalia ensiformis* (Jack bean) (Sigma, USA, C2010). The slides were covered, and the images were acquired using a Life Technology EVOS FL Auto Cell Imaging System fluorescent microscope on an RFP light channel.

2.3.7.4 *In vitro* standard curve of fluorophore (SNARF 5AM)

A fluorescence standard curve for SNARF-5F was generated using a fluorescent microplate reader (FLUOstar Omega, BMG LABTECH) by loading 10 µM of SNARF-5F AM into different pH_e (6.0, 6.5, 7.0, 7.5, and 8.0) solutions of 50 mM

potassium phosphate (K_2HPO_4) buffer mixture (Sigma, P-5504) and KH_2PO_4 (BDH Laboratory Supplies, 102034B) as in the table below. The fluorophore was excited at 580 nm and the emission acquired at 640 nm.

Table 2: Preparation of potassium phosphate buffer (50 mM) and final pH obtained.

Component	Molarity (mM)				
K_2HPO_4	6.9	14.9	26.8	34.8	42.8
KH_2PO_4	43.1	35.1	23.2	15.2	7.2
pH	6.0	6.5	7.0	7.5	8.0

2.3.8 Lysotracker assay

LysoTracker™ Green DND-26 (Invitrogen, L 7526) was used to stain the cellular lysosomes. After sperm collection and washing, they were incubated with Lysotracker for 30 min at a final concentration of 100 nM in a 5% CO_2 incubator at 37^oC, then the sperm were washed three times in PBS by centrifugation at 2400 rpm for 5 min. Washed cells were resuspended in M2 medium and about 20 μl of suspension were smeared onto pre coated microscopic slide with Con A to immobilize the sperm, followed by application of a drop of Hoechst to stain

the DNA. The coverslip was placed on top of the slide and pressed to remove the excess solution. The samples were evaluated immediately using a fluorescent microscope EVOS^{TM} FL Auto Imaging System. The fluorophore was detected using the GFP light channel and DAPI light channel for the DNA fluorophore.

2.4 Sperm Energy Analysis

2.4.1 Measurement of ATP content

Total ATP concentration was measured using an ATP Colourimetric Assay Kit (Sigma, UK; MAK 190). The ATP assay protocol relies on the phosphorylation of glycerol to generate a product can reacted with a developer and quantified by colourimetric method. In brief, following sperm incubation for 1 hour, 1 x 10^6 mice sperm were collected and washed with PBS by centrifugation at 2400 rpm for 5 min at 4^{o}C, then resuspended in 100 µl of the manufacturer's ATP lysis buffer. The supernatant was collected and incubated with an ATP probe. The colourimetric change reflecting ATP content was measured at a wavelength of 595 nm using a 96-well microplate reader (Tecan Sunrise). The ATP concentration was calibrated with supplied standard ATP. The results are presented as a comparison of the ATP concentration of WT versus TPC2KO sperm.

2.4.2 Measurement of GAPDH activity

Sperm GAPDH enzyme activity was quantified using a GAPDH Activity Assay Kit (Abcam, ab204732). GAPDH catalyzes conversion of glyceraldehyde 3-phosphate (GAP) into 1, 3-Bisphosphate Glycerate (BPG) and an intermediate, which reacts with a developer to form a coloured product that absorbs maximally at 450 nm. Following the incubation, 1 x 10^6 mouse sperm were collected and dissolved in GAPDH assay buffer. The lysate was used to measure the GAPDH activity using a 96 well plate in accordance with the manufacturer's protocol. The absorbance of colorimetric change was recorded at 450 nm in kinetic mode using a Tecan Sunrise microplate reader every 2 min for 30 min.

2.4.3 NAD/NADH assay

The NAD / NADH ratio, which is a quantitative assay, was assessed by use of the colorimetric total NAD/NADH assay kit (ab65348; Abcam, Cambridge, U.K.). NAD cycling enzyme catalyses NAD cycling substrate to NAD cycling product in presence of NAD^+/NADH intermediate that reacted with a colourimetric probe. The assay was performed according to the manufacturer's guidance. Isolated sperm were first washed in PBS by centrifugation. The pellets were then suspended in 100 μl of the NAD / NADH extraction buffer and incubated on dry ice for 20 min and for 10 min at room temperature at 15 x 10^6 cell density. The

samples were centrifuged for 5 min at 13,000 rpm at 4^{o}C to remove the insoluble materials. The soluble lysate was divided into 3 equal volumes; the first one was heated at 60^{o}C for 30 min to convert NAD to NADH. The second contained both NAD and NADH (NADt) while the third portion was used as a background. The enzyme was added to the samples and the colourimetric change of NADH and NADt content was measured at a wavelength of 450 nm as an end point using a 96-well microplate reader (Tecan Sunrise). The NAD^{+} / NADH ratio was calculated by subtracting the total NADt from NADH relative to the value of NADH.

2.4.4 Energy metabolism phenotype

A Panel PM-M1 was used for energy metabolism microarray analysis (Biolog USA). A 96 well plate contained a variety of cytoplasmic and mitochondrial energy sources. Metabolism of substrates was assessed by the colorimetric change of a reduction of tetrazolium redox dye to produce formazan. Approximately, 70 x 10^{3} of sperm were loaded in each well and incubated with dye at 37^{o}C for 30 min. Then, the colorimetric change of the redox reaction was assessed at a wavelength of 595 nm using a 96-well microplate reader (Tecan Sunrise) in a kinetic mode of 5 cycles with a 20 sec interval every 30 min.

2.4.5 Glycerol 3-Phosphate (G3P) Reduction Assay

Isolated sperm were washed in PBS and resuspended in M2 medium. Approximately, 1 x 10^6 cells were loaded into 96 well plates in triplicates at a 100 μl final volume and 10 μl of redox dye was added to each sample except for a negative control. The sperm were divided into 3 groups in which the first group was treated with 20 mM G3P in M2 medium, and the second group did not have a treatment. The third group had the treatment without the redox dye as a negative control for the redox reaction. The plate was then sealed and incubated in a non-CO_2 incubator at 37°C. The colorimetric change of the redox rection was obtained at 595 nm using an absorbance 96 well microplate reader in a kinetic mode of 3 cycles with a 20 sec interval every 30 min. For naringenin (as a TPC2 inhibitor), gemfibrozil (as a PPARα agonist) (Cayman Chemical Company, 14835), and GW 6471 (Selleckchem Company, S2798) (as a PPARα inhibitor) treatment, the same protocol was used with drug concentrations at 80 μM, 50 mM, and 20 μM respectively.

2.4.6 Oxygen Consumption Rate (OCR) and Extracellular Acidification Rate (ECAR) assessment

An XFe96 extracellular flux analyser (Seahorse, Agilent) was used to measure the OCR and ECAR of mouse sperm. The Agilent Seahorse XFe96 extracellular flux analyser plate kit is composed of a cartridge sensor, utility plate, and

extracellular flux analyser 96 well plate (Figure 2-1). One day prior to the assay, the cartridge sensor was hydrated by pipetting 200 µl of double distilled water into the utility plate and incubated overnight in a 37°C non-CO_2 incubator.

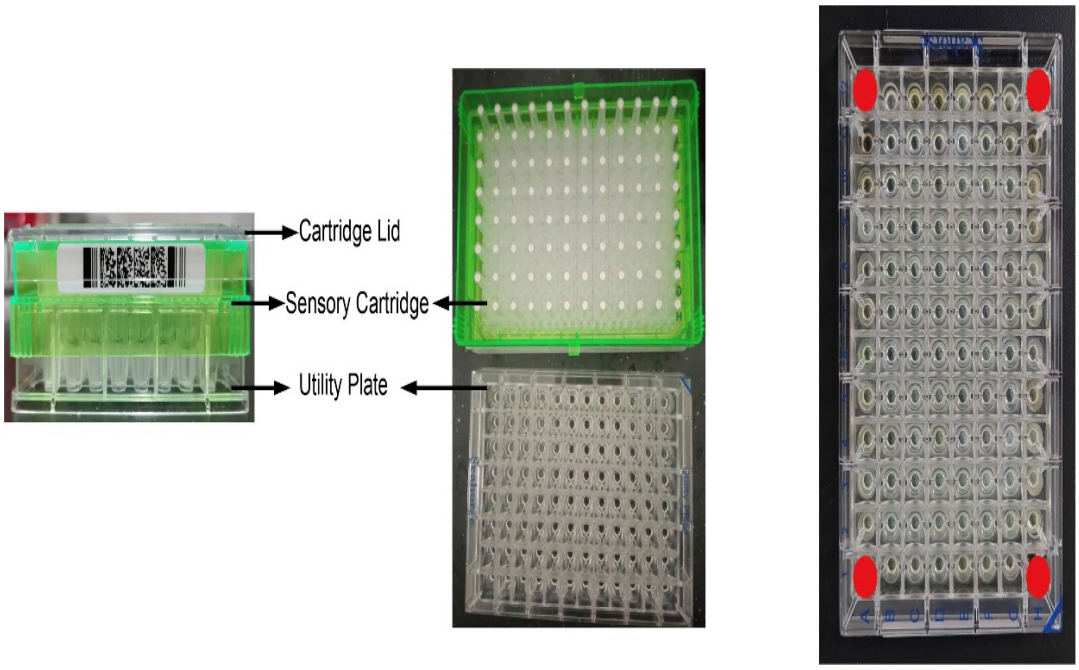


Figure 2-1 The Agilent Seahorse XFe96 extracellular flux analyser plate kit. (Adopted from Gu et. al, 2021).

Concanavalin A (Con A) was used to attach the sperm to the bottom of the extracellular flux analyser 96-well plate by loading 50 µl of 0.5 mg/ml Con A in each well and leaving the plate with the lid open overnight to let it dry. On the day of the assay, the distilled water in the cartridge was replaced with 200 µl of prewarmed Seahorse XF Calibrant Solution (Agilent, 100840-000). The isolated

sperm were washed and incubated for 15 min in TYH medium containing 4 mg BSA/ml with low HEPES contains 138 mM NaCl, 4.7 KCl (Sigma, P-3911), 1.7 mM $CaCl_2$ (Sigma, C3306), 1.2 mM KH_2PO_4 (Sigma, M-7506), 1.2 mM $MgSO_4$ (, 5.6 mM Glucose (Sigma, G-7528), and 1 mM HEPES (Sigma, H-8651). The sperm were loaded into the extracellular plate at a density of 1 x 10^6 sperm per well to a final volume of 180 μl except for the four corner wells which contained only the medium that used as a background. After loading the sperm, the plate was centrifuged for 1 min at 1000 rpm at room temperature and the plate oriented 180^o and centrifuged again at the lowest braking rate to ensure the sperm are evenly distributed and adhered in the bottom of the well. The sensor cartridge containing the calibrant solution was placed into the extracellular flux analyser to start the assay calibration that takes 10 – 15 min while the sample plate was placed in a 37^{o}C non-CO_2 incubator. Once the calibration was finished, the calibration plate was replaced with the sperm plate, and the assay was continued. The measurement was performed at 37^{o}C for at least 60 min. The first reading was recorded after 30 – 40 min after the sperm collection, taking into account the time spent on sperm counting, seeding, and machine equilibration.

2.4.7 Mitochondrial membrane potential assay

The JC-1 (Abcam, ab113850) fluorescent probe was used to assess the mitochondrial membrane potential ($\Delta\Psi_M$) of the sperm using two different approaches involving a fluorescent microplate reader and fluorescent microscope imaging. JC-1 is a cationic dye that accumulates in the mitochondria in a potential dependent manner to measure the mitochondrial membrane polarization based on the negative charge inside the mitochondria. The probe generally produces a green fluorescence upon excitation. When there is more negative charge in the mitochondria, JC-1 accumulates and form J aggregate which emits a red fluorescence. On the other hand, at low membrane potential or apoptosis in the mitochondria, the dye still passes to the mitochondria and is unable to form a sufficient concentration of J aggregate to generate the red fluorescence, and instead it exhibits the normal green fluorescence. Hence, the ratio of red to green fluorescence of the dye in the mitochondria can be regarded as a direct evaluation of the status of mitochondrial polarisation, with the greater the red shift of the dye, the higher the $\Delta\Psi_M$. (Sivandzade et al., 2019). Following the sperm isolation, sperm were collected and washed in PBS 2 times by centrifugation at 2400 rpm for 5 min at room temperature. The pellet was resuspended in M2 medium and loaded into a 24 well plate that was incubated in 5% CO2 at 37^{O}C. JC-1 was dissolved in DMSO and 5 μl was applied to the sperm

at a final concentration at 1 μM and incubated in the dark for 30 min. Samples were taken and measured at different time points. After 30 min of incubation, sperm were collected in a 1.5 ml Eppendorf tube and washed with pre warmed PBS 3 times by centrifugation for 5 min at 2400 rpm at room temperature to remove the excess dye then the sperm were resuspended in M2 medium for the assessment. The sample underwent two methods to assess the $\Delta\Psi_M$.

2.4.7.1 Fluorescent microplate reader

Sperm were loaded into a 96 well plate at a density of 1 x 10^6 sperm per well. The fluorescent intensity reading was obtained at 36^{o}C in the end point mode using a FLUOstar Omega microplate reader. JC-1 dye was excited at 480 nm and the emission was set at 520 for monomer detection and at 590 for the J aggregate detection to obtain the sperm $\Delta\Psi_M$. The 590/520 fluorescence intensity ratio of the dye was measured and represented as a direct evaluation of the condition of mitochondrial polarisation.

2.4.7.2 Microscopic imaging

Sperm were immobilized by loading 10 μl of the sperm suspension onto a pre treated microscope slide with 0.5 mg/ml Con A. Following this, DAPI was added to the slide for nuclei detection, the cover slip was placed on the slide and the sperm were observed immediately under a fluorescent microscope EVOS ™ FL

Auto Imaging System using the DAPI, GFP, and RFP light channels. The red / green fluorescence intensity ratio of the dye was analysed and depicted.

2.5 Sperm Protein Analysis

2.5.1 Protein extraction and electrophoresis (SDS-PAGE)

2.5.1.1 Protein extraction

Sperm were collected and washed with PBS then the pellet was suspended in M2 medium and loaded into a 24 well plate that had been divided into two groups, and the plate was incubated in a 5% CO_2 incubator at 37^{o}C. The first group was treated with 80 μM naringenin whereas the second group was treated with DMSO as a control group. The plates were incubated with the treatment for 30 min. The samples were collected in a 1.5 ml Eppendorf tube and washed with PBS 3 times. The first two washes were at 4000 rpm at room temperature for 5 min and the last wash was at a maximum speed of 13000 rpm for 5 min to remove all the solutions. Following the washing, the sperm were suspended in 30 μl of 5 x SDS lysis buffer (1.67 ml ddH_2O, 5.83 ml of 0.5 mM Tris-base pH 6.8 (Sigma, T1503), 2.5 ml glycerol (Sigma, G6279), 833 mg SDS (Fisher Scientific, BPE166) and 1 mg Bromophenol blue (Sigma, b-7021), total 10 ml) and mixed by pipetting up and down for homogenization, boiled at 95^{o}C for 4 min and centrifuged once more at maximum speed 13000 rpm for 10 min at room

temperature. The supernatants were transferred into a new tube and supplemented with 10% of the total volume β-mercaptoethanol (β -ME) (Sigma, m-6250) and boiled again for 3 min. The protein samples were either used for electrophoresis or stored at -80^{o}C until use.

2.5.1.2 Protein electrophoresis and immuno-blotting

Protein electrophoresis was carried out using a Mini PROTEAN® 3 Cell system (Bio-Rad). Protein samples and protein ladder Page Ruler™ Plus Pre-stained Protein Ladder, 10 to 250 kDa (Thermo Scientific, 26619) were loaded into a 4 – 20% Mini-PROTEAN TGX precast protein gel (Biorad, 4561094) and electrophoresed at 100 mV in 1 x Tris Glycine SDS buffer (TGS buffer, Bio-Rad 1610732) (25 mM Tris, 192 mM glycine, 0,1% W/V SDS at pH 8.3) for 1.5 hour. The gel was transferred to polyvinylidene difluoride PVDF membrane (Immobilon®-P PVDF Membrane 0.45 μm pore size, Millipore IPVH00010) in cold Tris-Glycine transfer buffer (25 mM Tris, 192 mM glycine pH 8.3 with 20 % methanol V/V) at 75 V for 1 to 1.5 hours at room temperature. Non-specific antibody interaction sites in the membrane were blocked using Intercept (TBS) Protein-Free Blocking Buffers (LI-COR, 927-80001) for 1 hour at room temperature. Blocked membranes were incubated with the primary antibodies (1:1000 dilution) listed in table 2. either overnight at 4^{o}C or 1 hour at room temperature. The blots were washed in 1 x Tris Buffered Saline (TBS) (50 mM

Tris-HCl and 150 mM NaCl (Sigma, S9888) with 0.1 % Tween V/V (Sigma, P7949) three times, 5 min for each wash, followed by incubation with an appropriate secondary antibody (1:10000 dilution) for 1 hour at room temperature. The membranes were washed again with TBST three times for 5 min every wash, and the immunoreactive bands were detected using a LICOR Odyssey M Imaging System.

2.5.2 Indirect immunofluorescence assay

Isolated sperm were washed with PBS by centrifugation and suspended in PBS to a final concentration of 10 x 10^6 cells ml^{-1}. The sperm were fixed with 4 % paraformaldehyde (PFA) in PBS (Chem Cruz, sc-281692) to a final concentration of 2% for 30 min at room temperature. 20 μl of the cell suspension was smeared onto a microscopic slide coated with poly D-lysine and air dried then rinsed three times with PBS for 20 sec each. Approximately, 0.5 % of triton in PBS v/v was used for sperm permeabilization for 30 min at room temperature followed by washing in PBS three times. The sperm were blocked in the blocking buffer containing 2 % goat serum in PBS, and 0.1 % Tween 20 in PBS for 1 hour at room temperature. The sample was incubated with the primary antibody, which was diluted at 1:200 in 1 % BSA in PBS and 0.1 % Tween 20 in PBS, overnight at 4^{o}C in a humid chamber. After 3 washes with PBS, the smears were incubated with

the secondary antibody goat anti-mouse IG-g H&L Alexa fluor 647 (Abcam, ab150115) for 1 hour at room temperature then the last wash was performed three times in PBS. The slides were mounted using ProLong™ Diamond Antifade Mountant with DAPI (Invitrogen, P36966) and covered with coverslip, and then sealed using nail polish for assessment. Samples were evaluated using an Olympus BX40 fluorescence microscope equipped with 40x lenses and the image was acquired through a CCD camera fitted with the microscope. The images were processed and analysed using Image-J, Fiji.

2.6 Testis and Sperm RNA Analysis

2.6.1 Testis and sperm RNA extraction and cDNA synthesis

2.6.1.1 RNA extraction

A GeneJET RNA Purification Kit was used for RNA extraction (Thermo Scientific, K0732). Testis was isolated from the euthanised mouse and collected in PBS. About 20 mg of fresh testis was homogenised and grinded thoroughly on dry ice by mortar and pestle. The ground tissue was transferred into a 1.5 ml Eppendorf tube containing 300 μl of lysis buffer supplemented with 2 % of 14.3 M β-ME and mixed by vortex mixer. 300 μl of proteinase K diluted in 1:60 in Tris-EDTA buffer (10 mM Tris HCl, pH 8.0 and 1 mM EDTA) was added to the lysate, the mixture incubated for 10 min, then centrifuged for 10 min at 13000 rpm at room temperature to remove the tissue debris.

For sperm RNA extraction, after the sperm isolation, collection, and washing in PBS, 300 μl of lysis buffer supplemented with 2 % of 14.3 M β-ME was added to the sperm and mixed by vortex mixer. The supernatant of the testis lysate and the sperm lysate were mixed by pipetting up and down with 300 μl of 95 % ethanol and transferred into a Gene JET RNA Purification Column and centrifuged for 1 min at 13000 rpm at room temperature. The flow through was discarded, while the lysate that binds to the column was washed by washing buffer 1 and 2 for 1 min at 13000 rpm at room temperature, then 30 μl of nuclease-free water was used to elute the RNA by centrifugation using the same

parameters of washing. The RNA was quantified using a Nanodrop 1000 (Thermo Scientific) and stored at -80 ^{o}C until ready for use.

2.6.1.2 cDNA Synthesis for RT-qPCR

A High-Capacity RNA to cDNA Kit (Applied Biosystems by Thermo Fisher Scientific, 4387406) was used to perform reverse transcription of isolated RNA to generate complementary DNA. The RNA template was mixed with reaction mixture as described in Table 2. The mixture was incubated for 1 hour at 37^{o}C followed by 5 min incubation at 95^{o}C and stored at -20^{o}C until ready for use.

Table 3: Template mixture of cDNA synthesis from testis and sperm RNA.

Component	Volume µl
2X RT Buffer Mix	10
20X RT Enzyme Mix	1
RNA sample	5
Nuclease-free H_2O	4
Total per reaction	20

2.6.1.3 Quantitative reverse transcription PCR

The quantitative reverse transcription polymerase chain reaction (qRT-PCR) reactions were performed in 96-well PCR plates (Roche); each run was evaluated in triplicate for the gene of interest and actin was used as a reference gene. Negative controls excluding cDNA were used to evaluate the reliability of each

experiment. The cDNA template was mixed with reaction mixture as described in Table 2. PowerUp™ SYBR™ Green Master Mix (Applied Biosystems™ by Life Technology, A27542) was used to detect the formation of double-stranded DNA by a fluorescent dye. qRT-PCR experiments were conducted in a Light Cycler 480 Real Time PCR System (Roche). The thermal cycling conditions was programmed in the machine as follows: firstly, the cDNA samples were initiated for 2 min at 50^{o}C for Uracil DNA Glycosylase (UGD) activation to eliminate carryover PCR products and prevent contamination and another 2 min at 95^{o}C for DNA polymerase activation. Then 40 cycles were set up for the template denaturation at 95^{o}C for 15 sec followed by template annealing and extension at 60^{o}C for 1 min. The fluorescence was acquired at the melting phase of each cycle at 60^{o}C. The gene expression fold change for each condition was calculated relative to the WT control, using the relative gene expression formula ($2^{-\Delta\Delta Ct}$). The primers were designed using the NCBI database and Primer PLAST tool.

Table 4: Composition of one reaction mixture used for RT-qPCR.

Component	*Volume*
SYBR green master mix	5 µl
Forward primer	0.5 µl (final concentration 500 nM)
Reverse primer	0.5 µl (final concentration 500 nM)
RNA free water	2 µl
cDNA Template	1 µl
Total	10 µl

2.7 *In Vitro* Fertilization (IVF)

2.7.1 Oocyte isolation

4 to 5 weeks old WT female mice were injected intraperitoneally (IP) with 7.5 IU (100 μl) of Pregnant Mare Serum Gonadotropin (PMSG) (MSD, PMSG Intervet 5000 IU) followed by another injection of 7.5 IU of human Chorionic Gonadotropin (hCG) (MSD, Chorulon® 1500 IU) 48 hours after the first injection. Between 12 to 14 h after the second injection, the female mice were euthanised to isolate the oocytes. The oviducts were isolated and collected into the oil that covered the fertilization drop. Then, the cumulus oocyte complexes (COCs) were released from the oviduct by piercing the ampulla with 27 gauge needle and dragged into the fertilization drop (200 μl of human tubal fluid HTF (Sigma, Embryo Max™ Human Tubal Fluid, MR 070-D) containing 4 mg/ml bovine serum albumin (BSA) (Sigma, A9418) and 1 mM reduced glutathione (GSH) (Fisher Bioreagents™, BP2521-1)), then covered with 3.5 ml of paraffin oil (Cooper Surgical, Liteoil LGOL-500).

2.7.2 Sperm collection and oocyte insemination

The cauda epididymis of 8 – 12 weeks old male mice were isolated and collected in the paraffin oil that covered the sperm drop of M2 medium containing 4 mg/ml BSA. The cauda was pierced in the sperm drop to allow the sperm to swim

out for 30 min. 2 μl of the sperm suspension was transferred into the fertilization drop containing the COCs incubated at 37°C in a 5% CO_2 incubator to induce IVF. 4 hours later, the oocytes were collected from the fertilization drop and washed in three drops of HTF and incubated again for another day. On the second day, 2-cell embryo formation was observed under the microscope and the ratio of 2-cell embryo formation was calculated by dividing the number of 2-cell embryos by the total original number of oocytes.

2.8 Data presentation and statistical analysis

Statistical analyses were conducted including a student's unpaired T-Test to compare two independent means. One way or two-way analysis of variance (ANOVA) testes were also performed to analyse the differences between more than two independent means, and any interaction between them. This was done by using Tuckey's or Šídák's test for multiple comparison to investigate the source of any differences seen. All results are represented as mean ± standard error of the mean (SEM). All statistical analysis and graphs were generated by using graph pad prism version 9.1.1. $P < 0.05$ was considered significant. The level of significance is presented as stars on the figures (* $P < 0.05$; ** $P < 0.01$; *** $P < 0.001$, **** $P < 0.0001$).

List of primers

Table 5: List of primers used for RT-qPCR.

Name of Gene	Primer
Mitochondrial NADH dehydrogenase 1 mt-ND1	Forward CTA GCA GAA ACA AAC CGG GC
	Reverse CCG GCT GCG TAT TCT ACG TT
Mitochondrial NADH dehydrogenase 5 mt-ND5	Forward ACC CAA TCA AAC GCC TAG CA
	Reverse AGG ACT GGA ATG CTG GTT GG
mitochondrial glycerol phosphate dehydrogenase 2 (Gpd2, or mGPDH)	Forward CTA ACA TTC AGG CCC GGG GT
	Reverse GTC GGG GGA CTC TAG GGA CT
Mitochondrial ATP synthase alpha subunit 1Atp5a1	Forward CCA TTT TGT GCC AGT CGT CC
	Reverse TTT TTG GAG ACC AGT CCC GC
Two-pore calcium channel 2 TPC2	Forward GAG CTC TGC ATA GAC CAG GCT GTG G
	Reverse CCA GGA AGG CAA GCA AGC AGA ACG C
Peroxisome proliferator activated receptor alpha PPARα	Forward TGA CGT TTG TGG CTG GTC AA
	Reverse CAG ATG GGG CTC TCT GTG TC
Peroxisome proliferator activated receptor gamma PPARγ	Forward CGC GGA AGA AGA GAC CTG G
	Reverse GTG TGA CTT CTC CTC AGC CC
Cytochrome c oxidase subunit 5B Cox5b	Forward GCG TTG TTA GAC TCC CAC CAA
	Reverse GCG AAG TAA CCT TGA AGC CA
	Forward ACT CTC AGT AAG GGG CTG GT

Peroxisome proliferative activated receptor, gamma, coactivator 1 alpha Ppargc1a	Reverse CAA CCA GAG CAG CAC ACT CT
Beta Actin	Forward GTG ACG TTG ATC TCC GTA AAG A
	Reverse GCC GGA CTC ATC GTA CTT AGA
Mitochondrial transcription factor A, mTFA	Forward GTC ACG AAG CTC AGT AGG CAG
	Reverse TGG GTA GCT GTT CTG TGG AAA
Superoxide dismutase 1 (SOD1)	Forward GGGAAGCATGGCGATGAAAG
	Reverse CCCCATACTGATGGACGTGG
Superoxide dismutase 2 (SOD2)	Forward GTAGGGCCTGTCCGATGATG
	Reverse CGCTACTGAGAAAGGTGCCA

List of Antibodies

Sirt 1 SirT1 (D1D7) Rabbit mAb 9475 Cell Signalling Technology

PGC1a Anti-PGC1 alpha + beta antibody (ab72230) Abcam

mTFA Anti-mtTFA antibody - mitochondrial marker (ab47517) Abcam

p-PKA Phospho-PKA Substrate (RRXS*/T*) (100G7E) Rabbit mAb 9624 Cell Signalling Technology

p-Tyr Anti-Phosphotyrosine antibody [PY20] (ab10321) Abcam

Tubulin Anti-alpha tubulin antibody [DM1A] - Loading Control (ab7291) Abcam

Actin β-Actin (8H10D10) Mouse mAb 3700. Cell Signalling Technology

Chapter 3

Characterization of Sperm Motility and Metabolism in TPC2 KO Mice Sperm

3.1 Introduction

The sperm is one of the most clearly differentiated cells and has an exclusive target during its lifespan. The main function of the sperm is to penetrate the oocyte and release its DNA content inside the latter to accomplish the fertilization process. To achieve this goal, it must migrate from the male body to the female reproductive system and continue its journey to fulfil its purpose. Reduced sperm motility and incapability for capacitation-induced hyperactivation of motility are common causes of human male infertility (Nayak et al., 2019; Suarez and Dai 1992). The process of sperm formation for the first part of their lives, takes place in the testes, where they can grow and develop until they reach structural maturation in the epididymis wherein, they become actively motile and ready to leave the male body (Cornwall and von Horsten 2007). When the sperm are ejaculated in the female reproductive system, they are still unable to fertilize oocytes because they are functionally immature (Freitas et al., 2017). They need to spend a certain time in the female genital tract to become functionally active cells. They undergo multiple physiological and biochemical modifications, a process that is referred to as capacitation and in which the sperm becomes able to fertilize the oocyte (Ickowicz et al., 2012). During this process, the sperm motility pattern changes to become more vigorous and hyperactivated, a process whereby the flagellum speed is

increased and become more forceful (Cancel et al., 2000). This enhanced motility helps the sperm to swim along the female genital tract and penetrate the cumulus and zona pellucida to reach the oocyte, which is necessary for a successful fertilization.

Throughout the time of this journey, the flagellum which houses the motile apparatus requires an adequate source of energy to sustain the motility of the sperm (Tash, 1989). As for most other animal cells, adenosine triphosphate (ATP) is the main energy source used at the cellular level that the sperm must produce to sustain its motility. Glycolysis and oxidative phosphorylation are considered the major metabolic pathways to produce ATP in mammalian cells and they are regulated by various signal transduction pathways (Takei et al., 2014).

Calcium is a versatile cellular secondary messenger. Changes in the intracellular calcium ion (Ca^{2+}) concentration play a key role in the regulation of a variety of physiological processes. Ca^{2+} signals can be induced via influx of extracellular Ca^{2+} and by release of Ca^{2+} from intracellular stores (Galione et al., 2011). While the major well-known intracellular store is the endoplasmic reticulum (ER), another Ca^{2+} store identified by Antony Galione is the acidic endolysosomal compartment. Nicotinic acid adenine dinucleotide phosphate (NAADP) is the second messenger that triggers Ca^{2+} release from this store through two-pore

channels (TPCs). Studies using TPC knockout (KO) mice have shown that TPC1 and TPC2 play roles in processes including brown adipose tissue thermogenesis, intracellular trafficking, immunity, neo-angiogenesis, and cancer hallmarks such as proliferation, metastasis, and abnormal cellular energy metabolism (Lear et al., 2015; Favia et al., 2014; Müller et al., 2021; Cang et al., 2013). This current study set out to investigate a potential role for TPC2 in sperm based on investigating the effect of abolishing TPC2 gene on sperm motility and energy production/utilisation.

3.2 Chapter Aims

The aims of this chapter were to characterise sperm motility and metabolism in the sperm of WT and TPC2 KO mice and potential related molecular regulatory proteins.

3.3 Results

3.3.1 General characterization of gene expression, viability, and lysosomes in the sperm of WT and TPC2 KO mice

TPC2 KO mice have been established by the Parrington and Galione groups (Department of Pharmacology, University of Oxford). I first measured the transcriptional expression of the TPC2 gene in KO mice sperm relative to the wild type (WT) sperm (Figure 3-1 A). The data show that the gene expression level is significantly reduced more than 80 % compared to WT with a $p < 0.0001$.

Figure 3-1B, shows that there are no significant differences in the viability between the WT and TPC2 KO sperm. As the sperm of TPC2 KO mice have not been studied previously, the general expression, viability, and localization of the lysosomes in such sperm were evaluated to assure us that will not have an impact on the model. The fluorescent images in Figure 3-1 C show the staining of the lysosomal acidic compartment. It is generally localised in the head and the midpiece of the sperm as shown in both WT and TPC2 KO sperm. It seems that TPC2 KO sperm have normal viability and no differences in the location of the lysosomes compared to WT mice sperm.

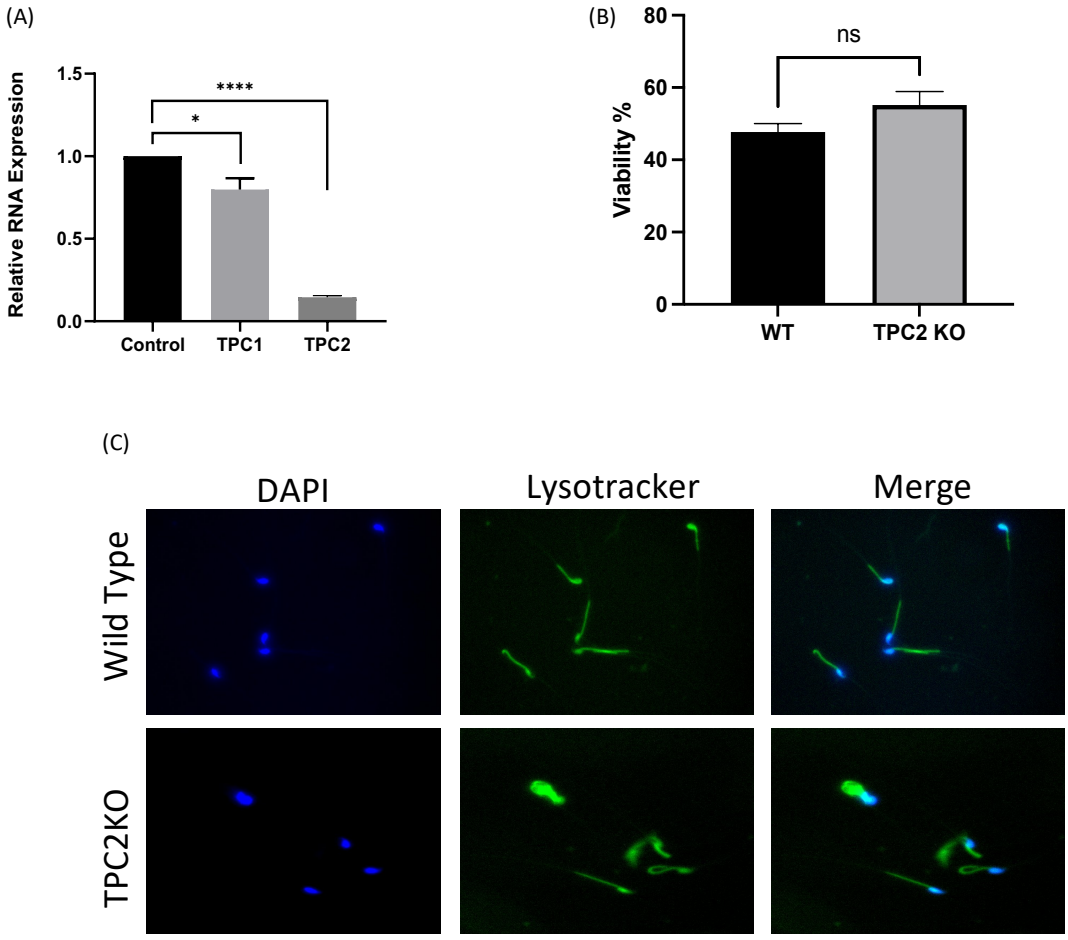


Figure 3-1: Characterization of sperm from WT and TPC2 KO mice.

(A) Quantitative RT-PCR analysis of relative mRNA expression of the TPC2 gene in the WT and TPC2 KO sperm using (n=3) RNA samples from 3 WT and 3 TPC2 KO mice, unpaired two-tailed Student's t-test. (B) Sperm viability analysis using eosin and nigrosine staining assay with more than 200 sperm counted from three mice each for WT and TPC2 KO. (C) The localization of the lysosomes in the WT and TPC2 KO sperm using green lysotracker dye. Nuclear staining (DAPI, blue), lysosomes staining (lysotracker, green). Data is represented as mean +/− SEM. Asterisks show statistical significance where * $p < 0.05$, ** $p < 0.01$, ** $p < 0.001$, **** $p < 0.0001$.

3.3.2 TPC2 KO sperm show an enhancement in sperm motility parameters

TPC2 KO sperm were used to investigate the role of TPC2 in sperm motility parameters such as total motility (MOT), progressive motility (PROG), straight line velocity (VSL), average path velocity (VAP), curvilinear velocity (VCL), lateral head (ALH), beat cross frequency (BCF), and linearity (LIN) during different time points using Computer Automated Sperm Assessment (CASA). The total motility indicates the percentage of total sperm that are motile while the progressive motility refers to the percentage of the rapidly motile sperm. To our surprise, the percentage of total and progressive motility of TPC2 KO sperm were significantly higher than wild type at the early point of measurement (Figure 3-2 A and B). However, the data shows no significant differences in the percentage of total and rapid motile sperm at the later time points of 0.5 and 1.5 hours. Noticeably, the data show that the VAP, VCL, and VSL, of TPC2 KO sperm were significantly higher than that of WT sperm at all time points (Figure 3-2 C-E). Also, the BCF is significantly decreased after 0.5 h of swimming (Figure 3-2 G). However, the other parameters such as ALH and LIN showed no significant differences between the WT and TPC2 KO sperm (Figure 3-2 F-H). It appears then that TPC2 KO sperm are more active and swim faster than WT sperm and might reach the status of hyperactivation more rapidly compared to the WT sperm. The graphs 3-2 A to E show that there is a decrease in the motility and kinetic

parameters with time for both WT and TPC2 KO sperm. The data suggest that the absence of TPC2 was associated with enhancement in some sperm kinetic parameters that could accelerate the process of sperm hyperactivation and this may be linked to the influence that the TPC2 lysosomal channel has upon the cellular Ca^{2+}. This phenotype could be a consequence of cellular modifications at the molecular level of the cellular machinery that regulates and maintains sperm motility.

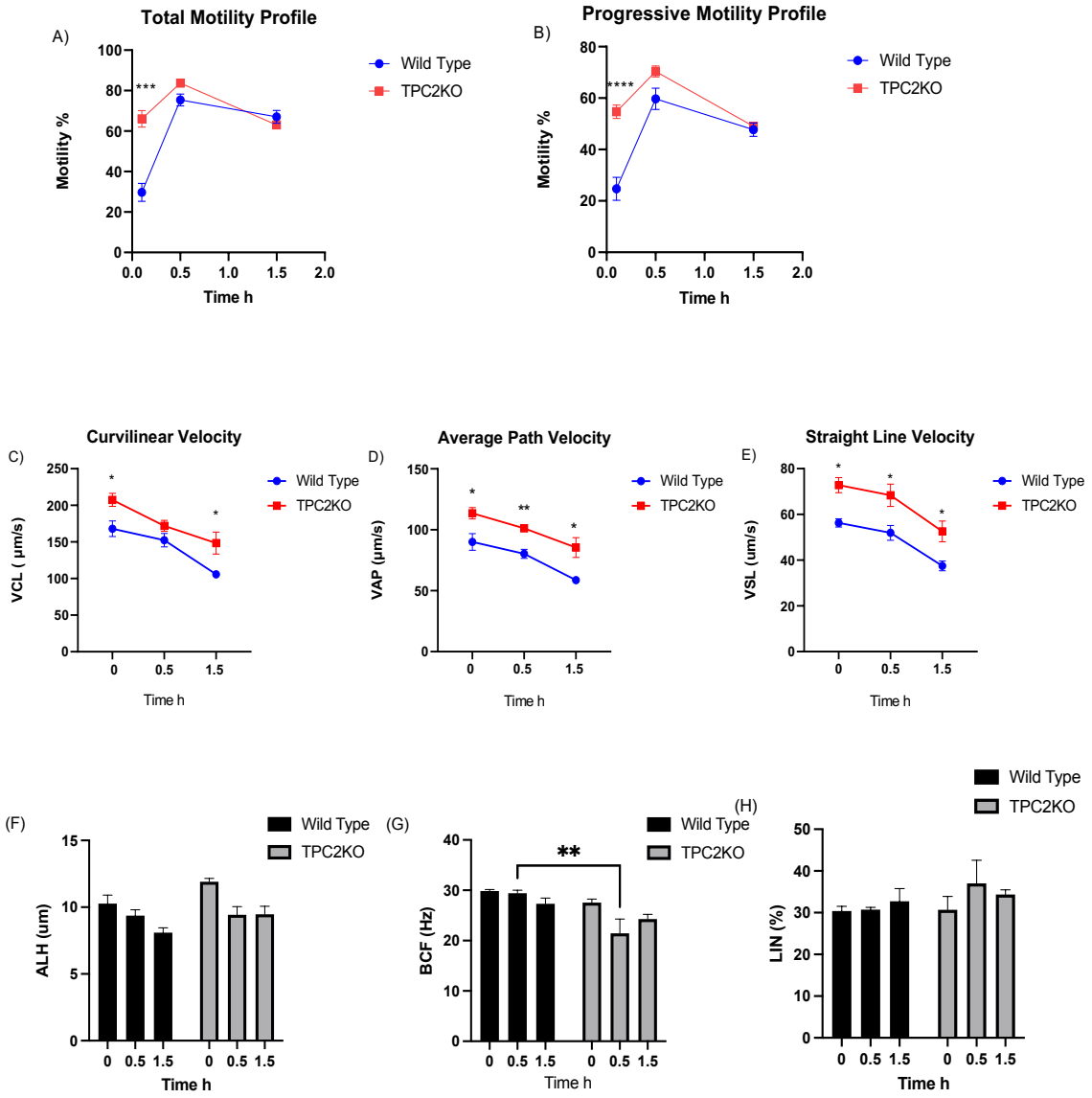


Figure 3-2: Sperm motility and kinetic parameters of WT and TPC2 KO.

Analysis of the sperm motility parameters using computer assisted sperm analysis (CASA) at different time points for WT and TPC2 KO sperm. (A) the percentage of motile sperm. (B) the percentage of the sperm that move in a forward straight line. (C) VSL, straight line velocity (µm/s); the average velocity of the sperm head along the straight line between its first detected position and its last. (D) VCL, curvilinear velocity (µm/s); the average velocity of the sperm through its real path. (E) VAP, average path velocity (µm/s); velocity of a sperm head along its average path that is computed by smoothing the curvilinear path. (F) ALH, amplitude of lateral head displacement (µm); the magnitude of the lateral sperm head displacement of its average path. (G) BCF, beat cross frequency (Hz); the average rate at which the curvilinear path crosses the average path. (H) LIN, straightness (%); the percentage of straightness of sperm path. All data are presented as average ± s.e.m of three animals. Asterisks show statistical significance where * $P < 0.05$, ** $P < 0.01$, *** $P < 0.001$, **** $P < 0.0001$ using unpaired student's t-test.

3.3.3 TPC2 KO sperm exhibits increased energy production.

Maintaining mammalian sperm motility for a long period requires continuous energy production. ATP is considered as the primary cellular energy source from substrate metabolism and is used to maintain the intracellular environment for sperm processes such as motility, capacitation, hyperactivation, and the acrosome reaction, which are all necessary for successful fertilization. Sperm ATP content was measured after one hour incubation to see if there were any differences in this energy source that might explain the differences in sperm motility of TPC2 KO compared to WT sperm. Sperm from TPC2 KO mice showed a significant elevation in ATP levels compared to that in WT sperm (Figure 3-3 A). Glyceraldehyde 3-phosphate dehydrogenase (GAPDH) is an enzyme which, catalyses the transformation of glyceraldehyde 3-phosphate (GAP) to 1,3-biphosphoglycerate (1,3 BPG), which is involved in the process of glycolysis to produce ATP. In addition, it produces pyruvate which is the precursor of oxidative phosphorylation in the mitochondria and is localised in the principal piece of the sperm that plays a role in energy regulation and cellular metabolism. Hence, the activity of GAPDH was measured in the WT and TPC2 KO sperm to assess the rate of energy production in the sperm. Figure 3-3 B shows the kinetic activity of GAPDH in the WT and TPC2 KO sperm during the time. It appears that

the TPC2KO sperm exhibit more activity compared to the WT sperm during the assay. Thus, the higher motility parameters of TPC2 KO sperm might be seen as a reflection of greater energy production.

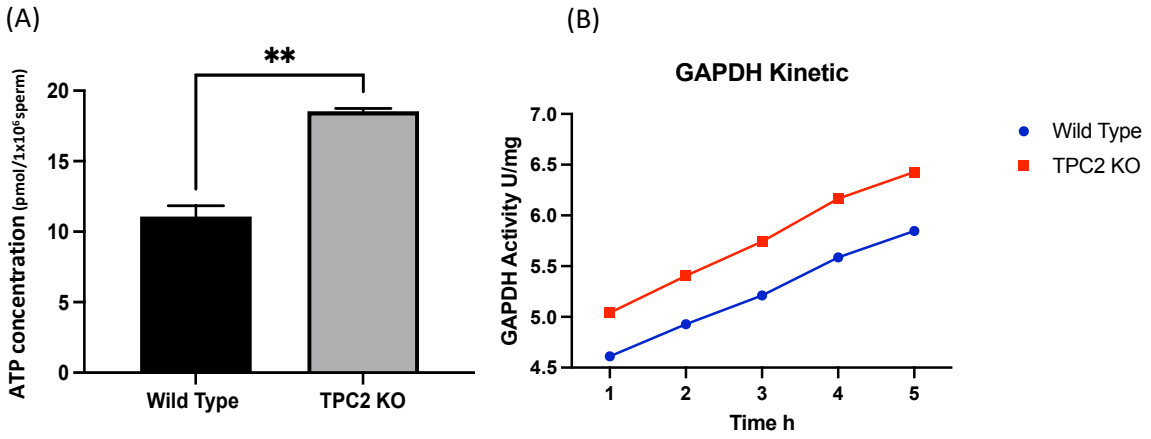


Figure 3-3: Sperm ATP Content and GAPDH activity of WT and TPC2KO mice.

(A) The level of ATP in sperm from WT and TPC2 KO mice. (B) GAPDH activity of WT and TPC2 KO sperm. The data are presented as an average ± s.e.m of sperm from three animals of each type. Asterisks show statistical significance where * $P < 0.05$; ** $P < 0.01$; *** $P < 0.001$, **** $P < 0.0001$, using unpaired Student's *t*-test.

3.3.4 Another factor plays a role in the change in motility in TPC2 KO sperm

It has been shown that AMP-activated protein kinase (AMPK) is the central regulator of cellular energy homeostasis in mammalian sperm. This kinase signalling mechanism involved in regulating sperm motility has been studied in both mice and boars. Since AMPK acts as a sensor of the cellular energy state and regulates metabolism and motility accordingly, its role was studied in WT versus TPC2 KO sperm using $CdCl_2$ as an AMPK inhibitor along similar lines to Wang et. al. (2016). WT and TPC2KO sperm were treated with 10 μM $CdCl_2$ and incubated for 30 min to assess the inhibitory effect of AMPK on sperm motility. $CdCl_2$ markedly decreased the total and progressive motility of both WT and TPC2 KO sperm (Figure 3-4 A and B). However, the TPC2 KO sperm were much less susceptible to the inhibitory effect of $CdCl_2$ compared to WT sperm. The graph shows that the AMPK inhibitor sharply decreased the percentage of total motility of WT sperm from 70% to 20% with more than 70% reduction in the motile sperm whereas the drop in the TPC2 KO sperm was much less at around 30% of the motile sperm. A similar effect occurred with progressive motility, there being a 70% and 30% reduction in motile WT and TPC2 KO sperm, respectively. This reduction in the motility of the WT and TPC2 KO sperm was found to be significantly decreased ($P < 0.01$) in the WT sperm compared to the TPC2 KO sperm. However, the kinetic parameters did not show significant

differences within each group in response to the AMPK inhibitor (Figure 3-4 C-E).

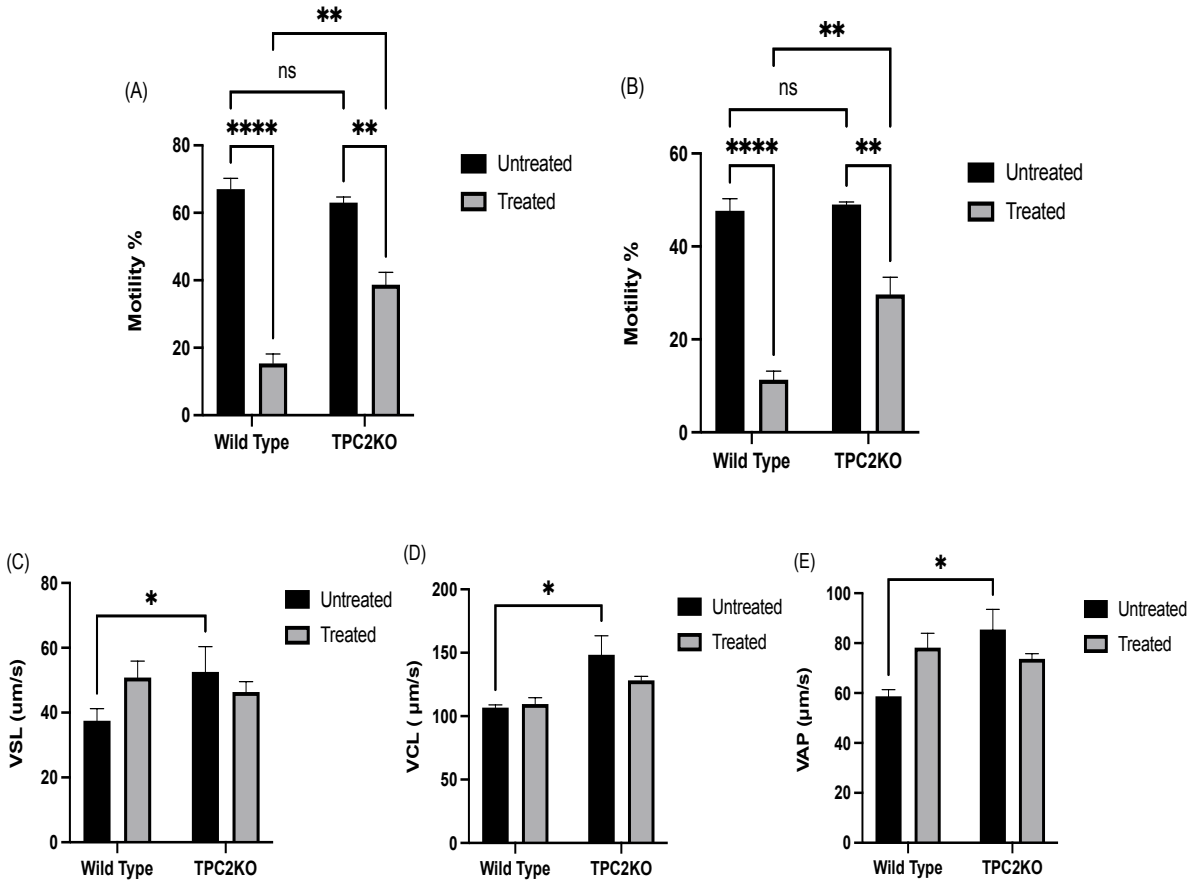


Figure 3-4: The effect of $CdCl_2$ treatment on motility parameter of WT and TPC2KO sperm.

The effect of 10 µM $CdCl_2$ treatment on the percentage of the total motility (A), and the progressive motility (B), of wild type and TPC2 KO sperm. (C)-(E) the treatment effects on the sperm kinetics of WT and TPC2 KO sperm. (C) VSL, straight line velocity (µm/s); the average velocity of the sperm head along the straight line between its first detected position and its last. VCL, curvilinear velocity (µm/s); the average velocity of the sperm through its real path. (E) VAP, average path velocity (µm/s); velocity of a sperm head along its average path that is computed by smoothing the curvilinear path. All data are presented as average ± s.e.m of three animals. Asterisks show statistical significance where * $P < 0.05$; ** $P < 0.01$; *** $P < 0.001$, **** $P < 0.0001$ using 2-way ANOVA test.

3.3.5 Glycerol 3 phosphate as an energy source that drives ATP production in TPC2 KO sperm via oxidative phosphorylation.

Sperm energy production is generated from cytosolic substrate metabolism and mitochondrial respiration. Utilisation of several substrates was tested at different time points using a colorimetric energy metabolism microarray panel to identify the metabolic pathway that sperm use to produce energy. Glycerol 3 phosphate (G3P) was the most obvious substrate that produced energy in sperm (Figure 3-5 A). The rate of G3P substrate metabolism was greater in the TPC2 KO sperm compared to that in WT sperm during the incubation period.

Glycerol 3 phosphate dehydrogenase 2 (GPD2) is the enzyme that catalyses hydrolysis of G3P to produce dihydroxyacetone phosphate (DHAP), which can either produce energy from glycerol hydrolysis or feed into gluconeogenesis. Hence, the expression level of GPD2 mRNA was measured in TPC2 KO and WT sperm using RT-qPCR to check whether there is functional enhancement of expression of this gene in TPC2 KO sperm. The findings show that the GPD2 expression level is significantly highly upregulated in TPC2 KO sperm compared to WT sperm (Figure 3-5 B). This suggests that this GPD2 upregulation could be the cause of the increased ATP levels in the TPC2 KO sperm.

A Seahorse energy analyser was used to assess the pattern of sperm energy production in the WT and TPC2 KO sperm since they have obvious differences in ATP production. The Seahorse analyser evaluates whether energy is produced

through the glycolytic system or via oxidative phosphorylation in the mitochondria. The rates of glycolysis and oxidative phosphorylation are obtained simultaneously through measuring the extracellular acidification rate (ECAR) and the oxygen consumption rate (OCR) in an extracellular flux analyser. The glycolytic rate is measured by evaluating the extracellular acidification rate that derives from lactic acid formation from glycolysis. However, the metabolic reaction that takes place in the mitochondria requires the oxygen to convert the energy stored in the nutrient substances to ATP, so the OCR is a direct measurement of the oxygen consumed by the cells that occurs during oxidative phosphorylation. The graphs C-F in Figure 3-5 show the ECAR and OCR of WT and TPC2 KO sperm in the presence of 20 mM G3P, measured for 1 hour. It is clear that there are no significant differences in the glycolysis rate between WT and TPC2 KO sperm in the presence of G3P, however the rate of oxidative phosphorylation in TPC2 KO sperm is significantly higher than that of WT sperm. Our data indicate that the higher levels of ATP in the TPC2 KO sperm could be a result of an increase in the activity of GDP2 which catalyses more G3P metabolism and processes it into greater energy in the form of ATP.

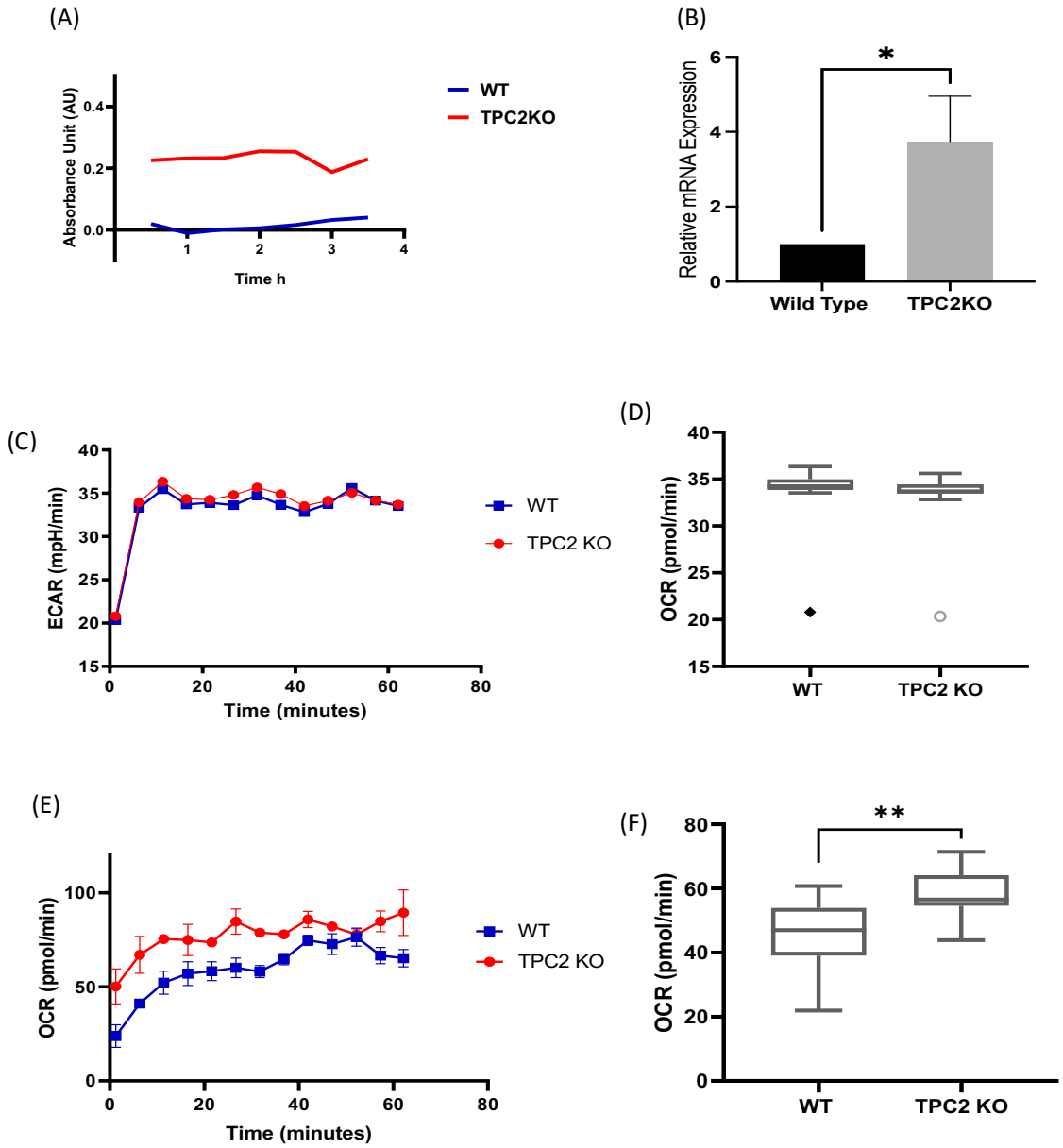


Figure 3-5: The metabolic rate of G3P and gene expression of GPD2 in WT and TPC2KO sperm.

(A) The utilization rate of G3P of the WT and TPC2KO sperm measured using redox dye. The oxidation of substrate was shown by the reduction of the dye and generation of colour as measured by microplate reader. (B) The expression of the GPD2 gene in the TPC2KO sperm was quantified relative to WT sperm. It is normalised to the expression of housekeeping gene (β-actin). (C) Extracellular acidification rate (ECAR) in the presence of 20 mM G3P for 1 hour evaluation. (D) The analysis of the mean ECAR of WT and TPC2 KO sperm over the time of assessment. (E) The oxygen consumption rate (OCR) of WT and TPC2 KO sperm in the presence of 20 mM G3P. (F) The analysis of the mean OCR of sperm during the experiment. Values are represented as average ± s.e.m. of 3 independent experiments. Asterisks show statistical significance where * $P < 0.05$; ** $P < 0.01$; *** $P < 0.001$, **** $P < 0.0001$ using unpaired Student's t-test.

3.3.6 Inhibition of TPC2 enhances GPD2 activity.

To pharmacologically validate the effect of loss of TPC2 functionality on the activity of GPD2 protein, both WT and TPC2 KO sperm were treated with 80 µM naringenin, which is a TPC2 inhibitor, and the redox reaction was assessed over 3 hours. The data show an elevation in the redox activity of GPD2 protein for the treated WT sperm compared to untreated sperm over the first 2 hours of the measurement (Figure 3-6 B) whereas after 2 hours of incubation treated and untreated WT sperm behave similarly. Figure 3-6 C shows the effect on the GPD2 activity of naringenin treatment in the WT sperm compared to the TPC2 KO sperm. Despite the fact that naringenin enhances the GPD2 activity in the WT sperm it has less effect on this parameter than in TPC2 KO sperm (Figure 3-6 C and D).

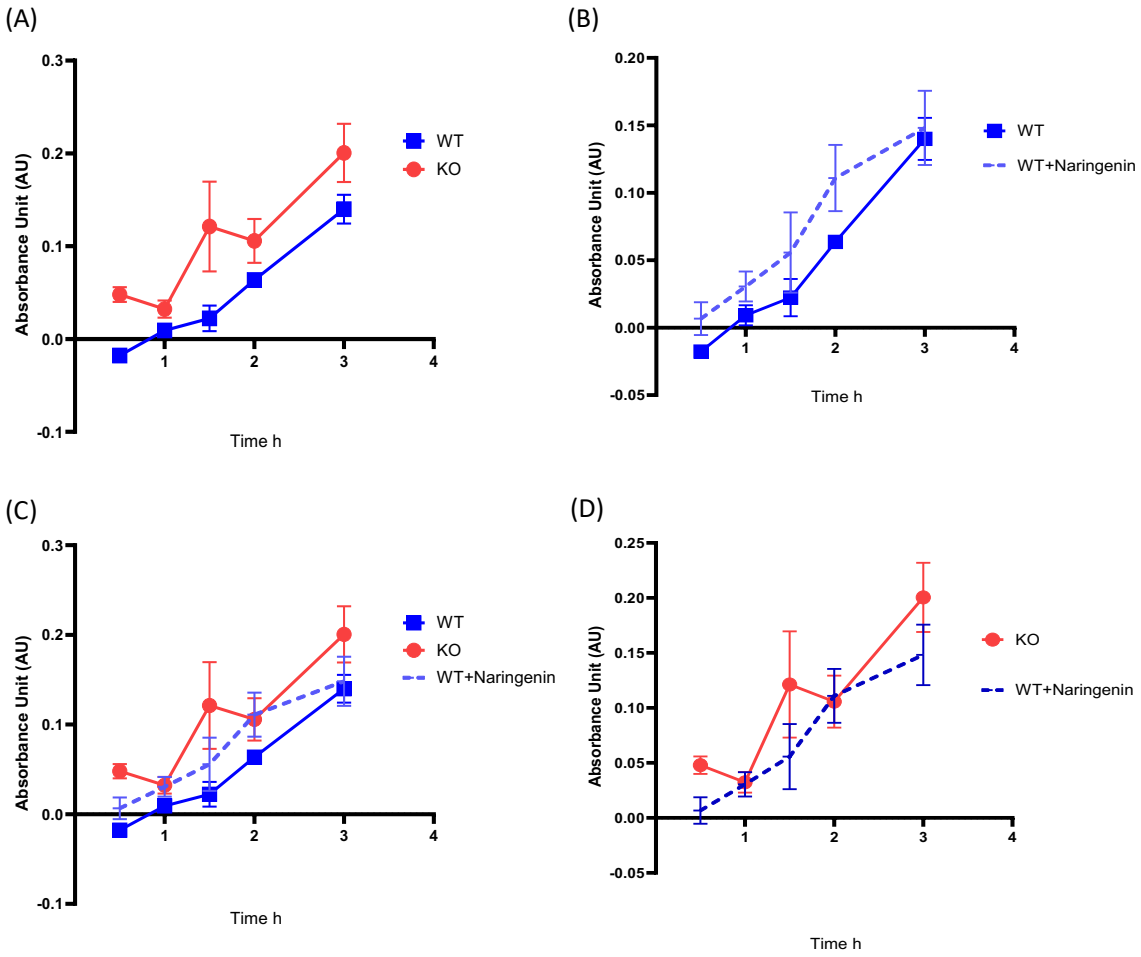


Figure 3-6: The effect of naringenin treatment on the GDP2 activity of the sperm in WT and TPC2 KO mice.

(A) the redox reaction of the sperm in the presence of 20 mM G3P of WT and TPC2 KO sperm for 3 hours measurement showing the colorimetric change every 30 minute interval. (B) the effect of 80 μM naringenin on the WT sperm. (C) and (D) the comparison between the redox reaction between WT and TPC2 KO with treated WT with naringenin. All data are presented as average ± s.e.m of three animals.

3.3.7 TPC2 KO may enhance GPD2 activity through PPARs.

To gain further insight into the molecular mechanism underlying the enhancement of GPD2 activity, which participates in the process of gluconeogenesis from glycerol (Madiraju et. al, 2014), I subsequently evaluated some genes that are involved in the regulation of lipid metabolism and that might possibly be regulating the activity of GPD2.

Peroxisome proliferator-activated receptors (PPARs) are nuclear receptor proteins that play a significant role in the regulation of fatty acid oxidation as well as glucose and lipid metabolism via modulation of the expression of genes that have a regulatory effect on energy homeostasis and metabolism (Montaigne, et. al, 2021). There are three isoforms of PPAR that have been identified and expressed in various tissues, which are PPARα, PPARβ/δ, and PPARγ. These isoforms have been investigated and well-studied in the male reproductive system and attributed roles in sperm motility enhancement, testis lipid metabolism which is vital for sex hormone production, and modification of lipid membrane composition (Mousavi et. al, 2019 and Duliban et. al, 2021). In addition, it has been reported that GPD2 is regulated by PPARα (Patsouris et al., 2004); consequently, the effect on GPD2 activity of pharmacologically activating PPARα in the WT and TPC2 KO sperm was assessed.

Figure 3-7 A and B illustrate the effect of activating PPARα on the activity of GPD2 in the WT and TPC2 KO sperm. The sperm of WT and TPC2 KO mice was treated with PPARα activator (50 mM Gemfibrozil); this increased the activity of GPD2 markedly in both WT and TPC2 KO sperm with $p < 0.01$ and $p < 0.0001$ respectively. In contrast, application of a PPARα inhibitor (20 μM GW6471) led to a reduction in the utilization of G3P in both WT and TPC2 KO sperm, but the inhibitory effect was only significant in the WT sperm.

I next showed that I could rescue the inhibition of GPD2 that resulted from the application of GW6471 by adding naringenin, with both WT and TPC2 KO sperm shows such an enhancement effect on GPD2 activity. However, the effect was more significant in the WT sperm, in line with the idea that GPD2 activity was already inhibited in the TPC2 KO sperm.

Since PPARα influences G3P utilization, the mRNA expression level of PPARα in WT and TPC2 KO sperm was evaluated. Our data showed that the level of expression of PPARα mRNA was significantly increased in the TPC2 KO sperm compared to the WT sperm with a $P < 0.01$ (Figure 3-7 C). The level of the increase in the PPARα mRNA in TPC2 KO sperm was double that in the WT sperm. It is possible that this nuclear gene contributes to the motility and metabolism enhancement in the TPC2 KO sperm.

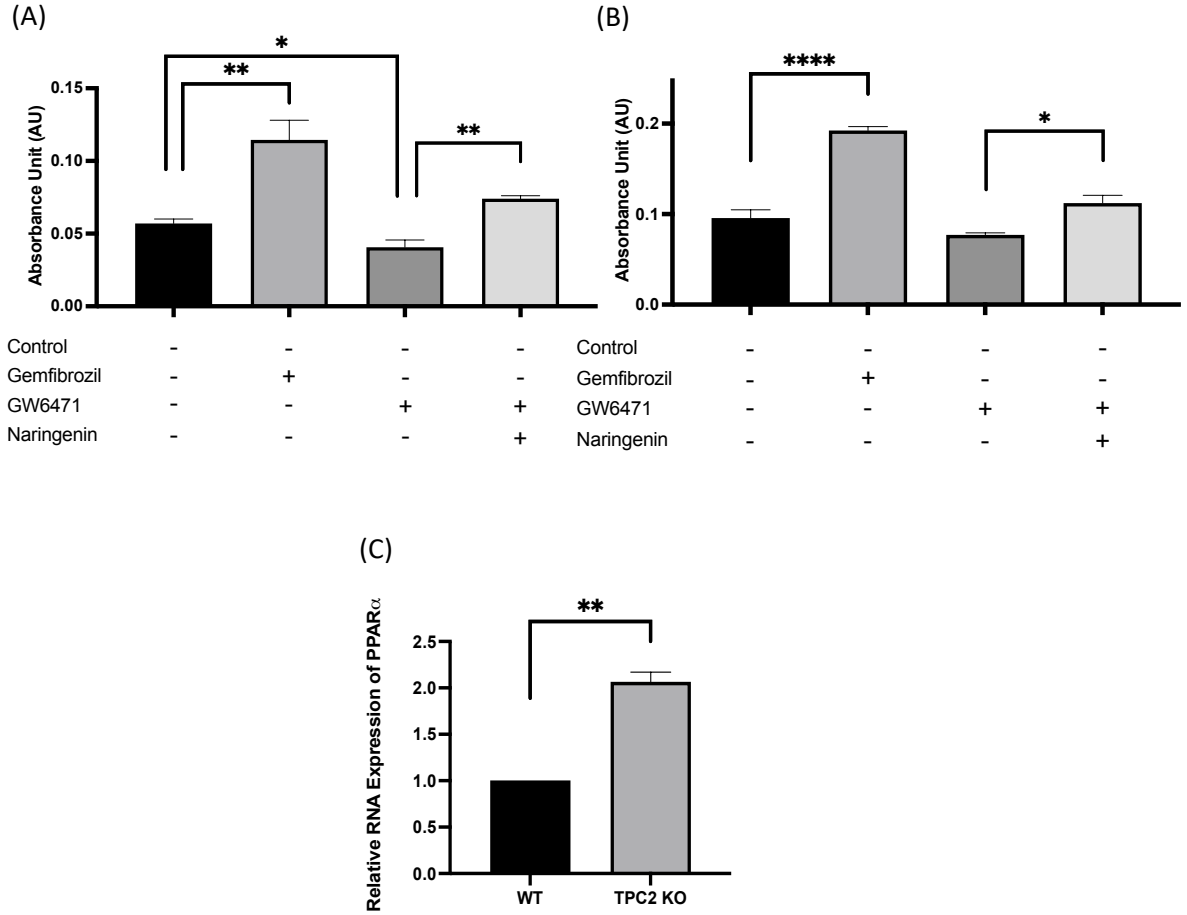


Figure 3-7: The effect of PPARα agonists and antagonists on GPD2 activity.

(A) The analysis of the utilization of glycerol 3 phosphate by WT sperm treated with 50 mM Gemfibrozil as PPARα activator, 20 μM GW6471 as a PPARα inhibitor, and 80 μM Naringenin as TPC2 inhibitor for 2 hours. (B) The analysis of the utilization of glycerol 3 phosphate by TPC2 KO sperm treated with 50 mM Gemfibrozil, 20 μM GW6471, and 80 μM Naringenin inhibitor for 2 hours. (C) The gene expression of PPARα of TPC2 KO sperm relatively to the WT which normalized to the β-actin as a housekeeping gene. The data are presented as average ± s.e.m of three animals. Asterisks show statistical significance where * $P < 0.05$; ** $P < 0.01$; *** $P < 0.001$, **** $P < 0.0001$ using ordinary one-way ANOVA test and unpaired Student's t-test.

3.4 Discussion

Sperm motility is a principal factor in the movement of the sperm to the fertilization site and in oocyte penetration. Sperm maturation is required for successful fertilization and several functional modifications occur in the sperm to accomplish this mission. The changing pattern of motility is one of the alterations that plays a fundamental role in the sperm's ability to reach and penetrate the oocyte. The sperm becomes more dynamic and requires an increased energy supply. ATP is the main cellular energy source that operates the flagellum motility machinery, and it is mainly produced via glycolysis and oxidative phosphorylation. Maintained cellular energy production is essential for sperm motility.

Changes in the concentration of intracellular Ca^{2+} play a major role in various physiological processes. Ca^{2+} can influx into the cell through the plasma membrane from external sources or increase in the cytoplasm via release from intracellular Ca^{2+} stores. TPC2 is a key regulator of Ca^{2+} release from endolysosomal compartments. It has been shown that TPC2 plays roles in cancer cell motility, and metabolism. Accordingly, this study set out to investigate the role of TPC2 in sperm motility and energy utilisation.

The motility of sperm is one of the factors that determines sperm health and their capacity for fertilization. My data showed that TPC2 KO sperm exhibit

enhanced kinetic properties compared to WT sperm. VCL, VAP, and VSL were significantly higher in the sperm of TPC2 KO mice during the incubation period while the other motility parameters showed no significant differences. It has been reported that VCL, LIN, and reduction in BCF are kinetic parameters that contribute to capacitation-induced sperm hyperactivation (Suarez, 2008; Cancel et al., 2000; Ooi et al., 2014). In addition, it has been shown that sperm that were incapable of being hyperactivated failed to penetrate the egg (Suarez and Dai 1992). My findings showed that the VCL was significantly higher in the TPC2 KO sperm and that the BCF was significantly reduced in such sperm after 0.5 hours of sperm swimming, suggesting that the disruption of TPC2 function could lead to improvements in sperm motility and hyperactivation.

The activation of sperm flagellar motility requires both the stimulation of energy metabolism and the activation of the motile machinery. ATP is the cellular energy source for flagellar movement with hydrolysis of ATP being used to power the motor of the axoneme acting against the microtubule and create flagellar movement (Miki et al., 2004). It has been reported that the velocity of sperm swimming is related to the sperm production rate of ATP and to the ATP content in the sperm (Fitzpatrick et al., 2009; Tourmente et al., 2015). Since glycolysis plays a major role in ATP production for flagellar movement, GAPDH plays a key role as a glycolysis rate limiting enzyme (Takei et al., 2014).

Additionally, genetic deletion of the GAPDH isomer leads to infertility which has been attributed to extremely low ATP levels and severe motility reduction (Miki et al., 2004). My findings show that ATP content and GAPDH activity of the TPC2 KO sperm is greater than that of the WT sperm which is consistent with the increased kinetic parameters of the TPC2 KO sperm. It seems likely that TPC2 KO sperm show more ability to maintain the energy source required for motility via glucose hydrolysis.

AMPK is a crucial regulatory protein that plays a major role in energy metabolism homeostasis. AMPK is part of a key signalling pathway involved in mammalian sperm motility (Martin-Hidalgo et al., 2018). Transgenic mice with depletion of the α1AMPK gene were used to study the effect of loss of AMPK function on sperm motility. The study showed a marked decrease in the sperm motility of AMPK KO mice compared to normal mice (Tartarin et al., 2012). It has also been shown that $CdCl_2$ decreases sperm motility via inhibition of AMPK. When I treated sperm with $CdCl_2$, I found a marked decrease in the total and progressive motility percentages of WT sperm compared to those of TPC2 KO sperm while the kinetic parameters showed a slightly negative effect which was consistent with the findings reported by Wang et al. about WT sperm in 2016. However, although the finding indicates a slight increase in VSL and VAP, these were not significant changes. It seems that $CdCl_2$ has more influence on WT sperm

compared to TPC2 KO sperm since the progressive motility of WT sperm showed a much greater decline than TPC2 KO sperm after treatment with this AMPK inhibitor. Although $CdCl_2$ is used to study the role of AMPK on sperm motility, other pharmacological AMPK activators such as A769662 and metformin have also been used to study AMPK role in sperm; such studies showed influences on sperm motility of these chemicals, but the findings remain controversial. Metformin enhanced sperm motility while A769662 led to a downregulation of motility in human and boar sperm (Zhu et al., 2018; Calle-Guisado et al., 2017). Moreover, some pollutants such as sulphur and ammonia enhance the protein level of AMPK but cause a decline in mouse sperm motility (Zhao et al., 2016). It seems therefore that the role of AMPK in sperm motility is still not clear.

Based on the total motility percentages, it has been shown that sperm are highly affected by the toxicity of the $CdCl_2$ and that this was due to the generation of more reactive oxygen species that induce cellular oxidative stress and cause cell death (Branca et al., 2020). TPC2KO sperm may therefore be more tolerant to oxidative stress, and this needs to be further investigated.

As I have also shown that ATP levels in sperm were greater in the absence of TPC2 protein, metabolic phenotyping could reveal the alternative metabolic pathway used to release energy in such sperm. My data shows that TPC2 KO

sperm utilize more G3P than WT sperm. This substrate is a glycerol precursor that is catalysed via GPD2, and it can either can feed glycolysis, or gluconeogenesis pathways via glycerol hydrolysis pathway (Berg et al., 2002; Blanco and Blanco, 2017; Madiraju et al., 2014). Additionally, the role of GPD2 in sperm function has been studied using GPD2 KO mice. GPD2 activity shows a correlation with sperm hyperactivation and tyrosine phosphorylation during capacitation. It has been reported that the percentage of hyperactivated sperm were lower for the GPD2KO sperm compared to WT controls (Kota et al., 2010). My findings showed that mRNA expression of the catalytic enzyme GPD2 is significantly enhanced in the TPC2 KO sperm which may contribute to the higher motility parameters of the TPC2 KO sperm. The increased ATP production, glycolysis rate, and enhanced mRNA expression of GPD2 provide clues as to the likely role of TPC2 in normal sperm hyperactivation, but the underlying mechanisms need to be ascertained.

PPARs are fundamental nuclear receptors that play a role in the regulation of fatty acid β-oxidation and lipid metabolism (Ament et al., 2012). Lipid metabolism is an essential feature of normal testis and sperm function to synthesise the sex hormones, maintain the energy required for sperm motility, and facilitate sperm membrane lipid composition modification during the

process of capacitation (Duliban et al., 2021; Jones, and Bubb 2000; Shan et al., 2021). PPARα is one of the three isotypes of PPARs which has a crucial role in the regulation of lipid metabolism. Moreover, overexpression of PPARα has a positive correlation with rapid sperm motility, VSL, VAP, VCL and LIN, and a negative correlation with slow motility, in ram sperm (Kadivar et al., 2016). It has been shown that GPD2 mRNA expression in hepatocytes was not affected in the fasting state in PPARα null mice, which could indicate that PPARα regulates the GPD2 activity (Patsouris et al., 2004). When I treated sperm with Gemfibrozil which is a PPARα agonist, and then measured the redox reaction of the sperm in the presence of G3P, I observed a significant increase in both WT and TPC2 KO sperm with more effect in the TPC2 KO sperm suggesting that the effect is augmented in the TPC2 KO sperm. The data show a consistency with the findings of Patsouris et al. (2004) who showed that cells treated with Wy14643 which is a PPARα agonist, led to an increase in the expression level of GPD2 mRNA. In addition, I found that application of the PPARα antagonist GW6471 led to a reduction in G3P utilization in the WT and TPC2 KO sperm which indicates that PPARα is required for the activity of GPD2. The data confirm the indispensable role of PPARα for GPD2 activity.

TPC2 KO leads to an overexpression of PPARα which could explain the enhancement of GPD2 activity in TPC2 KO sperm. To test the hypothesis that TPC2 may directly regulate PPARα expression, WT sperm were treated with naringenin, and this led to an enhancement in G3P utilization compared to untreated sperm which suggests that TPC2 has an influence on PPARα. When the sperm treated with GW6471 were rescued with naringenin, there was an improvement in the GPD2 activity in both WT and TPC2 KO sperm but this was less significant in the TPC2 KO sperm compared to the WT sperm, which could indicate that the effect was partially a consequence of affecting TPC2 activity. The increase in the activity of GPD2 in the TPC2 KO sperm suggests that naringenin may also have TPC2-independent effects on PPARα and this is in line with a previous observation that naringenin induces the overexpression of PPARα in a dose dependant manner in human hepatic cells and cardiomyocytes (Goldwasser et. al, 2010 and Zhang et. al, 2019).

3.5 Conclusion

Sperm motility plays an essential role in male fertility. Maintenance of sufficient intracellular energy production is necessary to power the motility of the sperm and allow it to fertilize the oocyte. My data indicate that the disruption of TPC2 leads to a modification of energy metabolism in a way that enhances sperm

motility parameters. The data show an enhancement in the activity of GPD2 in the TPC2 KO sperm that leads to an improvement in the energy production which is regulated via PPARα. The exact nature of the molecular mechanism of TPC2 signalling that underlies the regulation of sperm motility remains to be fully ascertained. Understanding the role of TPC2 in sperm motility could lead to the development of new therapeutic approaches to treat male infertility.

Chapter 4

Potential molecular mechanism for TPC2 KO sperm underlying the metabolism enhancement.

4.1 Introduction

Mitochondria are significant and unique organelles, and current studies are revealing new ways in which they contribute to cellular processes. Mitochondria are known to be essential for sperm cells, but their exact roles and functions appear to be complicated. These organelles participate in numerous cellular functions. Apart from ATP production, other processes include calcium homoeostasis, reactive oxygen species (ROS) creation, the intrinsic apoptotic pathway, and steroid hormone biosynthesis (Dumollard et al., 2004; Marchetti et al., 2002; Stocco and McPhaul, 2006). Although sperm motility is a fundamental requirement for a successful fertilization, mitochondrial function is not only necessary for fuelling the sperm with energy for flagellar movement, it also plays a role in hyperactivation, the acrosome reaction, and fertilization (Barbagallo et al., 2020 and Giaccagli et al., 2021). Recent studies of sperm physiology have linked mitochondrial function and activity with the sperm's health and fertility. Dysfunction in the sperm mitochondria is involved in pathogenesis of sperm oxidative stress which could be fatal to the sperm and lead to male infertility (Amaral et al., 2013). Mitochondrial activity also seems to play a key role in sperm becoming competent to fertilize the egg.

Peroxisome proliferator-activated receptor γ coactivator 1α (PGC1 α) is a transcriptional coactivator that plays a critical role in the regulation of

mitochondrial biogenesis and function. PGC1 α is involved in the regulation of energy metabolism, oxidative stress, and mitochondrial biogenesis (Fernandez-Marcos and Auwerx, 2011). The importance of PGC1α in mitochondrial function has been demonstrated in numerous studies, and its dysregulation has been associated with various diseases, including neurodegenerative disorders, metabolic disorders, and cancer (Zolezzi et al., 2017; Rowe et al., 2010; Wu et al., 2016). It has been suggested that PGC1α has a regulatory effect on nuclear respiratory factor 1 (NRF-1) and mitochondrial transcription factor A (mTFA) which are responsible for mitochondrial activity and biogenesis (Puigserver and Spiegelman, 2003). Furthermore, PGC1α has been shown to be involved in the regulation of other factors that impact on sperm function, such as the antioxidant defence system. This suggests that PGC1α may play a critical role in the maintenance of sperm function and fertility (Rius-Pérez et al., 2020; Wagner et al., 2018).

PGC1α gene expression regulation is complex. It has been suggested that PGC1α is regulated by Ca^{2+} through both calcineurin and the calcium/calmodulin-dependent protein kinase (CaMK) signalling pathway in skeletal muscle (Kusuhara et al., 2007). CaMK triggers the phosphorylation of cAMP-response element binding protein (CREB). This can activate PGC1α which has a binding

site for CREB in its gene promoter suggesting that Ca^{+2} induces CaMK phosphorylation and CREB activation and induces PGC1α gene expression (Herzig et al., 2001).

AMPK is another regulator which is a key element in energy homeostasis and mitochondrial function. It has been shown that the activity of PGC1α is mediated via AMPK which phosphorylates PGC1α and induces its activity (Jager et al., 2007).

It has been revealed that the insulin signalling pathway plays an important role in the regulation of mitochondrial activity via PGC1α in the myocytes which stimulates AKT phosphorylation (Pagel-Langenickel et al., 2008). Southgate et al., (2005) demonstrated that AKT affects the expression of PGC1α via phosphorylation of FoxO1 through the insulin pathway. Hence, AKT activity plays a significant role in PGC1α regulation.

Recently, it has been shown that there is an interaction between TPC2 and Mammalian Target of Rapamycin (mTOR) activity in autophagy regulation in response to changes in intracellular ATP (Cang et al., 2013). In addition, several investigations have demonstrated the complex interaction between the PI_3K/AKT/mTOR pathway and various cellular functions such as autophagy, metabolism, proliferation, and cell cycle regulation. Taken together, it is possible

that TPC2 could affect sperm mitochondrial function and biogenesis through modulating the activity of PGC1α.

4.2 Aims of this chapter

To study the mitochondrial activity and biogenesis of WT and TPC2 KO sperm and understand the role of TPC2 as a regulator of mitochondrial activity.

4.2.1 Results

4.2.2 TPC2 KO sperm have enhanced mitochondrial oxidation phosphorylation.

As ATP, the cellular energy source, is produced in the sperm via both glycolysis and oxidative phosphorylation in the mitochondria, and our data as shown in Figure 4-1 A demonstrates an increases in overall intracellular sperm ATP in TPC2 KO sperm compared to WT controls, I studied the sperm metabolic profile using a Seahorse analyser to evaluate the sperm ECAR, which reflects the rate of glycolysis, and OCR which reflects the energy produced by the mitochondria, in both WT and TPC2 KO sperm, in order to gain an insight into the energy production pattern and investigate potential molecular mechanisms.

The rate of glycolysis in the sperm was no different between WT and TPC2 KO sperm during 1 hour of evaluation of ECAR, as shown in Figures 4-1 A and C, which shows the ECAR at each time point of evaluation and the mean of glycolysis rate during the assay, respectively. Simultaneously, the mitochondrial respiration rate was also assessed by measuring the OCR every 5 min for 1 hour. Figure 4-1 B illustrates the OCR of sperm at each time point while Figure 4-1 D demonstrates the mean of the OCR of the sperm over 1 hour. The oxidative phosphorylation rate of TPC2 KO sperm was found to be greater than that of WT sperm, with a P value < 0.05. It therefore seems that the mitochondrial activity

of the TPC2 KO sperm is considerably more active than that of the WT sperm, and this needs to be further investigated.

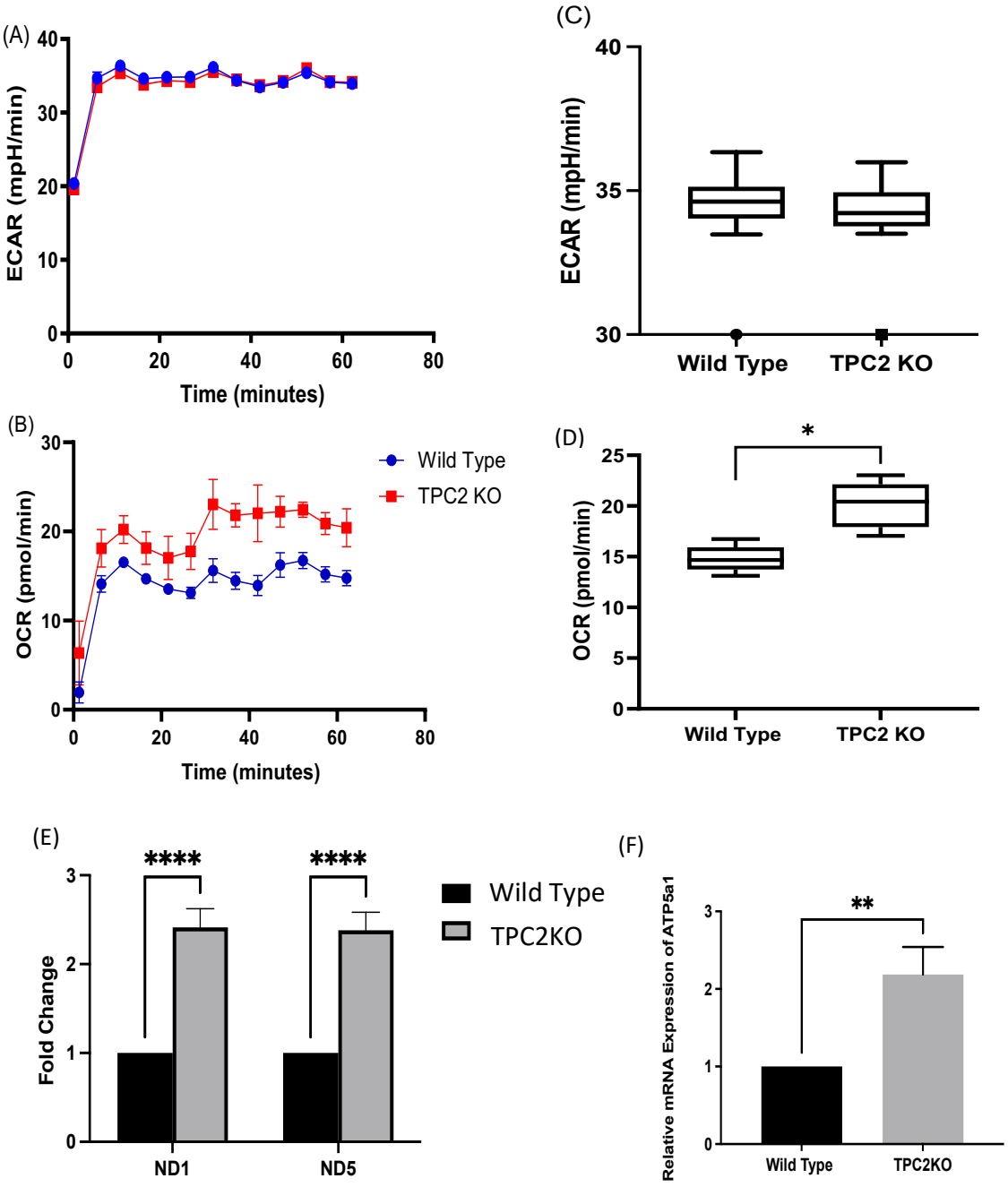


Figure 4-1: The metabolic profile and expression of markers of mitochondrial activity of WT and TPC2 KO sperm.

(A and C) Analysis of the extracellular acidification rate (ECAR) in WT and TPC2 KO sperm which reflects the glycolysis rate. (B and D) The oxygen consumption rate (OCR) in WT and TPC2 KO sperm which reflects the oxidative phosphorylation activity of cells. (E-F) The expression level of ND1, ND2, and ATP5a1 genes in the TPC2KO sperm were quantified relative to WT sperm and normalised to the expression of a housekeeping gene (β-actin). Data are represented as average ± s.e.m. of 3 independent experiments. Asterisks show statistical significance where * $P < 0.05$; ** $P < 0.01$; *** $P < 0.001$, **** $P < 0.0001$ using unpaired Student's t-test.

We examined the mRNA levels of some mitochondrial markers that are involved in mitochondrial ATP production such as those involved in the respiratory electron transport chain and proton pumping system. These markers are ATP synthase (ATP5a1), and NADH-ubiquinone oxidoreductase chain 1 and 5 (ND1 and ND5) genes. ATP5a1 is a subunit of the mitochondrial ATP synthase that catalyses ATP synthesis, known as complex V. It generates ATP from ADP in the presence of a proton gradient across the membrane created by the electron transport chain of respiratory complexes (Cadonic et al., 2016). ND1 and ND5 code for NADH-ubiquinone oxidoreductase chain 1 and 5 proteins which are subunits of complex 1 that dehydrogenates NADH to form NAD^+ and produces the hydrogen ions that are pumped out into the mitochondrial intramembrane space (Yusnita et al., 2010; Urra et al., 2017). It also transfers the electrons generated from NADH oxidization to coenzyme Q. The data in Figures 4-1 E and F show the levels of ND1, ND5, and ATP5a1 mRNAs in WT and TPC2 KO sperm. The data show that there is a substantial increase in the mRNA levels of ND1 and ND5 in TPC2 KO sperm compared to that in WT sperm with a $p < 0.0001$. Additionally, the level of the ATP5a1 mRNA is also substantially higher in the TPC2 KO sperm than in the WT sperm with a $p < 0.01$ (Figure 4-1 F).

4.2.3 The mitochondrial membrane potential is greater in TPC2 KO sperm than in WT sperm.

The mitochondrial membrane potential $\Delta\Psi m$ is considered to be a key indicator of mitochondrial activity (Lee et al., 2019). It reflects the processes of electron transport and oxidative phosphorylation which drive the production of ATP. The $\Delta\Psi m$ is generated when the mitochondrial complexes I, III, and IV pump out protons from the mitochondrial matrix into the intermembrane space so that the proton gradient between these two compartments is increased and the intermembrane space becomes more positively charged (Zorova et al., 2018). This difference in the proton concentration drives proton re-entry into the matrix through the ATP synthase (complex V) and this generates ATP in the presence of ADP (Vedel et al., 1999).

I used JC-1 fluorescent dye, which is a lipophilic and cationic dye, as an indicator of the $\Delta\Psi m$. It generally produces a green fluorescence when it is excited. However, when JC-1 enters the mitochondria where there is a negative charge, it accumulates and forms a fluorescent J aggregate that emits a red fluorescence. When there is a low membrane potential or apoptosis in the mitochondria, the dye still passes to the mitochondria and is unable to form a sufficient concentration of J aggregate to generate the red fluorescence, and instead it exhibits the normal green fluorescence. Hence, the ratio of red to green fluorescence of the dye in the mitochondria can be regarded as a direct

evaluation of the status of mitochondrial polarisation, with the greater the red shift of the dye, the higher the $\Delta\Psi m$ (Sivandzade et al., 2019).

The data shows a comparison of the $\Delta\Psi m$ between WT and TPC2 KO sperm after 60 and 90 min of sperm swimming. The fluorescent microplate reader results reveal that the ratio of red to green fluorescence which indicates the $\Delta\Psi m$, is significantly higher in the TPC2 KO sperm compared to the WT with a $p < 0.01$ at two points of measurements (Figure 4-2 A). Moreover, the fluorescence microscopic evaluation shows that the TPC2 KO sperm exhibit more red fluorescence than WT controls, showing that there is more J aggregate formed which indicates more negative charge in the TPC2 KO sperm mitochondria. The green fluorescence of the WT sperm is greater compared to the TPC2 KO which means the mitochondria of WT sperm have a lesser degree of polarization since the dye generated its originally green fluorescence (Figure 4-2 B). The ratio of red to green fluorescence in the microscopic data shows that this is considerably higher in the TPC2 KO sperm than in the WT sperm (Figure 4-2 C), which to some degree is consistent with the fluorescent microplate reader data.

Next, sperm were treated with 80 μM naringenin to confirm that the enhancement of mitochondrial membrane potential is related to the loss of TPC2 function. The analysis of the fluorescence data shows there is a significant increase in the ratio of the fluorescence in the WT sperm that were treated with

naringenin with a $P < 0.05$ while there is no significant difference in the fluorescence ratio in the treated TPC2 KO sperm, or between the treated WT sperm and the untreated TPC2 KO sperm, which suggests that the enhancement of $\Delta\Psi m$ in the TPC2 KO sperm is directly related to loss of TC2 function (Figure 4-2 D).

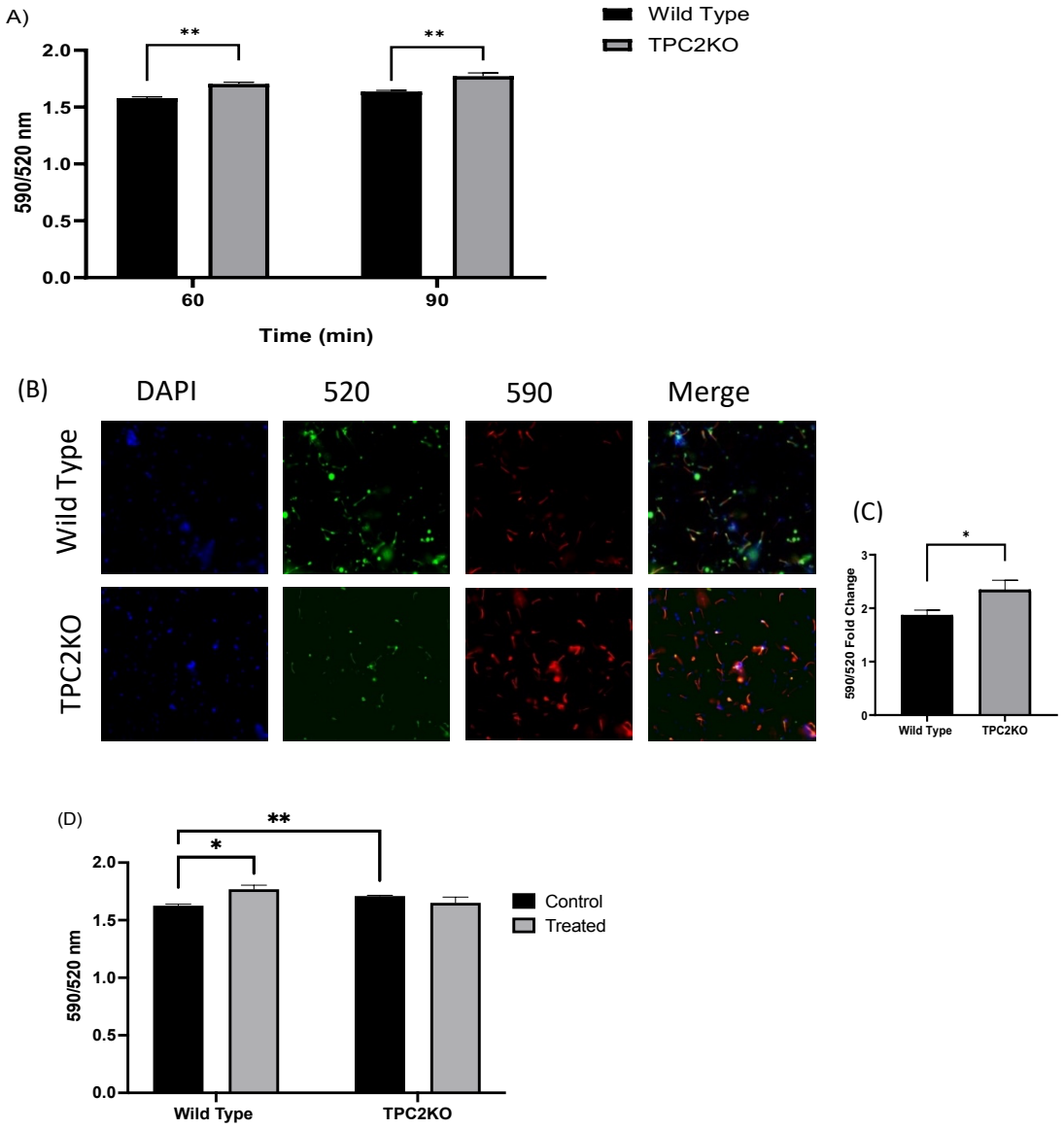


Figure 4-2: The mitochondrial membrane potential of WT and TPC2 KO sperm.

(A) The analysis of the JC-1 dye ratio used for $\Delta\Psi m$ assessment of WT and TPC2 KO sperm that was measured with a microplate reader at emission wavelength 590 nm and 520 nm 30 and 60 min after incubation with non-capacitated media. (B) JC-1 staining of live WT and TPC2 KO sperm immobilized on a pre-treated microscopic slide with 0.5 mg/ml concanavalin A and imaged with an EVOS FL Auto Cell Imaging System fluorescent microscope using RFP and GFP channels. (C) The analysis of red to green dye of TPC2 KO sperm relative to WT controls using Image Studio™ Lite Quantification software, Li-Core Bioscience. (D) The analysis of JC-1 dye ratio of WT and TPC2 KO sperm treated with 80 μM naringenin for 30 min using FLUOstar Omega, BMG LABTECH fluorescent microplate reader. The data are presented as average ± s.e.m of three animals. Asterisks show statistical significance where * $P < 0.05$; ** $P < 0.01$; *** $P < 0.001$, **** $P < 0.0001$ using Tukey two-way ANOVA test and unpaired Student's t-test.

4.2.4 Interfering with TPC2 may enhance cellular protection from oxidative damage.

Reactive oxygen species (ROS) are a natural by-product of cellular oxidative metabolism and NADPH oxidation and are a source of oxidative stress. Various cellular processes such as protein phosphorylation, transcription factors, inflammation, metabolism, and cell survival are regulated by cellular ROS levels (Pizzino et al., 2017). ROS have both a physiological and a pathological effect on male reproduction. At the physiological level, they play a key role in the processes of sperm maturation, capacitation, the acrosome reaction, and fertilization (O'Flaherty et al., 2006; de Lamirande et al., 1998). Conversely, when ROS accumulates due to overwhelming antioxidant effects, they can be harmful to the cellular structure and to proteins, lipids, and nucleic acids, and they can cause damage which develops from the oxidative stress (Tremellen, 2008). As ROS are generated during the mitochondrial oxidative metabolism and other mitochondrial processes and signalling, they could reflect the degree of mitochondrial biogenesis; accordingly, the ROS levels of WT and TPC2 KO sperm were evaluated.

The overall cellular ROS was assessed in WT and TPC2 KO sperm 30 min after sperm isolation. The data show a significant reduction in the ROS level of TPC2 KO sperm compared to WT sperm with a $p < 0.01$ (Figure 4-3 A). The reduction

in ROS is observed in the sperm following the knocking out of the TPC2 gene, so naringenin which is a TPC2 inhibitor was used to pharmacologically mimic the effect of the absent gene and confirm the phenotype. Both WT and TPC2 KO sperm were treated with 80 μM naringenin. Figure 4-3 B shows that there was a reduction in the ROS of the WT sperm following the exposure to the naringenin whereas there was no such effect on the TPC2 KO sperm and no differences between the mean ROS levels of treated WT and non-treated TPC2 KO sperm.

The reduction in the ROS levels could be either due to a decrease in the production of free radicals or to an ability of the cells to elicit the defence mechanism against the ROS via antioxidant enzymes. Several antioxidant enzymes, such as catalase, superoxide dismutase, and glutathione reductase, are involved in the ROS defence system in the sperm and seminal fluid (Papas et. al, 2019). Superoxide dismutase is one of the antioxidants that is highly activated in human sperm and seminal fluid (Peeker et. al, 1997). Moreover, it is highly expressed in the mouse testis compared to catalase and glutathione reductase based on the NCBI Gene Database which shows that there are three forms of genes coding for superoxide dismutase. These are the soluble superoxide dismutase (SOD1), the mitochondrial version (SOD2), and the extracellular one (SOD3). Accordingly, the mRNA expression levels of cellular

SOD1 and SOD2 were examined in the WT and TPC2 KO sperm to evaluate their expression levels. The data reveal that the expression level of SOD1 is almost three times as high in the TPC2 KO sperm relative to the expression in WT sperm with a $P < 0.01$ Figure 4-3 C. Similarly, the same enhancement was found for the SOD2 mRNA levels in the TPC2 KO sperm compared to WT sperm with a $P < 0.05$ (Figure 4-3 D).

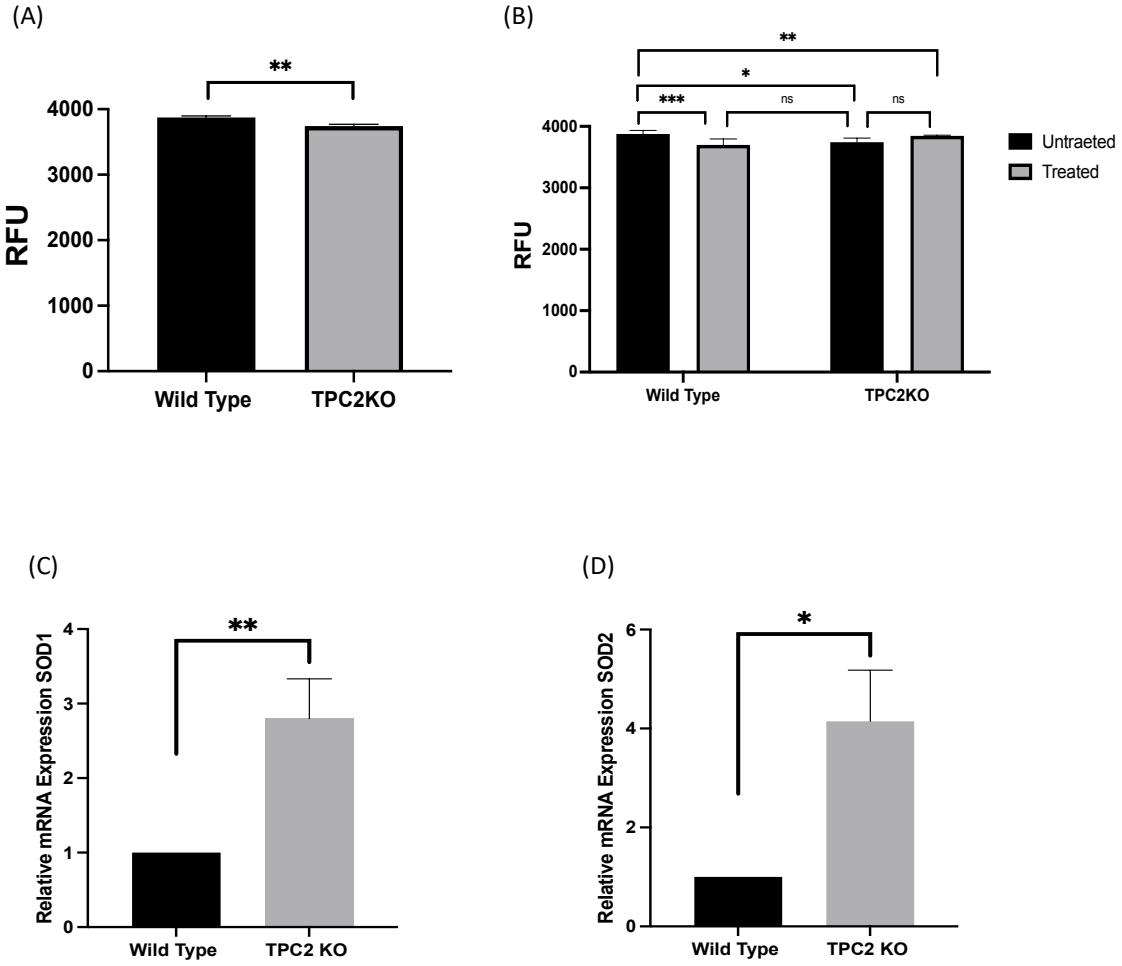


Figure 4-3: ROS generation in the sperm of WT and TPC2 KO mice.

(A) The analysis of ROS generated from WT and TPC2 KO sperm incubated with 10 μM DCFDA / H_2DCFDA for 30 min using a fluorescent microplate reader that excited at 485 nm with the reading acquired at 535 nm. (B) The analysis of ROS generated from WT and TPC2 KO sperm treated with 80 μM naringenin for 30 min. (C and D) The relative gene expression of SOD1 and SOD2 of TPC2 KO sperm compared to WT controls and normalized to β-actin as the housekeeping gene. The data are presented as average ± s.e.m of three animals. Asterisks show statistical significance where * $P < 0.05$; ** $P < 0.01$; *** $P < 0.001$, **** $P < 0.0001$ using Tukey two-way ANOVA test and unpaired Student's t-test.

4.2.5 TPC2 KO sperm induces mitochondrial biogenesis and oxidative phosphorylation via activation of the PGC-1α pathway.

PGC-1α interacts with various transcriptional factors that are involved in mitochondrial biogenesis and metabolism. To explore the mechanistic basis of the enhancement of the mitochondrial activity following loss of TPC2 function, I evaluated the transcriptional and protein expression level of mitochondrial biogenesis related molecules such as PGC-1α and its downstream target mTFA in WT and TPC2 KO sperm. Quantitative RT-PCR analysis shows there is a significant up regulation of expression of the genes PGC-1α and mTFA that are associated with mitochondrial biogenesis, in the TPC2 KO sperm compared to WT sperm with a $P < 0.05$ (Figures 4-4 B and C). Similarly, the protein of PGC-1α and mTFA is enhanced in the TPC2 KO sperm with a P value < 0.05 and < 0.001 respectively (Figures 4-4 F and G). It has been reported that PGC-1α is activated via Sirt-1 which interacts and deacetylates the PGC-1α that enhances and promotes mitochondrial activity and maintains its function (Lagouge et. al, 2006). Since the upstream regulator of PGC-1α is Sirt1, the Sirt-1 mRNA level and protein expression level were measured in WT and TPC2 KO sperm. Our data analysis shows an increase in the transcriptional expression level of Sirt 1 in the TPC2 KO sperm with $P < 0.05$ compared to WT controls (Figure 4-4 C). The

expression level of Sirt1 protein was also significantly increased in the TPC2 KO sperm by almost 50 % compared to that in WT sperm with a P value < 0.05 (Figure 4-4 E).

I also pharmacologically inhibited TPC2 by application of 80 μM naringenin to investigate if this mimicked the effect of TPC2 KO on PGC-1α, sirt1, and mTFA protein expression, thereby independently confirming the involvement of TPC2 loss in this. Analysis of the levels of PGC-1α, Sirt1, and mTFA protein after the treatment showed these to be dramatically elevated in both WT and TPC2 KO sperm compared to the non treated sperm (Figures 4-5 B – D). However, the data showed no significant differences in the mean of the protein levels in the treated TPC2 KO sperm compared to the WT sperm.

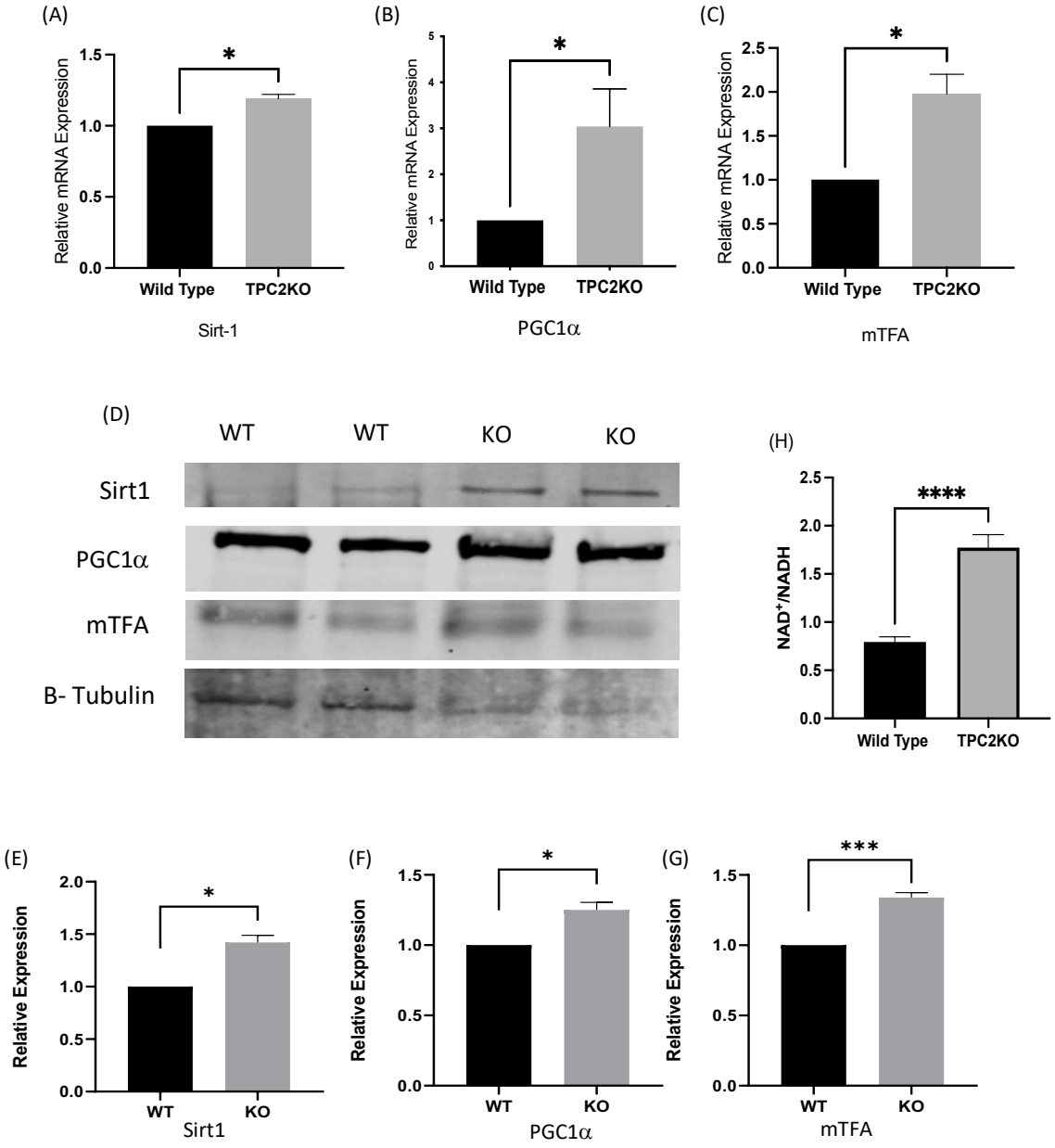


Figure 4-4: TPC2 KO sperm enhances the mitochondrial activity.

(A-C) The relative gene expression of Sirt1, PGC1α and SOD2 of TPC2 KO sperm compared to WT controls and normalized to β-actin as the housekeeping gene. (D) The protein expression of Sirt1, PGC1α, and mTFA of WT and TPC2 KO sperm normalized to β-tubulin. (E-G) The analysis by western blot of Sirt1, PGC1α, and mTFA of WT and TPC2 KO sperm, normalized to β-tubulin protein expression. (H) The ratio of NAD^+/NADH of WT and TPC2 KO sperm using 15 x 10^6 cell density. The data are presented as average ± s.e.m of 3 animals. Asterisks show statistical significance where * P < 0.05; ** P < 0.01; *** P < 0.001, **** P < 0.0001 using unpaired Student's t-test.

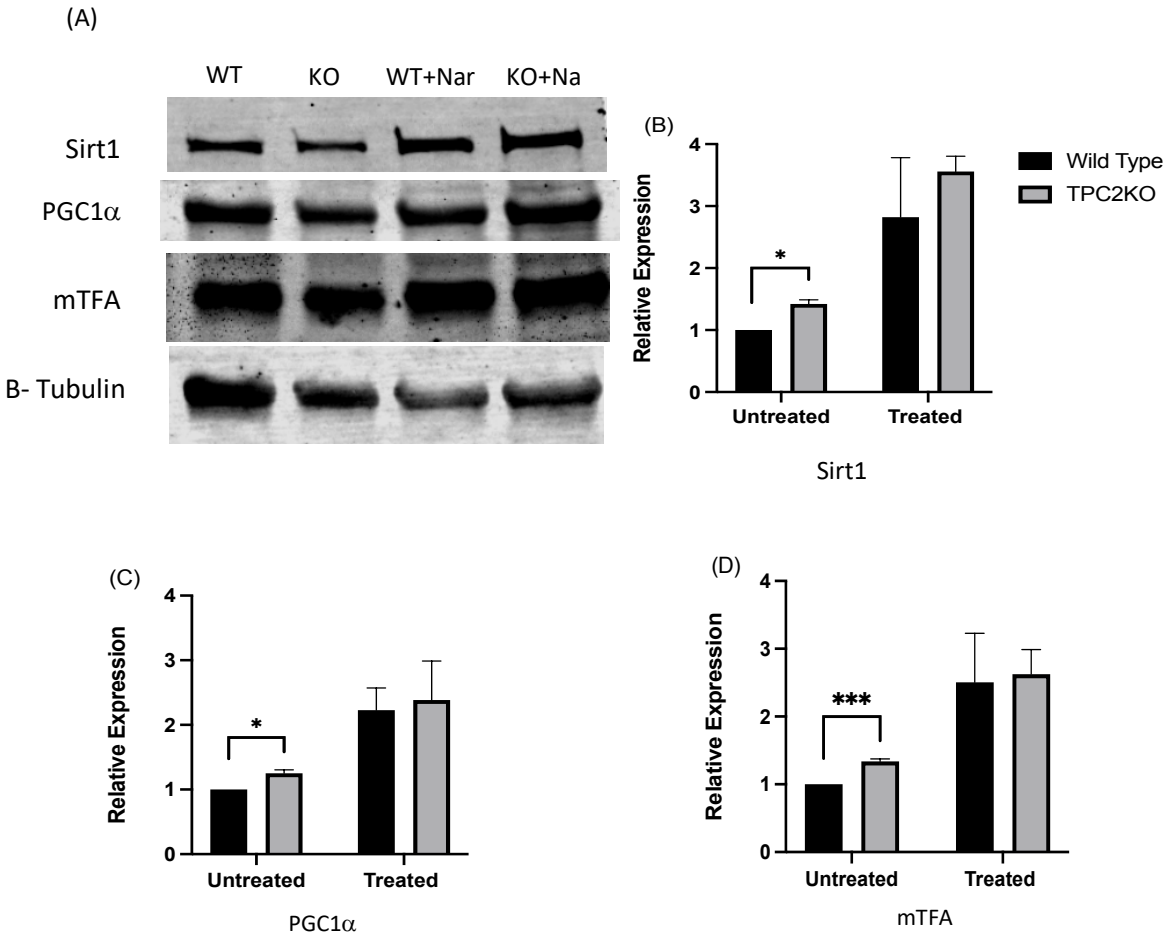


Figure 4-5: The effect of TPC2 inhibitor on proteins involved in mitochondrial function in WT and TPC2 KO sperm.

(A) The protein expression of Sirt1, PGC1α, and mTFA of WT and TPC2 KO sperm treated with 80 μM naringenin normalized to β-tubulin. (E-G) The analysis by western blot of Sirt1, PGC1α, and mTFA of WT and TPC2 KO sperm treated with 80 μM naringenin, normalized to β-tubulin protein expression. The data are presented as average ± s.e.m of 3 animals. Asterisks show statistical significance where * $P < 0.05$; ** $P < 0.01$; *** $P < 0.001$, **** $P < 0.0001$ using unpaired Student's t-test.

4.3 Discussion

The mitochondrion is a cellular organelle known as the powerhouse of the cell, which is responsible for generating the ATP for various cellular functions, through oxidative phosphorylation. It can play a fundamental role in Ca^{2+} homeostasis, ROS generation for other cellular functions, involvement in the cellular apoptosis pathway, and biosynthesis of some hormones. Particularly, in the sperm, these contributions are vital for sperm motility, hyperactivation, capacitation, the acrosome reaction, and even for the fertilization process.

Mitochondrial metabolism can determine the functional status of the sperm's condition. It has been reported that reduction in the ΔΨm, which reflects mitochondrial health status and function, is an early step in sperm apoptosis prior to other signs such as ROS generation, DNA fragmentation, and membrane permeability (Marchetti et al., 2002). Furthermore, Giaccagli et al., (2021) demonstrates that the sperm mitochondrial activity is essential for a successful fertilization. When the sperm were treated with CCCP, this reduced the sperm hyperactivation in a dose dependant pattern. Additionally, the *in vitro* fertilization rate was significantly reduced in sperm that had been treated with a mitochondrial uncoupling agent indicating the fundamentality of the mitochondria in sperm function.

The TPC2 depleted sperm displayed an increase in the OCR measured using a Sea Horse analyser which suggests an enhanced capacity of oxidative phosphorylation to generate more ATP than in WT sperm. The results demonstrate no differences between the WT and TPC2 deficient sperm in the ECAR which is compatible with the ATP production shown in Figure 3-3 A. Additionally, the transcriptional expression of the mitochondrial markers ND1 and 2, and ATP51a, which are subunits of the mitochondrial complexes I and V respectively, shows a significant elevation in the TPC2 KO sperm that could play a pivotal role in mitochondrial complexes' biogenesis. Iommarini et al., (2018) demonstrated that ablation of ND-1 reduced mitochondrial respiration while the abundance of ND-1 induced respiration which is in line with the transcriptional data for the ND1 gene. The results suggest an enhancement in the energy of TPC2 KO sperm through cellular oxidative phosphorylation.

The JC-1 assay is another approach used to evaluate the mitochondrial membrane potential that reflects the health and activity of mitochondria and their ability to generate an electrochemical gradient via the mitochondrial electron transport chain. This electrochemical gradient is essential for ATP generation by H^+ in the inner mitochondrial membrane space being pumped into

the mitochondrial matrix to produce ATP (Zorova et al., 2018). The ΔΨm of TPC2 KO sperm is elevated indicating that the oxidative phosphorylation activity is higher in the depleted TPC2 sperm. The proton is passed through complex V and leads to ATP generation resulting from ADP phosphorylation in the mitochondrial matrix (Cadonic et al., 2016). The abundance of transcriptional expression of ATP51a is also in line with the energy produced in the TPC2 KO sperm being due to enhanced oxidative phosphorylation in comparison with the WT sperm. Overall, the ΔΨm assay supports there being higher mitochondrial activity in TPC2 KO sperm.

Mitochondrial respiration is one of the major ROS generation sources resulting from the ETC during oxidative phosphorylation. It has been estimated that 90 % of the ROS are produced in the mitochondria (Balaban et al., 2005). Since the deficient TPC2 cells demonstrate a greater mitochondrial activity compared to the WT sperm, it might be anticipated that the TPC2 KO sperm have an elevation in ROS production. Interestingly, the level of ROS in the TPC2 null sperm was less than that in the WT sperm. TPC2 KO sperm display an increase in the relative mRNA expression levels of SOD1 and SOD2 which protect the mammalian sperm from the harmful effect of ROS (Perumal, 2014). This elevation in the antioxidant

enzymes in the deficient TPC2 sperm could be attributed to the reduction in ROS generation.

Since naringenin inhibits TPC2 activity, further pharmacological analysis was used to investigate whether the elevation of mitochondrial activity and reduction of generated ROS was due to a loss of TPC2 activity. Naringenin markedly enhances the ΔΨm of the WT sperm which is compatible with Wang et al.'s finding (2017), while the TPC2 KO sperm display no significant effect between the treated and non-treated sperm. Furthermore, the level of generated ROS of WT cells in the presence of naringenin is noticeably reduced whereas the ROS level was not changed in the TPC2 KO sperm after naringenin treatment. The naringenin treatment did not affect the ΔΨm and the ROS generation in the TPC2 KO sperm; instead, a change was found only in the WT sperm that could be due to an increase in the expression of SOD1 and SOD2 via naringenin upregulating the antioxidant expression level (Li et al., 2020). It seems that the improvement of the mitochondrial activity and ROS scavenging reaction can be attributed to the impairment of TPC2 activity.

The findings suggest that disruption of TPC2 can enhance mitochondrial activity and biogenesis in sperm, potentially via the PGC1α pathway. PGC1α is known to

be a master regulator of mitochondrial biogenesis. The results show an elevation in the mRNA and the protein level of PGC1α in the TPC2 KO sperm which is consistent with the observed enhancement of the mitochondrial activity of TPC2 KO sperm. mTFA protein, one of the downstream effectors of the PGC1α pathway, which is involved in mtDNA transcription, repair, and replication is regulated via PGC1α (Picca and Lezza, 2015). It displays an upregulation at the mRNA and protein levels in the TPC2 KO sperm. In addition, the pharmacological impairment of the TPC2 activity leads to a similar effect on the protein levels of the mitochondrial regulators supporting the idea that interfering with TPC2 activity enhances the mitochondrial function.

The potential regulator that enhances the PGC1α effect in the deficient TPC2 sperm could be the AKT protein. Hepatic cell metabolism is directly inhibited via AKT activation through inhibition of PGC1α that indicates AKT has a key role in regulating PGC1α activity (Li et al., 2007). Lin et. al, (2015) showed a reduction in the AKT activity in the skeletal muscle of TPC2 KO mice. Additionally, the phosphorylation of AKT is inhibited in the presence of the NAADP signalling pathway inhibitor Ned-19 suggesting that local Ca^{2+} released via TPC2 is essential for AKT activity (Favia et al., 2014). Naringenin, which inhibits TPC2 has also been shown to inhibit the PI3K/AKT pathway in prostate and ovarian cancers and may act through inhibition of TPC2 supporting the idea that impairment of TPC2

affects the activity of AKT (Lim et al., 2017 and Xu et al., 2022). Hence, it might be impairment of TPC2 activity that upregulates the expression of PGC1α via inhibition of AKT activity.

4.4 Conclusion

Maintaining sufficient intracellular energy production is crucial for sperm function and fertilization. The data demonstrate the effect of disruption of TPC2 on the sperm energy production and the potential molecular mechanisms that underlie the energy enhancement. The results suggest that interfering with TPC2 leads to an enhancement in mitochondrial activity and biogenesis. TPC2 KO sperm tends to utilize more energy via oxidative phosphorylation. PGC1α, which plays a key role in the regulation of cellular metabolism has been upregulated in the deficient TPC2 cells and it is thus likely to be the protein that is responsible for this phenotype. However, the exact mechanism of PGC1α activity regulation via TPC2 remains to be fully understood.

Chapter 5

Role of TPC2 in sperm capacitation and fertilization enhancement

5.1 Introduction

Freshly ejaculated sperm or epididymal sperm are not able to fertilize the oocyte until they have resided in the female reproductive tract system for a certain time (Chang, 1951). The environment of the male tract is acidic while the female one is alkaline being enriched with bicarbonate (HCO_3^-) (Vishwakarma, 1962). During the time the sperm is swimming in the female tract, it undergoes multiple physiological and biochemical modifications that are known as capacitation (De Lamirande et. al., 1997). The major modifications associated with sperm capacitation include alterations in the sperm plasma membrane lipid reorganization resulting from cholesterol efflux, HCO_3^- influx into the sperm cytosol, elevation of soluble adenylyl cyclase (sAC), an increase in cyclic adenosine monophosphate (cAMP) levels, and an increase in the activity of protein kinase A (PKA), and tyrosine phosphorylation residues which could be activated indirectly as the PKA inhibitors block the capacitation-dependent increases in protein tyrosine phosphorylation in sperm in a concentration-dependant manner (Visconti et. al., 1995; Travis and Kopf, 2002, Ickowicz et. al., 2012). These modifications lead to the initiation of sperm hyperactivated motility, activation of the acrosome reaction, and interaction with the zona pellucida and inducement of sperm-oocyte fusion.

Maintenance of the intracellular pH (pH_i) within the physiological range is essential for cellular processes. Changes in the pH_i affect the ionic state of the cellular biomolecules and may potentially their function (Boron, 2004). Several crucial ion transporters in the sperm are pH_i dependent for their activity and elimination of proteins such as the CatSper channel, Slo_3 channel, Na^+/H^+ exchanger, and sAC can lead to infertility (Ren et. al., 2001, Santi et. al., 2010 Wang et. al., 2003). Hence, regulation of spermatozoa pH_i is essential for sperm function and fertilization.

It has been reported that TPC2 plays an essential role in the regulation of acidic compartment ions such as Ca^{2+}, Na^+, and H^+. Pitt et. al., (2010) have suggested that the activation of TPC2 via NAADP leads to an excretion of Ca^2 and to an alkalinization of the Ca^{2+} store which via an efflux of H^+ into the cytosol could also affect the intracellular pH level.

In the current study, I investigated the effect of interfering with TPC2 activity on sperm capacitation and the ability to undergo the fertilization process.

5.2 Chapter Aims

Cellular pH regulation is a crucial aspect of sperm physiological processes such as sperm motility, capacitation, the acrosome reaction, and fertilization. The primary goal of this chapter to investigate the effect of loss of TPC2 activity on the cellular pH and its impact on sperm capacitation and capacity for fertilization.

5.3 Results

5.3.1 Loss of TPC2 function makes the sperm intracellular pH more alkaline.

It has been shown that intracellular pH plays a fundamental role in sperm motility, capacitation, and fertilization in mammals. Intracellular pH regulation is critical for initiation of sperm motility since the dynein ATPase activity which is the motor for the flagellar beat is pH dependent. Moreover, intracellular pH is essential for the influx and efflux of the intracellular and extracellular anions and cations that regulate sperm function (Giroux-Widemann et. al, 1991). Meanwhile, it has been reported that TPC2 contributes to the regulation of lysosomal pH homeostasis in skeletal muscle and melanocytes that may affect the intracellular pH (Lin et. al, 2015 and Ambrosio et. al, 2016). Since the intracellular pH has a significant role in sperm function, accordingly, I measured the value of the pH_i in the sperm of the WT and TPC2 KO mice.

I used SNARF-5F AM dye which is a pH indicator fluorescent probe that exhibits a pH dependent excitation value. The data demonstrates the intracellular pH value of the WT and TPC2 KO sperm (Figure 5.1). Graph 5-1 B shows the microscopic fluorescence intensity change in response to the effect of changing the intracellular pH on the WT sperm indicating that the higher the pH the higher the fluorescent emission generated. TPC2 KO sperm have a greater pH_i value compared to the WT controls as shown in Figures 5-1 C and D. The graph 5-1 C

shows that the TPC2 KO sperm has a more alkaline pH than the WT sperm with a value of 7.1 ± 0.12 and 7.4 ± 0.07 respectively with a P value < 0.05. The microscopic data displays a similar phenotype in the TPC2 KO sperm compared to the WT controls (Figure 5.1 D).

To confirm that it is the lack of TPC2 that affects the pH_i of the sperm, TPC2 was also pharmacologically inhibited using 80 μM naringenin with incubation with this for 30 min before the assessment of the pH_i. As shown in Figure 5-1 E the pH_i of treated WT sperm significantly increased with a pH value around 0.3 with a P value < 0.01. The data also shows no significant differences in the pH_i between the treated WT and TPC2 KO sperm. However, naringenin had some effect on the intracellular pH of the TPC2 KO sperm as well as the WT sperm but this was not a significant increase which may indicate that the naringenin has a TPC2 independent effect on the sperm pH_i. The findings suggest that TPC2 may contribute to the regulation of the lysosomal pH and possibly the intracellular pH homeostasis.

Overall, the findings suggest that TPC2 plays a role in regulating intracellular pH homeostasis in sperm and that its absence may lead to changes in pH_i that could impact on sperm function.

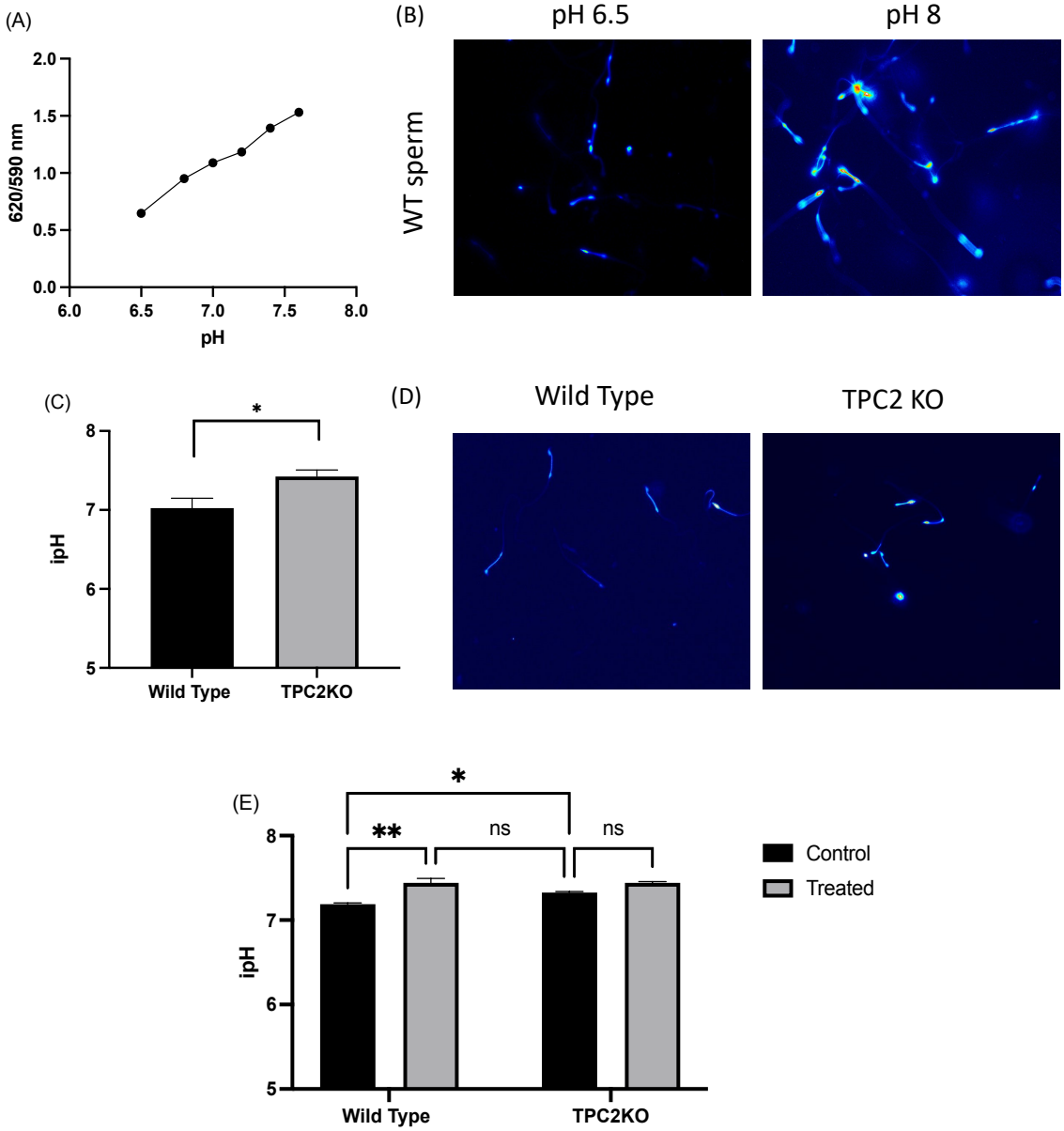


Figure 5-1: TPC2 effects on the intracellular pH.

(A) The ratio of the fluorescent intensity of the SNARF-5F AM dye in potassium phosphate buffer at different pH values that excited at 480 nm and emitted at 620 nm and 590 nm. (B) The fluorescence intensity of the WT sperm in a high K^+ medium (120 mM KCl, 25 mM HEPES and 1 mM $MgCl_2$) with different pH_e (6.5 and 8) loaded with 10 µM of nigericin to equilibrate the pH_e and pH_i. (C) The pH_i value of WT and TPC2 KO sperm obtained by calibration of the sperm in different pH_e (of 6.0, 6.5, 7.0, 7.5, and 8.0,). The linear correlation is obtained, and the pH_i is calculated using the slope equation. A fluorescent microplate reader was used to measure the fluorescence intensity. (D) Intracellular pH staining of live WT and TPC2 KO sperm with 10 µM SNARF-5F AM then loaded with 10 µM of nigericin to equilibrate the pH_e and pH_i. Sperm were immobilized on a pre-treated microscopic slide with 0.5 mg/ml Concanavalin A and imaged with an EVOS FL Auto Cell Imaging System fluorescent microscope. (E) The pH_i value of control and treated WT and TPC2 KO sperm with 80 µM naringenin obtained from calibration of the sperm in different pH_e (of 6.0, 6.5, 7.0, 7.5, and 8.0). The linear correlation is obtained, and the pH_i is calculated using the slope equation. The fluorescent microplate reader was used to measure the fluorescence intensity. The data are presented as average ± s.e.m of three animals. Asterisks show statistical significance where * $P < 0.05$; ** $P < 0.01$; *** $P < 0.001$, **** $P < 0.0001$ using a Tukey two-way ANOVA test and unpaired Student's t-test.

5.3.2 TPC2 KO could enhance the activity of CatSper channel.

The CatSper channel allows Ca^{2+} influx into the sperm tail and induces the flagellar hyperactivation motility. It is a pH dependent ionic channel whose activity is improved by an alkaline pH. It has been demonstrated that the CatSper channel in human sperm is sensitive to progesterone. In addition, the channel activity is initiated through a receptor directly associated with the channel.

To better understand the role of TPC2 as a potential regulator of the CatSper channel, I conducted an experiment to assess the Ca^{2+} response profile of non capacitated sperm from both WT and TPC2 KO mice induced by progesterone, using fluo 4 AM dye (Figure 5-1). Interestingly, TPC2 KO sperm exhibit a significantly greater Ca^{2+} response profile compared to WT controls (Figure 5-1 A and B). The mean of the fluorescence change due to progesterone treatment in TPC2 KO sperm is significantly increased compared to WT controls with $P < 0.05$. In addition, the ionophore A 23187 was used as a positive control to induce global Ca^{2+} and this was slightly greater in the WT sperm but the mean of the Ca^{2+} elevation is not significant compared to the mean of that in the TPC2 KO sperm (Figure 5-1 C).

To further investigate the role of TPC2 on CatSper channel activity, a TPC2 inhibitor was used to mimic the effect of loss of TPC2 function on the CatSper

channel. Specifically, WT and TPC2 KO sperm were treated with 80 μM naringenin for 30 min and the Ca^{2+} response profile evaluated using a fluorescence microplate reader.

The result of this investigation reveals an elevation in the Ca^{2+} response profile of the treated WT sperm, with the mean of the Ca^{2+} response increasing; however, this increase was not statistically significant. Interestingly, the elevation of the Ca^{2+} response of the treated WT sperm exhibits no significant differences with the control TPC2 KO sperm. Additionally, the treated TPC2 KO sperm shows similarities in the Ca^{2+} response with the control non treated TPC2 KO sperm, suggesting that impairment of TPC2 activity may enhance the progesterone evoked Ca^{2+} influx.

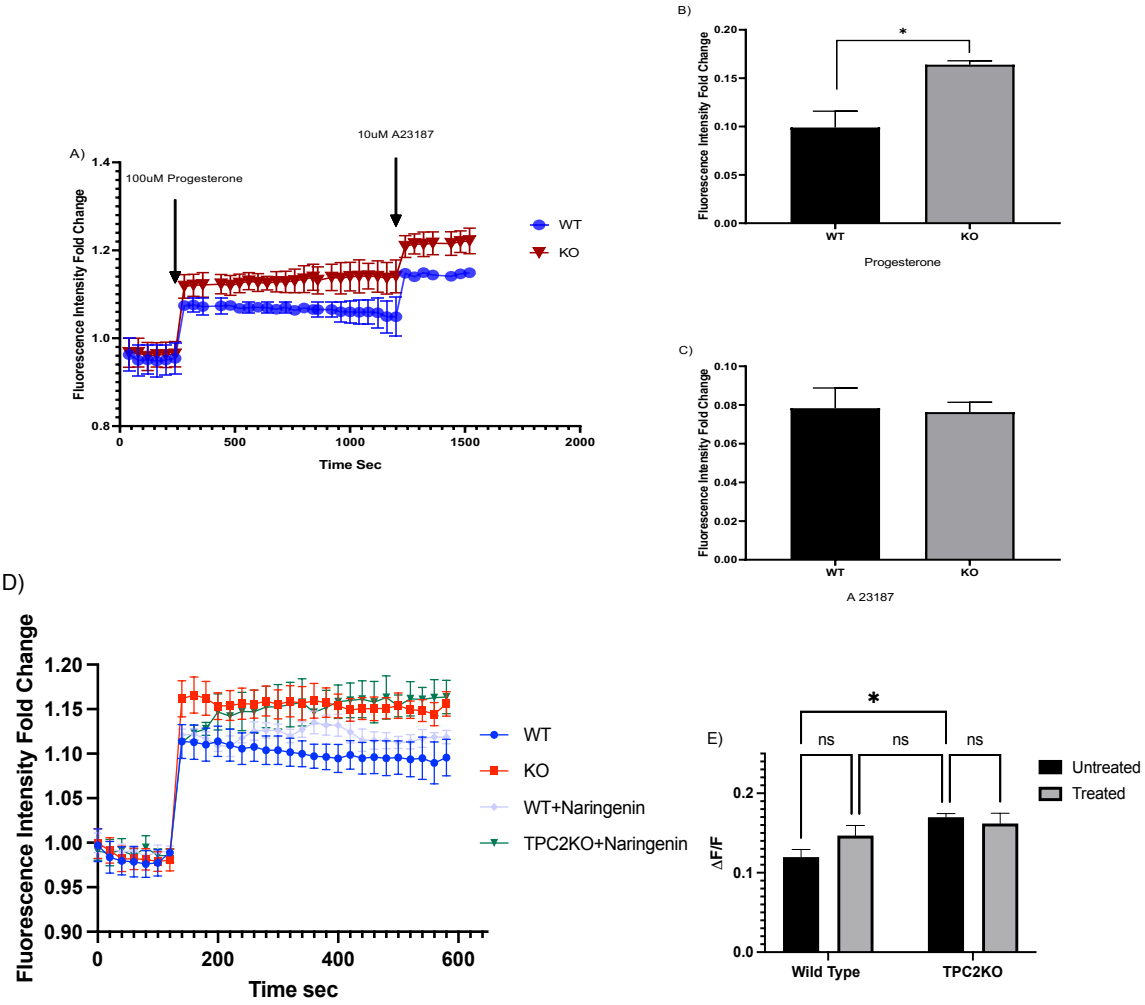


Figure 5-2: Ca^{2+} response to progesterone and ionomycin in the sperm of WT and TPC2 KO sperm.

(A) The Ca^{2+} response profile of WT and TPC2 KO sperm incubated with 100 μM progesterone and 10 μM A 23187 ionophore. The signal was measured in a fluorescence plate reader using 5 μM Fluo 4 AM. (B and C) The analysis of the mean of the Ca^{2+} response in the WT and TPC2 KO sperm incubated with progesterone and A 23187. (D) The Ca^{2+} response profile of control and treated WT and TPC2 KO sperm with 80 μM naringenin incubated with 100 μM progesterone and 10 μM A 23187 ionophore. (E) The analysis of the mean of the Ca^{2+} response in the control and naringenin treated WT and TPC2 KO sperm incubated with progesterone. The data are presented as average ± s.e.m of three animals. Asterisks show statistical significance where * $P < 0.05$; ** $P < 0.01$; *** $P < 0.001$, **** $P < 0.0001$ using two-way ANOVA test and unpaired Student's t-test.

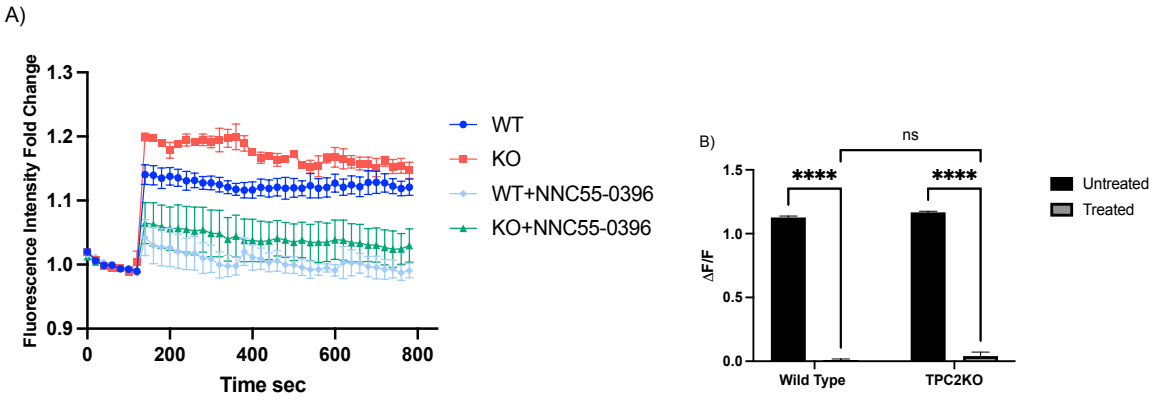


Figure 5-3: Ca^{2+} response to CatSper inhibitor of WT and TPC2 KO sperm.

(A) Progesterone induced-Ca^{2+} response profile of WT and TPC2 KO sperm are inhibited by NNC 55-0396. (B) The analysis of progesterone induced-Ca^{2+} signals by NNC 55-0396. The data are presented as average ± s.e.m of three animals (n=3). Asterisks show statistical significance where * P < 0.05; ** P < 0.01; *** P < 0.001, **** P < 0.0001 using two-way ANOVA test.

To further validate whether the Ca^{2+} response is due to the activation of the CatSper channel or not, I incubated the sperm of the WT and TPC2 KO mice with a CatSper inhibitor (NNC-55-0396) prior to the injection of the progesterone to test the Ca^{2+} response. The result of the evaluation demonstrates that there was a sharp reduction in the Ca^{2+} response evoked by progesterone in both WT and TPC2 KO sperm (Figure 5-3 A and B). Importantly, this reduction in the Ca^{2+} response shows no differences between the WT and TPC2 KO sperm indicating

that the absence of TPC2 did not significantly affect the CatSper channel's response to the inhibitor. This finding is particularly noteworthy, as it indicates that TPC2 plays an important role in regulating the Ca^{2+} influx that is associated with the progesterone-evoked response in sperm.

5.3.3 PKA-P activity is increased in the absence of TPC2 activity.

Sperm capacitation is a crucial process that occurs in the female reproductive tract and is essential for the fertilization of the oocyte. It involves a series of molecular and biochemical changes that enable the sperm to undergo the acrosome reaction and penetrate the oocyte. One of the hallmarks of sperm capacitation is the increase in protein tyrosine phosphorylation that is up regulated by cAMP analogues and inhibited via PKA inhibitors suggesting the indirect regulation of tyrosine phosphorylation, which mediated by the HCO_3^- induced cAMP / PKA pathway (Visconti et al, 1995). I investigated the p-PKA activity in WT and TPC2 KO sperm to find out the effect of the absence of TPC2 on sperm capacitation by measuring the amount of active p-PKA that elevates the sperm protein tyrosine phosphorylation in the model. The data shows the amount of p-PKA in non capacitated sperm of WT and TPC2 KO mice (Figure 5-4). The western blot for p-PKA demonstrates a greater degree of phosphorylation of PKA in the TPC2 KO sperm (Figures 5-4 A and B). Notably,

when the TPC2 has been pharmacologically inhibited by naringenin, this also led to an increase in the phosphorylation of PKA in WT sperm, with no significant difference observed between the treated WT sperm and TPC2 KO sperm (Figures 5-4 C and D). Additionally, the phosphorylation state of PKA in the treated TPC2 KO sperm exhibits no differences in the mean when compared to the control group, non-treated TPC2 KO sperm. Overall, to some degree the data shows that interfering with TPC2 activity seems to enhance the phosphorylation status of PKA.

Tyrosine phosphorylation activity that is involved in modulating sperm physiology and function was also evaluated in the WT and TPC2 KO sperm. Figure 5-5 demonstrates that interfering with TPC2 activity leads to enhancement of Tyr-p in the sperm. The total phosphorylation degree of tyrosine residues in the TPC2 KO sperm and the naringenin inhibited TPC2 KO sperm were significantly higher compared to the WT sperm (Figure 5-5 A and C). Interestingly, the localization of Tyr-p in the WT sperm was distributed around the head and the tail of the sperm while in the TPC2 KO sperm, it was mainly located in the tail of the sperm (Figure 5-5 B).

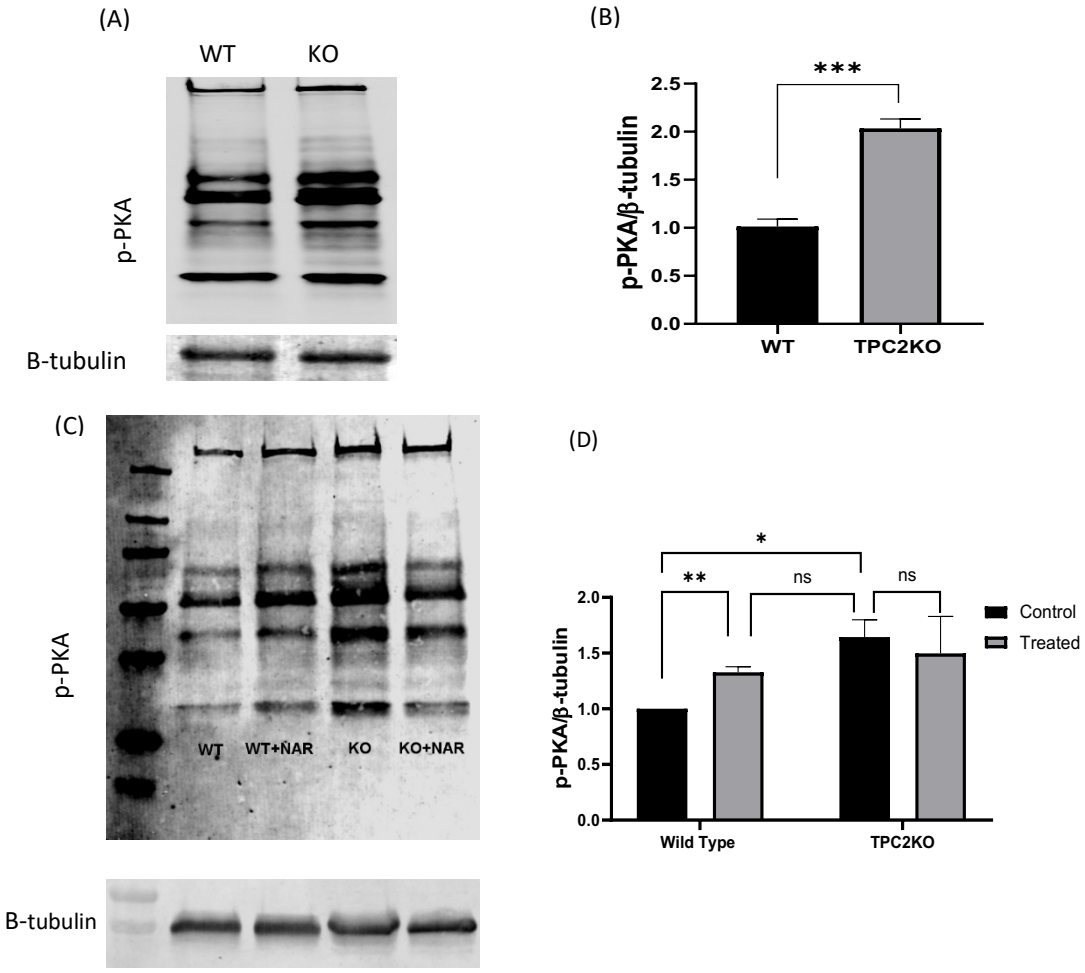


Figure 5-4: p-PKA activity in the WT and TPC2 KO sperm.

(A) Protein extracts of WT and TPC2 KO sperm (C) Sperm protein extracts of control and 80 μM naringenin treated WT and TPC2 KO sperm were analysed for phosphorylation by western blotting using anti-p-PKA as a primary antibody and the loading control was β-tubulin. (B and D) Relative amount of signal quantified in each membrane using Image studio. The data are presented as average ± s.e.m of two animals. Asterisks show statistical significance where * $P < 0.05$; ** $P < 0.01$; *** $P < 0.001$, **** $P < 0.0001$ using two-way ANOVA test and unpaired Student's t-test.

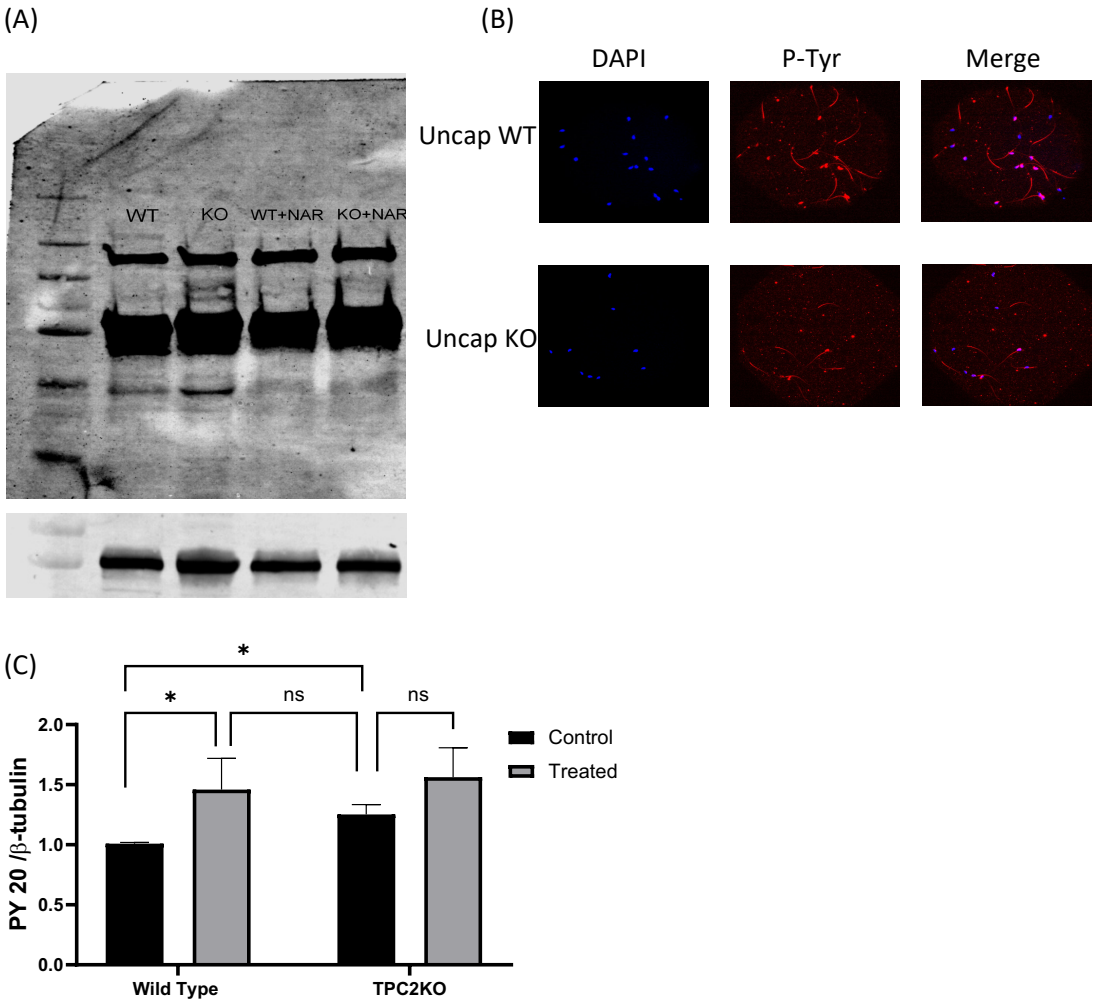


Figure 5-5: Tyrosine phosphorylated protein in WT and TPC2 KO sperm.

(A) Protein extracts of control and 80 μM naringenin treated WT and TPC2 KO sperm were analysed for tyrosine phosphorylation (Tyr-p) by western blotting using PY 20 as a primary antibody and the loading control was β-tubulin. (B) The localization of Tyr-p of WT and TPC2 KO sperm before and after the capacitation process. (C) Western blot analysis of Tyr-p of WT, TPC2 KO, untreated and treated sperm with 80 μM naringenin normalized to β-tubulin protein expression. The data are presented as average ± s.e.m of two animals. Asterisks show statistical significance where * $P < 0.05$; ** $P < 0.01$; *** $P < 0.001$, **** $P < 0.0001$ using two-way ANOVA test.

5.3.4 TPC2 KO sperm exhibit enhancement of the sperm capacitation and fertilization rate.

Sperm capacitation is a crucial physiological process that is essential for successful fertilization of the oocyte, and the acrosome reaction is a critical step in sperm-oocyte interaction during oocyte penetration. Since I have demonstrated that TPC2 KO sperm show an enhancement in the PKA and tyrosine phosphorylation; consequently, the acrosome reaction of WT and TPC2 KO sperm was evaluated. The results showed that TPC2 KO sperm had a higher percentage of reacted acrosomes compared to WT cells at different time points, suggesting that TPC2 KO sperm was more likely to be more rapidly capacitated than WT sperm (Figure 5-6 A and B).

Furthermore, *in vitro* fertilization (IVF) was performed on oocytes of female WT mice to evaluate the fertility rate of non-capacitated sperm to validate the capacitation status of the sperm of WT and TPC2 KO since capacitation is crucial for fertility. Figure 5-7 demonstrates the fertility rate of non-capacitated WT and TPC2 KO sperm compared to capacitated WT sperm. The results showed that non-capacitated TPC2 KO sperm have higher fertilization rate than the non-capacitated WT sperm. When the fertilization rate of the evaluated sperm was compared to the positive control (capacitated WT sperm) there was no significant difference in the mean fertilization rate between TPC2 KO and control sperm, whereas there was a significant difference between non-capacitated WT

sperm compared to the positive control ($p < 0.05$). These findings suggest that absence of TPC2 may lead to increased capacitation and fertilization rates.

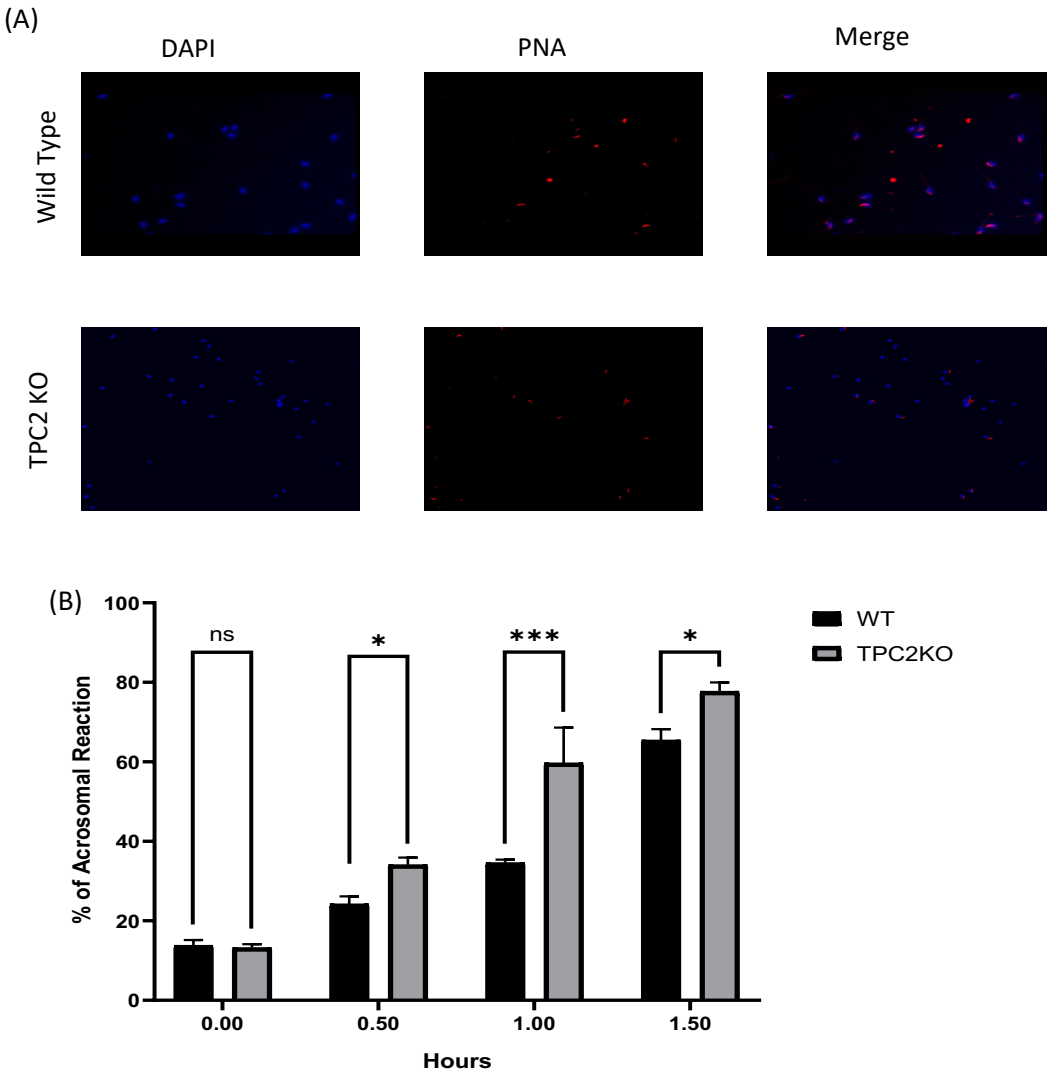


Figure 5-6: Acrosome reaction of WT and TPC2 KO sperm.

(A) The staining of the acrosome region of the WT and TPC2 KO sperm incubated with 10 µM ionomycin using lectin PNA and the images acquired every 30 min interval. The blue fluorescence is DAPI for nuclear staining, and the red staining is the lectin PNA showing the unreacted region of the acrosome. (B) The analysis of the acrosome rection where the reacted sperm were assessed by lack of reactivity towards the fluorescence of lectin PNA. The data are presented as average ± s.e.m of 200 spermatozoa of three independent experiments. Asterisks show statistical significance where * $P < 0.05$; ** $P < 0.01$; *** $P < 0.001$, **** $P < 0.0001$ using unpaired Student's t-test.

Table 6: Fertility rate of non-capacitated WT and TPC2 KO sperm.

GROUP	NUMBER OF FERTILIZED OOCYTE	FERTILITY RATE % (±SEM)
+ VE CONTROL	19/38	53.5 ± 3.5
WILD TYPE	11/60	18.33 ± 5.3 *
TPC2 KO	28/83	33.73 ± 5

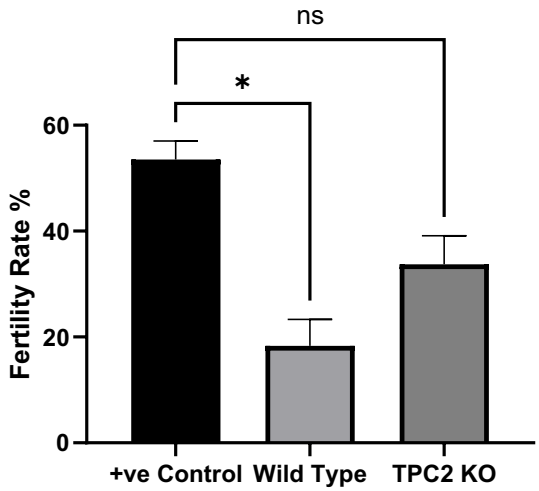


Figure 5-7: Fertility rate of non-capacitated WT and TPC2 KO sperm.

Analysis of fertility rate of non-capacitated WT and TPC2 KO sperm compared to the +ve control (capacitated WT sperm for 2 hours in HTF medium). The data are presented as average ± s.e.m of two animals. Asterisks show statistical significance where * P < 0.05; ** P < 0.01; *** P < 0.001, **** P < 0.0001 using one-way ANOVA test.

5.4 Discussion

Intracellular pH plays a crucial role in sperm physiology, so maintaining the pH_i within the normal range is essential for cellular function. Alteration in the pH_i affects the ionization of cellular molecules which eventually modify the activity of the cellular proteins (Boron, 2004). Additionally, cells tend to maintain the pH_i through generation, elimination, and transport of the H^+ across the cellular membrane which could affect the activity of plasma membrane transporters and then various molecules might be affected and alter the cellular activity (Nishigaki et al., 2014).

The finding shows that the intracellular pH of TPC2 KO sperm tends to be more alkaline compared to that of the WT sperm. It has been found that TPC2 agonists and NAADP alkalinize the lysosomes which means that there is more H^+ efflux through the TPC2 into the systoles, so is possible that TPC2 could have an influence on the systolic pH and that interference with TPC2 might alter the intracellular pH (Gerndt et al., 2020; Morgan and Galione, 2007). The contribution of TPC2 to the regulation of lysosomal pH might have an influence on intracellular pH homeostasis and might alter the intracellular pH.

Ca^{2+} signalling is essential for regulating sperm motility and is primarily mediated in human sperm by extracellular Ca^{2+} influx through CatSper channels. Progesterone, which is produced by the cumulus cell layer surrounding the

oocyte, can activate CatSper channels, resulting in a rapid Ca^{2+} entrance into sperm. The findings display an increase in the Ca^{2+} influx in the TPC2 KO sperm in response to the progesterone treatment. It is possible that the activity of the CatSper channel is altered since this channel is regulated by pH (Sun et al., 2017). The activity of CatSper resulting from the increase of the intracellular pH is consistent with the findings reported by Hwang et al., (2019) and Achikanu et al., (2018).

Protein kinases and phosphatases have proven their importance in sperm physiology. PKA participates in the sperm capacitation and tyrosine phosphorylation that induces the acrosome reaction (Lefievre et al., 2002). It has been shown that PKA inhibitors hinder sperm capacitation and the concomitant rise in protein tyrosine phosphorylation (Visconti et al, 1995; Leclerc et al, 1996), as well as the acrosome reaction (De Jonge et al, 1991), indicating that PKA is involved in these processes.

PKA is activated through the cAMP pathway which is induced by sAC. It has been shown that the enhancement of the level of cAMP affects the phosphorylation of PKA and induces sperm capacitation (Alonso et al., 2017). Visconti et al (1995) showed that an analogue of cAMP induces sperm capacitation through activation of PKA indicating that the cAMP/PKA signalling pathway plays a pivotal role in sperm capacitation. The cAMP/PKA pathway is mainly activated

via the abundance of intracellular sAC (Buffone et al., 2014). It has been proven that HCO_3^- influx is the first event associated with sperm capacitation. HCO_3^- is involved in the alkalinization of pH_i and different proton H^+ exchanger and transport (Delgado-Bermúdez et al., 2022). HCO_3^- induces sAC activation by direct binding to sAC and consequently activates the cAMP/PKA signalling pathway (Rossetti et al., 2021). Thus, alkalinization of pH_i activates the sAC and upregulates the cAMP/PKA signalling pathway which eventually induces sperm capacitation. The findings show an elevation in the level of the phosphorylated PKA of deficient TPC2 sperm compared to WT sperm. This phenotype could be attributed to the alkalized pH_i of TPC2 null sperm.

Tyrosine phosphorylation is one of the essential elements of sperm capacitation. Tyrosine phosphorylated proteins are not only important for sperm capacitation and hyperactive motility; they are also known to play a fundamental role in the sperm binding to the oocyte's zona pellucida (Naz and Ahmed, 1994). The changes in the localization of tyrosine phosphorylation during capacitation could indicate that a specific function of the sperm lay behind that region being phosphorylated. The phosphorylated tyrosine residue at the sperm flagellar proteins has been linked to the development of hyperactive motility of the sperm that is needed for cumulus and zona pellucida penetration of the oocyte (Nassar et al., 1999). Additionally, capacitation that induces the tyrosine

phosphorylation at the plasma membrane proteins in boar sperm are suggested to induce zona pellucida binding and the acrosome reaction (Flesch et al., 1999). The result shows that differences in the localization of the tyrosine phosphorylated proteins in WT and TPC2 KO sperm, with Tyr-p proteins in TPC2 KO sperm being more distributed around the flagellar and the acrosomal region, could explain why TPC2 null sperm are more hyperactive and have more capacity for the acrosome reaction.

It has been reported that in mammalian sperm, the cAMP/PKA pathway plays an important regulatory role in the activation of tyrosine phosphorylation of proteins. Furthermore, p-PKA has been induced via di butyryl cAMP (dbcAMP) and enhances the tyrosine phosphorylation suggesting that cAMP is essential for p-PKA activation (Liu et al., 2006). The findings show an enhancement in the tyrosine phosphorylated proteins of the TPC2 KO sperm that is consistent with an elevation in the level of phosphorylated PKA substrates suggesting that TPC2 KO sperm have a greater capacitation status than WT sperm.

Since the PKA regulates tyrosine phosphorylation and these phosphorylated proteins induce the acrosome reaction, which is a key factor in the fertilization process, so it is interesting that the findings show that the TPC2 KO sperm have a greater reacted acrosomal region and fertility rate compared to the WT sperm. Specifically, when the IVF was performed using non capacitated WT and TPC2

KO sperm with cumulus oocyte complexes, this showed that the TPC2 KO sperm were more capacitated than WT sperm even when incubated in non-capacitation medium.

5.5 Conclusion

The intracellular pH plays a significant role in sperm physiology, and its regulation is essential for maintaining cellular function. The activity of various cellular proteins is affected by the alteration in pH, which could impact on cellular activity. The TPC2 protein could have a critical role in regulating lysosomal pH and maybe the intracellular pH homeostasis. The findings suggest that interference with TPC2 may alter intracellular pH and increase Ca^{2+} influx through CatSper channels, affecting sperm motility. The cAMP/PKA signalling pathway is activated by HCO_3^- influx and plays a pivotal role in sperm capacitation. The findings indicate that the alkalization of pH_i could activate sAC, which upregulates the cAMP/PKA signalling pathway, eventually inducing sperm capacitation. Tyrosine phosphorylation is essential for sperm capacitation, hyperactive motility, and zona pellucida binding. The TPC2 null sperm had a different distribution of phosphorylated proteins than the WT sperm, which may lead to hyperactive motility and enhanced acrosome reaction. Overall, the findings provide valuable insights into the role of TPC2 in the regulation of

intracellular pH and protein activity in sperm physiology and may have implications in understanding fertility-related issues.

Chapter 6

General Discussion and Future Directions

6.1 General discussion

Sperm cells are highly specialized differentiated cells, making them distinct from other cell types. Their singular purpose is to successfully fertilize an oocyte and initiate the process of reproduction. The physiological function of sperm serves as a determining factor for successful fertilization. The characteristics and capabilities of sperm cells, such as motility, capacitation, and acrosome function, directly influence their ability to reach and penetrate the oocyte. Therefore, thorough understanding of sperm physiological function is crucial for achieving successful fertilization and improving outcomes in both natural and assisted reproductive contexts.

Sperm motility is a crucial factor that determines their health and capacity for successful fertilization. In my research, I observed that sperm lacking TPC2 gene function exhibited enhanced kinetic properties compared to WT sperm. Specifically, parameters such as VCL, VAP, and VSL were significantly higher in TPC2 KO sperm. The findings from previous studies have highlighted the importance of certain kinetic parameters, including VCL, LIN, and a reduction in BCF, in the capacitation-induced sperm hyperactivation that is a crucial aspect of sperm physiology and is required for successful fertilization (Suarez, 2008; Cancel et al., 2000; Ooi et al., 2014). The fact that such changes were observed

in the TPC2 KO sperm suggests that they might be capacitated more rapidly than WT sperm.

To better understand the basis of such enhanced motility, I studied the metabolism of TPC2 KO sperm, and found that they contain higher ATP levels than WT sperm since ATP is the energy source used to power the flagellar movement (Miki et al., 2004). Previous findings identified a central mediator of cellular homeostasis, AMPK, as playing a key role in sperm motility (Martin-Hidalgo, 2018). I exposed WT and TPC2 KO mice sperm to $CdCl_2$, an AMPK inhibitor (Wang et al., 2016), and found the motility of TPC2 KO sperm to be much less affected than WT sperm. Since the TPC2 KO sperm motility showed less response than WT sperm, this might suggest that alternative mechanisms modulate sperm motility in the absence of AMPK. Further studying AMPK activity in TPC2 KO sperm should reveal important insights about these mechanisms and the role of TPC2 as a mediator of motility in sperm in normal circumstances.

Glycerol 3 phosphate dehydrogenase 2 (GPD2) contributes to the gluconeogenesis process through hydrolysis of glycerol 3-phosphate. GPD2 displayed higher activity in the TPC2 deficient sperm compared to WT controls.

This enzyme has been reported to be involved in the process of capacitation and GPD2 KO sperm showed a reduction in the hyperactivated motility and tyrosine phosphorylation relative to WT sperm (Kota et al., 2010). My TPC2 KO sperm findings exhibit consistency with Kota et al., (2010)'s observations, supporting a link with GPD2 in the context of sperm motility.

Based on my finding regarding G3P substrate utilisation, further studies could make it as a starting point to conduct a comprehensive analysis of the role of this substrate in sperm motility, viability, DNA fragmentation, capacitation, tyrosine phosphorylation, and fertilization and investigate the molecular mechanisms underlying the role of G3P in sperm function.

The next part of my project was aimed at understanding the molecular mechanism underlying the modulation of GPD2 activity. Previous studies identified the role of PPARs in the regulation of fatty acid β-oxidation and glycerol metabolism via modulation of GPD2. Notably, PPARα gene expression was significantly increased in the TPC2 KO sperm suggesting that TPC2 may modulate the activity of GPD2 via PPARα as it has been confirmed that PPARα is necessary for GPD2 activity by Patsouris et al. (2004). However, when I inhibited PPARα using GW6471 in both WT and TPC2 KO sperm, the KO sperm

showed less response than WT controls suggesting that TPC2 could modulate the PPARα activity. In addition, the PAARγ isoform has been studied in sperm and shown to have a key role in lipid metabolism. A positive correlation between sperm motility and the expression of PAARγ has also been reported (Mousavi et. al, 2019). Additionally, human sperm capacitation, motility, and the acrosome reaction are enhanced by a PPARγ agonist (Aquila et. al, 2006). The potential effects of TPC2 KO on the expression of PAARγ would therefore also be worth exploring.

It is important to note that the assessment of GPD2 enzyme activity was conducted via an indirect assay through measurement of the redox reaction parameters ECAR, and OCR; therefore, that could be a limitation to this finding.

A second objective was the examination of mitochondrial biogenesis and the potential mechanism underlying this effect on the mitochondria through the absence of TPC2. The mitochondria are fundamental for human sperm movement, hyperactivation, and calcium responses as the mitochondria can act as a calcium store in the neck/midpiece, and the inhibition of the mitochondrial activity demonstrates a negative effect on ATP production and consequently on sperm motility in mouse studies (Costello et al., 2009; Kasai et al., 2002;

Tourmente et al., 2015). In my study, the TPC2 KO sperm displayed a significant increase in the OCR and $\Delta\Psi$m that reflect the oxidative phosphorylation and mitochondrial activity respectively, compared to WT controls. This elevation could be the reason for the high production of ATP in the TPC2 KO sperm. Since the TPC2 KO sperm displayed faster motility, so they must require an adequate supply of ATP to sustain all the enhanced motility of the KO sperm.

ROS are principally generated from the process of mitochondrial respiration that results from the ETC. As the TPC2 KO sperm exhibited higher oxidative phosphorylation and mitochondrial activity, it seemed likely that they would generate more ROS than WT. However, I found that TPC2 KO sperm in fact produced less ROS than WT controls. It is possible that this could be due to the ROS defence system. To investigate this issue further, I studied the expression of SOD, which is one of the antioxidant enzymes that is highly active in human sperm and found this to be highly expressed in the TPC2 KO sperm; this could explain the reduced ROS levels in the KO sperm. Additionally, the TPC2 inhibitor naringenin showed similar effect on the ROS levels in the WT sperm that could be via enhancement of the antioxidant enzymes as Li et al., (2020) previously found that naringenin upregulates the RNA expression of SOD.

The molecular mechanism underlying the enhancement of mitochondrial function in TPC2 KO sperm has been thoroughly investigated in the current study. One of the key master regulators of the mitochondrial biogenesis is PGC1α, known for its involvement in antioxidant activity (Lu at al., 2010; Rius-Pérez et al., 2020). The protein level of PGC1α was significantly increased in the TPC2 KO sperm, supporting the idea that this underlies the observed elevation of the mitochondrial activity and antioxidant activity. To further explore the relationship between this finding and the PGC1α signalling pathway, I examined the expression of key proteins involved in the pathway. Sirt1 which is the activator of PGC1α and mTFA which is the downstream target protein of PGC1α, are responsible for mitochondrial biogenesis. Both proteins were found to be elevated in the TPC2 KO sperm as well as in WT sperm in which TPC2 was pharmacologically inhibited. These findings suggest that TPC2 modulates the PGC1α pathway. However, the exact molecular mechanism by which TPC2 affects this pathway remains unclear. Further research is needed to elucidate the precise interactions and regulatory mechanisms involved. Understanding the intricate relationship between TPC2, PGC1α, and the downstream signalling pathways involved in mitochondrial biogenesis and antioxidant activity will provide valuable insights about the role of TPC2 as a mediator of mitochondrial activity and antioxidant activity in normal circumstances.

It has been reported that there is a reduction in the activity of AKT in the skeletal muscle of TPC2 KO mice and inhibition of the TPC2 activity using Ned-19 produces a similar response to the activity of AKT suggesting that TPC2 is essential for AKT activity (Lin et. al, 2015; Favia et al., 2014). It is plausible that TPC2 upregulates PGC1α through inhibition of the PIK_3/AKT pathway as naringenin downregulates the PIK_3/AKT activity (Lim et al., 2017 and Xu et al., 2022). Additionally, a previous study has reported that AKT activation downregulates the activity of PGC1α in hepatic cells (Li et al., 2007). This could be why PGC1α is highly expressed in the TPC2 KO sperm and this issue needs to be further examined in TPC2 KO sperm.

Furthermore, mammalian target of rapamycin (mTOR) is considered as the major growth regulator in animals and regulates most of the metabolic process and it also regulates mitochondrial biogenesis via PGC1α (Cunningham et al., 2007). mTOR, in addition, is one of the targeted proteins of the PIK_3/AKT signalling pathway which highlights the need to further investigate its role in this molecular pathway (Porta et al., 2014). Understanding the intricate interplay between TPC2 and the AKT, PGC1α, and mTOR signalling pathways will provide valuable insights into the regulatory mechanisms involved in mitochondrial biogenesis and cellular metabolism allowing us to gain a comprehensive

understanding of their roles in sperm physiology and potential therapeutic interventions.

A question that is raised by my findings is whether TPC2 KO leads to changes in other cell types and in isolated mitochondria.

Since the finding that TPC2 KO sperm shifted to elevation in the aerobic respiration, it is necessary to investigate this characteristic by studying the metabolism of other primary cells or immortalised cell lines by isolating their mitochondria and analysing their energetic profile to understand the mechanism underlying the shift in the aerobic respiration.

The next subject of investigation in the current project was how does interfering with TPC2 activity affect sperm functions such as capacitation and fertilization.

As the intracellular pH modulates the transportation of ions through the sperm membrane and TPC2 regulates the efflux of the H^+ from the acidic stores, the pH_i of the sperm was examined. The findings showed that the pH_i of TPC2 KO sperm tends to be more alkaline compared to the WT which is consistent with previous findings that the acidic stores become more acidic when the TPC2 activity has been interrupted and vice versa when TPC2 is activated, in which case it becomes more alkaline (Gerndt et al., 2020; Morgan and Galione, 2007).

The modification of the pH_i will consequently affect many ion transporters that are sensitive to the pH_i. This phenotype has affected Ca^{2+} influx through CatSper which is more active in an alkaline pH. There was more Ca^{2+} influx in the TPC2 KO sperm when they were exposed to progesterone suggesting that the CatSper channel is more active in the TPC2 KO sperm, and this was confirmed via inhibiting TPC2 in WT sperm using naringenin. Ca^{2+} influx and an alkaline nature of cells with interrupted TPC2 activity was also previously found by Hwang et al. (2019) and Achikanu et al. (2018).

In addition, several ion channel and transporters are involved in the regulation of lysosomal pH and pH_i including vacuolar (V)-ATPase localised to the acrosomal region, Hv1 located in the sperm tail, and NHEs expressed in the midpiece of the sperm (Ota et al., 2013; Lishko et al., 2010; Kang et al., 2021). These pH_i regulators have a crucial effect on other channels that are involved in sperm physiological function such as the sperm specific K^+ ion channel (SLO3) which is pH dependant and causes a membrane hyperpolarization through K^+ efflux which induces the capacitation process (Santi et al., 2010). TPC2 thus joins a growing list of ion channels and transporters that regulate pH_i at least in part through regulation of acidic organelle pH.

One of the limitations of the study is that naringenin has been shown to interact with large-conductance calcium-activated potassium channels (BK) of the rat that led to K^+ efflux from the mitochondria (Testai et al., 2013). Additionally, it can cause a membrane hyperpolarization of the vascular smooth muscle cells of rats indicating that naringenin can modulate the BK^+ channel that likely makes up the sperm big potassium (BK) channel (Slo1) (Yang et al., 2014; Mannowetz et al., 2013). It appears that the interference with TPC2 activity induces sperm capacitation via a complex cross talk between different channels and transporters that regulate sperm pH_i and additional work is needed to understand precisely how TPC2 regulates pH_i.

Phosphorylation of PKAs and tyrosine residues in sperm has been considered as markers for sperm capacitation that is activated via sAC that is induced by alkaline pH and Ca^{2+} and then activates the cAMP pathway (Travis and Kopf, 2002; Baldi et al., 2000). There was a significant increase in tyrosine phosphorylated proteins in the TPC2 KO sperm compared to WT controls in line with the notion that alkaline pH_i modulates PKAs and tyrosine phosphorylation. In line with sperm capacitation being pivotal for the sperm's ability to accomplish the fertilization process, I found a higher fertility rate for TPC2 KO sperm when the non-capacitated sperm of WT and TPC2 KO underwent IVF

compared to the capacitated sperm. The findings are in line with the idea that capacitation is a pre requirement for fertilization.

6.2 Overall conclusion

This thesis provides a comprehensive investigation into the impact of interrupting TPC2 activity on sperm function. It is the first study to examine the characteristics of sperm motility and metabolic alterations in the absence of TPC2 activity, shedding light on potential enzymes that play a role in this phenotype. The study investigated energy production in TPC2-deficient sperm, exploring the influence of TPC2 loss of function on mitochondrial activity and biogenesis, while also exploring the potential molecular mechanisms underlying this effect. Finally, the thesis examined the crucial aspects of sperm physiological function, such as capacitation, the acrosome reaction, and fertilization ability, to validate the positive effect of disrupting TPC2 activity on sperm function. These findings have the potential to lead to improvements in successful reproduction in clinical settings.

References:

Achikanu, C., Pendekanti, V., Teague, R. and Publicover, S., 2018. Effects of pH manipulation, CatSper stimulation and Ca^{2+}-store mobilization on $[Ca^{2+}]_i$ and behaviour of human sperm. *Human Reproduction*, *33*(10), pp.1802-1811.

Aitken, R.J. and Nixon, B., 2013. Sperm capacitation: a distant landscape glimpsed but unexplored. *Molecular human reproduction*, *19*(12), pp.785-793.

Albrizio, M., Moramarco, A.M., Nicassio, M., Micera, E., Zarrilli, A. and Lacalandra, G.M., 2015. Localization and functional modification of L-type voltage-gated calcium channels in equine spermatozoa from fresh and frozen semen. *Theriogenology*, *83*(3), pp.421-429.

Aley, P.K., Mikolajczyk, A.M., Munz, B., Churchill, G.C., Galione, A. and Berger, F., 2010. Nicotinic acid adenine dinucleotide phosphate regulates skeletal muscle differentiation via action at two-pore channels. *Proceedings of the National Academy of Sciences*, *107*(46), pp.19927-19932.

Alonso, C.A.I., Osycka-Salut, C.E., Castellano, L., Cesari, A., Di Siervi, N., Mutto, A., Johannisson, A., Morrell, J.M., Davio, C. and Perez-Martinez, S., 2017. Extracellular cAMP activates molecular signalling pathways associated with sperm capacitation in bovines. *MHR: Basic science of reproductive medicine*, *23*(8), pp.521-534.

Amaral, A., Lourenço, B., Marques, M. and Ramalho-Santos, J., 2013. Mitochondria functionality and sperm quality. *Reproduction*, *146*(5), pp. R163-R174.

Ambrosio, A.L., Boyle, J.A., Aradi, A.E., Christian, K.A. and Di Pietro, S.M., 2016. TPC2 controls pigmentation by regulating melanosome pH and size. *Proceedings of the National Academy of Sciences*, *113*(20), pp.5622-5627.

Ament, Z., Masoodi, M. and Griffin, J.L., 2012. Applications of metabolomics for understanding the action of peroxisome proliferator-activated receptors (PPARs) in diabetes, obesity, and cancer. *Genome Medicine*, *4*, pp.1-12.

Aquila, S., Bonofiglio, D., Gentile, M., Middea, E., Gabriele, S., Belmonte, M., Catalano, S., Pellegrino, M. and Andò, S., 2006. Peroxisome proliferator-activated receptor (PPAR) γ is expressed by human spermatozoa: Its potential role on the sperm physiology. *Journal of cellular physiology*, *209*(3), pp.977-986.

Arndt, L., Castonguay, J., Arlt, E., Meyer, D., Hassan, S., Borth, H., Zierler, S., Wennemuth, G., Breit, A., Biel, M. and Wahl-Schott, C., 2014. NAADP and the two-pore channel protein 1 participate in the acrosome reaction in mammalian spermatozoa. *Molecular biology of the cell*, *25*(6), pp.948-964.

Austin, C.R., 1951. Observations on the penetration of the sperm into the mammalian egg. *Australian journal of biological sciences*, *4*(4), pp.581-596.

Baker, H.G., 1996. Relationship between the zona pellucida (ZP) and ionophore A23187-induced acrosome reaction and the ability of sperm to penetrate the ZP in men with normal sperm-ZP binding. *Fertility and sterility*, *66*(2), pp.312-315.

Balaban, R.S., Nemoto, S. and Finkel, T., 2005. Mitochondria, oxidants, and aging. *cell*, *120*(4), pp.483-495.

Baldi, E., Luconi, M., Bonaccorsi, L., Muratori, M. and Forti, G., 2000. Intracellular events and signaling pathways involved in sperm acquisition of fertilizing capacity and acrosome reaction. *Frontiers in Bioscience-Landmark*, *5*(4), pp.110-123.

Barbagallo, F., La Vignera, S., Cannarella, R., Aversa, A., Calogero, A.E. and Condorelli, R.A., 2020. Evaluation of sperm mitochondrial function: a key organelle for sperm motility. *Journal of Clinical Medicine*, *9*(2), pp.363-374

Berg, J.M., Tymoczko, J.L. and Stryer, L. 2002. *Lecture notebook for biochemistry, fifth edition*. New York: W.H. Freeman and Co.

Berruti, G. and Paiardi, C., 2011. Acrosome biogenesis: revisiting old questions to yield new insights. *Spermatogenesis*, *1*(2), pp.95-98.

Billington, R.A., Ho, A. and Genazzani, A.A., 2002. Nicotinic acid adenine dinucleotide phosphate (NAADP) is present at micromolar concentrations in sea urchin spermatozoa. *The Journal of Physiology*, *544*(1), pp.107-112.

Björndahl, L., Söderlund, I., Johansson, S., Mohammadieh, M., Pourian, M.R. and Kvist, U., 2004. Why the WHO recommendations for eosin-nigrosin staining techniques for human sperm vitality assessment must change. *Journal of Andrology*, *25*(5), pp.671-678.

Blanco, G. and Blanco, A., 2017. *Medical biochemistry*. Academic Press.

Boron, W.F., 2004. Regulation of intracellular pH. *Advances in physiology education*, *28*(4), pp.160-179.

Brailoiu, E., Churamani, D., Cai, X., Schrlau, M.G., Brailoiu, G.C., Gao, X., Hooper, R., Boulware, M.J., Dun, N.J., Marchant, J.S. and Patel, S., 2009. Essential requirement for two-pore channel 1 in NAADP-mediated calcium signaling. *Journal of Cell Biology*, *186*(2), pp.201-209.

Branca, J.J., Fiorillo, C., Carrino, D., Paternostro, F., Taddei, N., Gulisano, M., Pacini, A. and Becatti, M., 2020. Cadmium-induced oxidative stress: focus on the central nervous system. *Antioxidants*, *9*(6), pp.492-512.

Bronson, R., 2011. Biology of the male reproductive tract: its cellular and morphological considerations. *American Journal of Reproductive Immunology*, *65*(3), pp.212-219.

Buffone, M.G., Wertheimer, E.V., Visconti, P.E. and Krapf, D., 2014. Central role of soluble adenylyl cyclase and cAMP in sperm physiology. *Biochimica Et Biophysica Acta (BBA)-Molecular Basis of Disease*, *1842*(12), pp.2610-2620.

Cadonic, C., Sabbir, M.G. and Albensi, B.C., 2016. Mechanisms of mitochondrial dysfunction in Alzheimer's disease. *Molecular neurobiology*, *53*, pp.6078-6090.

Calcraft, P.J., Ruas, M., Pan, Z., Cheng, X., Arredouani, A., Hao, X., Tang, J., Rietdorf, K., Teboul, L., Chuang, K.-T., Lin, P., Xiao, R., Wang, C., Zhu, Y., Lin, Y., Wyatt, C.N., Parrington, J., Ma, J., Evans, A.M., Galione, A., Zhu, M.X., 2009. NAADP mobilizes calcium from acidic organelles through two-pore channels. Nature 459, 596-600. https://doi.org10.1038/nature08030.

Calle-Guisado, V., Hurtado de Llera, A., González-Fernández, L., Bragado, M.J. and Garcia-Marin, L.J., 2017. Human sperm motility is downregulated by the AMPK activator A769662. *Andrology*, *5*(6), pp.1131-1140.

Cancel, A.M., Lobdell, D., Mendola, P. and Perreault, S.D., 2000. Objective evaluation of hyperactivated motility in rat spermatozoa using computer-assisted sperm analysis. *Human Reproduction*, *15*(6), pp.1322-1328.

Cang, C., Bekele, B. and Ren, D., 2014. The voltage-gated sodium channel TPC1 confers endolysosomal excitability. *Nature chemical biology*, *10*(6), pp.463-469.

Cang, C., Zhou, Y., Navarro, B., Seo, Y.J., Aranda, K., Shi, L., Battaglia-Hsu, S., Nissim, I., Clapham, D.E. and Ren, D., 2013. mTOR regulates lysosomal ATP-sensitive two-pore Na^+ channels to adapt to metabolic state. *Cell*, *152*(4), pp.778-790.

Chang, M.C., 1951. Fertilizing capacity of spermatozoa deposited into the fallopian tubes. *Nature*, *168*, pp.697-698.

Chávez, J.C., Darszon, A., Treviño, C.L. and Nishigaki, T., 2020. Quantitative intracellular pH determinations in single live mammalian spermatozoa using the ratiometric dye SNARF-5F. *Frontiers in Cell and Developmental Biology*, 7, pp.366-378.

Churchill, G.C., O'Neill, J.S., Masgrau, R., Patel, S., Thomas, J.M., Genazzani, A.A. and Galione, A., 2003. Sperm deliver a new second messenger: NAADP. *Current biology*, *13*(2), pp.125-128.

Cornwall, G.A. and von Horsten, H.H., 2007. Sperm maturation in the epididymis. In *The genetics of male infertility* (pp. 211-231). Humana Press.

Correia, J., Michelangeli, F. and Publicover, S., 2015. Regulation and roles of Ca^{2+} stores in human sperm. Reproduction (Cambridge, England), 150(2), pp. R65-R76.

Costello, S., Michelangeli, F., Nash, K., Lefievre, L., Morris, J., Machado-Oliveira, G., Barratt, C., Kirkman-Brown, J. and Publicover, S., 2009. Ca^{2+}-stores in sperm: their identities and functions. *Reproduction (Cambridge, England)*, *138*(3), pp.425-437.

Coy, P., Garca-Vzquez, F.A., Visconti, P.E. and Avils, M., 2012. Roles of the oviduct in mammalian fertilization. *Reproduction*, *144*(6), pp.649-660.

Cunningham, J.T., Rodgers, J.T., Arlow, D.H., Vazquez, F., Mootha, V.K. and Puigserver, P., 2007. mTOR controls mitochondrial oxidative function through a YY1–PGC-1α transcriptional complex. *nature*, *450*(7170), pp.736-740.

Darszon, A., Sánchez-Cárdenas, C., Orta, G., Sánchez-Tusie, A.A., Beltrán, C., López-González, I., Granados-González, G. and Treviño, C.L., 2012. Are TRP channels involved in sperm development and function? *Cell and Tissue Research*, *349*, pp.749-764.

De Jonge, C.J., Han, H.L., Lawrie, H., Mack, S.R. and Zaneveld, L.J.D., 1991. Modulation of the human sperm acrosome reaction by effectors of the adenylate cyclase/cyclic AMP second-messenger pathway. *Journal of Experimental Zoology*, *258*(1), pp.113-125.

De Lamirande, E., Leclerc, P. and Gagnon, C., 1997. Capacitation as a regulatory event that primes spermatozoa for the acrosome reaction and fertilization. *Molecular human reproduction*, *3*(3), pp.175-194.

de Lamirande, E.V.E., TSAI, C., HARAKAT, A. and GAGNON, C., 1998. Involvement of reactive oxygen species in human sperm arcosome reaction induced by A23187, lysophosphatidylcholine, and biological fluid ultrafiltrates. *Journal of Andrology*, *19*(5), pp.585-594.

Delgado-Bermúdez, A., Yeste, M., Bonet, S. and Pinart, E., 2022. A Review on the Role of Bicarbonate and Proton Transporters during Sperm Capacitation in Mammals. *International Journal of Molecular Sciences*, *23*(11), pp.6333-6352.

du Plessis, S.S., Agarwal, A., Mohanty, G. and Van der Linde, M., 2015. Oxidative phosphorylation versus glycolysis: what fuel do spermatozoa use? *Asian journal of andrology*, *17*(2), pp.230-235.

Duliban, M., Pawlicki, P., Gurgul, A., Tuz, R., Arent, Z., Kotula-Balak, M. and Tarasiuk, K., 2021. Peroxisome Proliferator-Activated Receptor γ, but Not α or G-Protein Coupled Estrogen

Receptor Drives Functioning of Postnatal Boar Testis—Next Generation Sequencing Analysis. *Animals*, *11*(10), pp.2868-2881.

Dumollard, R., Marangos, P., Fitzharris, G., Swann, K., Duchen, M. and Carroll, J., 2004. Sperm-triggered [Ca^{2+}] oscillations and Ca^{2+} homeostasis in the mouse egg have an absolute requirement for mitochondrial ATP production. *Development*, 131(13), pp. 3057–3067.

Eddy, E.M., Vernon, R.B., Muller, C.H., Hahnel, A.C. and Fenderson, B.A., 1985. Immunodissection of sperm surface modifications during epididymal maturation. *American Journal of Anatomy*, *174*(3), pp.225-237.

Favia, A., Desideri, M., Gambara, G., D'Alessio, A., Ruas, M., Esposito, B., Del Bufalo, D., Parrington, J., Ziparo, E., Palombi, F. and Galione, A., 2014. VEGF-induced neoangiogenesis is mediated by NAADP and two-pore channel-2–dependent Ca^{2+} signaling. *Proceedings of the National Academy of Sciences*, *111*(44), pp. E4706-E4715.

Fernandez-Marcos, P.J. and Auwerx, J., 2011. Regulation of PGC-1α, a nodal regulator of mitochondrial biogenesis. *The American journal of clinical nutrition*, *93*(4), pp.884S-890S.

Fitzpatrick, J.L., Craig, P.M., Bucking, C., Balshine, S., Wood, C.M. and McClelland, G.B., 2009. Sperm performance under hypoxic conditions in the intertidal fish Porichthys notatus. *Canadian journal of zoology*, *87*(5), pp.464-469.

Flesch, F.M., Colenbrander, B., van Golde, L.M. and Gadella, B.M., 1999. Capacitation induces tyrosine phosphorylation of proteins in the boar sperm plasma membrane. *Biochemical and biophysical research communications*, *262*(3), pp.787-792.

Florman, H.M. and Storey, B.T., 1982. Mouse gamete interactions: the zona pellucida is the site of the acrosome reaction leading to fertilization in vitro. Developmental biology, 91(1), pp.121-130.

Freitas, M.J., Vijayaraghavan, S. and Fardilha, M., 2017. Signaling mechanisms in mammalian sperm motility. *Biology of Reproduction*, *96*(1), pp.2-12.

Galione, A., Parrington, J. and Funnell, T., 2011. Physiological roles of NAADP-mediated Ca^{2+} signaling. *Science China Life Sciences*, *54*, pp.725-732.

Gerndt, S., Chen, C.C., Chao, Y.K., Yuan, Y., Burgstaller, S., Scotto Rosato, A., Krogsaeter, E., Urban, N., Jacob, K., Nguyen, O.N.P. and Miller, M.T., 2020. Agonist-mediated switching of ion selectivity in TPC2 differentially promotes lysosomal function. *Elife*, *9*, pp. e54712- e54774.

Gervasi, M.G. and Visconti, P.E., 2017. Molecular changes and signaling events occurring in spermatozoa during epididymal maturation. *Andrology*, *5*(2), pp.204-218.

Giaccagli, M.M., Gómez-Elías, M.D., Herzfeld, J.D., Marín-Briggiler, C.I., Cuasnicú, P.S., Cohen, D.J. and Da Ros, V.G., 2021. Capacitation-induced mitochondrial activity is required for sperm fertilizing ability in mice by modulating hyperactivation. *Frontiers in Cell and Developmental Biology*, *9*, pp.767161-767173.

Giroux-Widemann, V., Jouannet, P., Pignot-Paintrand, I. and Feneux, D., 1991. Effects of pH on the reactivation of human spermatozoa demembranated with Triton X-100. *Molecular reproduction and development*, *29*(2), pp.157-162.

Goldwasser, J., Cohen, P.Y., Yang, E., Balaguer, P., Yarmush, M.L. and Nahmias, Y., 2010. Transcriptional regulation of human and rat hepatic lipid metabolism by the grapefruit flavonoid naringenin: role of PPARα, PPARγ and LXRα. *PloS one*, *5*(8), pp. e12399- e12407.

Gu, X., Ma, Y., Liu, Y. and Wan, Q., 2021. Measurement of mitochondrial respiration in adherent cells by Seahorse XF96 Cell Mito Stress Test. *STAR Protocols*, 2(1), pp.100245-100256.

Harper, C., Wootton, L., Michelangeli, F., Lefièvre, L., Barratt, C. and Publicover, S., 2005. Secretory pathway Ca^{2+}-ATPase (SPCA1) Ca^{2+} pumps, not SERCAs, regulate complex $[Ca^{2+}]_i$ signals in human spermatozoa. *Journal of Cell Science*, *118*(8), pp.1673-1685.

Hedrich, R., Mueller, T.D., Becker, D. and Marten, I., 2018. Structure and function of TPC1 vacuole SV channel gains shape. *Molecular Plant*, *11*(6), pp.764-775.

Hereng, T.H., Elgstøen, K.B.P., Eide, L., Rosendal, K.R. and Skålhegg, B.S., 2014. Serum albumin and HCO3− regulate separate pools of ATP in human spermatozoa. *Human Reproduction*, *29*(5), pp.918-930.

Herzig, S., Long, F., Jhala, U.S., Hedrick, S., Quinn, R., Bauer, A., Rudolph, D., Schutz, G., Yoon, C., Puigserver, P. and Spiegelman, B., 2001. CREB regulates hepatic gluconeogenesis through the coactivator PGC-1. *Nature*, *413*(6852), pp.179-183.

Hwang, J.Y., Mannowetz, N., Zhang, Y., Everley, R.A., Gygi, S.P., Bewersdorf, J., Lishko, P.V. and Chung, J.J., 2019. Dual sensing of physiologic pH and calcium by EFCAB9 regulates sperm motility. *Cell*, *177*(6), pp.1480-1494.

Ickowicz, D., Finkelstein, M. and Breitbart, H., 2012. Mechanism of sperm capacitation and the acrosome reaction: role of protein kinases. *Asian journal of andrology*, *14*(6), pp.816-821.

Inaba, K., 2003. Molecular architecture of the sperm flagella: molecules for motility and signaling. *Zoological science*, *20*(9), pp.1043-1056.

Iommarini, L., Ghelli, A., Tropeano, C.V., Kurelac, I., Leone, G., Vidoni, S., Lombes, A., Zeviani, M., Gasparre, G. and Porcelli, A.M., 2018. Unravelling the effects of the mutation m. 3571insC/MT-ND1 on respiratory complexes structural organization. *International journal of molecular sciences*, *19*(3), pp.764-780.

Jager, S., Handschin, C., St-Pierre, J. and Spiegelman, B.M., 2007. AMP activated protein kinase (AMPK) action in skeletal muscle via direct phosphorylation of PGC-1alpha. *The Proceedings of the National Academy of Sciences*, V. 104, P. 12017-12022.

James, E.R., Carrell, D.T., Aston, K.I., Jenkins, T.G., Yeste, M. and Salas-Huetos, A., 2020. The role of the epididymis and the contribution of epididymosomes to mammalian reproduction. *International journal of molecular sciences*, *21*(15), pp.5377-5393.

Jimenez, T., McDermott, J.P., Sánchez, G. and Blanco, G., 2011. Na, K-ATPase α4 isoform is essential for sperm fertility. *Proceedings of the National Academy of Sciences*, 108(2), pp.644-649.

Jones, A.R. and Bubb, W.A., 2000. Substrates for endogenous metabolism by mature boar spermatozoa. *Journal of reproduction and fertility*, *119*(1), pp.129-136.

Jones, H.P., Lenz, R.W., Palevitz, B.A. and Cormier, M.J., 1980. Calmodulin localization in mammalian spermatozoa. *Proceedings of the National Academy of Sciences*, *77*(5), pp.2772-2776.

Jones, K.T., 2005. Mammalian egg activation: from Ca^{2+} spiking to cell cycle progression. *Reproduction*, *130* (6), pp. 813-823.

K. Naz, R. and Ahmad, K., 1994. Molecular identities of human sperm proteins that bind human zona pellucida: Nature of sperm–zona interaction, tyrosine kinase activity, and involvement of FA-1. *Molecular Reproduction and Development*, *39*(4), pp.397-408.

Kadivar, A., Khoei, H.H., Hassanpour, H., Ghanaei, H., Golestanfar, A., Mehraban, H., Davoodian, N. and Tafti, R.D., 2016. Peroxisome proliferator-activated receptors (PPARα, PPARγ and PPARβ/δ) gene expression profile on ram spermatozoa and their relation to the sperm motility. In *Veterinary research forum,* 7 (1), pp. 27-34.

Kang, H., Liu, M., Zhang, W., Huang, R.Z., Zhao, N., Chen, C. and Zeng, X.H., 2021. Na^+/H^+ exchangers involve in regulating the pH-sensitive ion channels in mouse sperm. *International Journal of Molecular Sciences*, *22*(4), pp.1612-1623.

Kasai, T., Ogawa, K., Mizuno, K., Nagai, S., Uchida, Y., Ohta, S., Fujie, M., Suzuki, K., Hirata, S. and Hoshi, K., 2002. Relationship between sperm mitochondrial membrane potential, sperm motility, and fertility potential. *Asian journal of andrology*, *4*(2), pp.97-103.

Kelu, J.J., Webb, S.E., Galione, A. and Miller, A.L., 2019. Characterization of ADP-ribosyl cyclase 1-like (ARC1-like) activity and NAADP signaling during slow muscle cell development in zebrafish embryos. *Developmental biology*, *445*(2), pp.211-225.

Kota, V., Rai, P., Weitzel, J.M., Middendorff, R., Bhande, S.S. and Shivaji, S., 2010. Role of glycerol-3-phosphate dehydrogenase 2 in mouse sperm capacitation. *Molecular Reproduction and Development*, *77*(9), pp.773-783.

Kumar, A., Majhi, R.K., Swain, N., Giri, S.C., Kar, S., Samanta, L. and Goswami, C., 2016. TRPV4 is endogenously expressed in vertebrate spermatozoa and regulates intracellular calcium in human sperm. *Biochemical and biophysical research communications*, *473*(4), pp.781-788.

Kusuhara, K., Madsen, K., Jensen, L., Hellsten, Y. and Pilegaard, H., 2007. Calcium signalling in the regulation of PGC-1α, PDK4 and HKII mRNA expression. *Journal of Biological Chemistry*, 388(5), pp. 481–488.

Lagouge, M., Argmann, C., Gerhart-Hines, Z., Meziane, H., Lerin, C., Daussin, F., Messadeq, N., Milne, J., Lambert, P., Elliott, P. and Geny, B., 2006. Resveratrol improves mitochondrial function and protects against metabolic disease by activating SIRT1 and PGC-1α. *Cell*, *127*(6), pp.1109-1122.

Lawson, C., Dorval, V., Goupil, S. and Leclerc, P., 2007. Identification and localisation of SERCA 2 isoforms in mammalian sperm. *Molecular Human Reproduction*, *13*(5), pp.307-316.

Lear, P.V., González-Touceda, D., Porteiro Couto, B., Viaño, P., Guymer, V., Remzova, E., Tunn, R., Chalasani, A., García-Caballero, T., Hargreaves, I.P. and Tynan, P.W., 2015. Absence of intracellular ion channels TPC1 and TPC2 leads to mature-onset obesity in male mice, due to impaired lipid availability for thermogenesis in brown adipose tissue. *Endocrinology*, *156*(3), pp.975-986.

Leclerc P, de Lamirande E, Gagnon C. Cyclic adenosine 3', 5'monophosphate-dependent regulation of protein tyrosine phosphorylation in relation to human sperm capacitation and motility. *Biol Reprod.* 1996; 55:684–692.

Lee, Y.X., Lin, P.H., Rahmawati, E., Ma, Y.Y., Chan, C. and Tzeng, C.R., 2019. Mitochondria Research in Human Reproduction. In *The Ovary* (pp. 327-335). Academic Press.

Lefievre, L., Jha, K.N., de LAMIRANDE, E.V.E., Visconti, P.E. and Gagnon, C., 2002. Activation of protein kinase A during human sperm capacitation and acrosome reaction. *Journal of andrology*, *23*(5), pp.709-716.

Lehti, M.S. and Sironen, A., 2017. Formation and function of sperm tail structures in association with sperm motility defects. *Biology of reproduction*, *97*(4), pp.522-536.

Li, H., Liu, M.W., Yang, W., Wan, L.J., Yan, H.L., Li, J.C., Tang, S.Y. and Wang, Y.Q., 2020. Naringenin induces neuroprotection against homocysteine-induced PC12 cells via the

upregulation of superoxide dismutase 1 expression by decreasing miR-224-3p expression. *Journal of Biological Regulators and Homeostatic Agents*, *34*(2), pp.421-433.

Li, X., Monks, B., Ge, Q., & Birnbaum, M. J. (2007). Akt/PKB regulates hepatic metabolism by directly inhibiting PGC-1α transcription coactivator. *Nature*, *447*(7147), 1012-1016.

Lim, W., Park, S., Bazer, F. W., & Song, G. (2017). Naringenin-induced apoptotic cell death in prostate cancer cells is mediated via the PI3K/AKT and MAPK signaling pathways. *Journal of cellular biochemistry*, *118*(5), 1118-1131.

Lin-Moshier, Y., Keebler, M.V., Hooper, R., Boulware, M.J., Liu, X., Churamani, D., Abood, M.E., Walseth, T.F., Brailoiu, E., Patel, S. and Marchant, J.S., 2014. The Two-pore channel (TPC) interactome unmasks isoform-specific roles for TPCs in endolysosomal morphology and cell pigmentation. *Proceedings of the National Academy of Sciences*, *111*(36), pp.13087-13092.

Lin-Moshier, Y., Walseth, T.F., Churamani, D., Davidson, S.M., Slama, J.T., Hooper, R., Brailoiu, E., Patel, S. and Marchant, J.S., 2012. Photoaffinity Labeling of Nicotinic Acid Adenine Dinucleotide Phosphate (NAADP) Targets in Mammalian Cells. *Journal of Biological Chemistry*, *287*(4), pp.2296-2307.

Lin, P.H., Duann, P., Komazaki, S., Park, K.H., Li, H., Sun, M., Sermersheim, M., Gumpper, K., Parrington, J., Galione, A. and Evans, A.M., 2015. Lysosomal two-pore channel subtype 2 (TPC2) regulates skeletal muscle autophagic signaling. *Journal of Biological Chemistry*, *290*(6), pp.3377-3389.

Lindemann, C.B. and Lesich, K.A., 2010. Flagellar and ciliary beating: the proven and the possible. *Journal of cell science*, *123*(4), pp.519-528.

Lishko, P.V. and Kirichok, Y., 2010. The role of Hv1 and CatSper channels in sperm activation. The Journal of physiology, 588(23), pp.4667-4672.

Liu, D.Y., Clarke, G.N. and Baker, H.W.G., 2006. Tyrosine phosphorylation on capacitated human sperm tail detected by immunofluorescence correlates strongly with sperm–zona pellucida (ZP) binding but not with the ZP-induced acrosome reaction. *Human reproduction*, *21*(4), pp.1002-1008.

Lu, Z., Xu, X., Hu, X., Fassett, J., Zhu, G., Tao, Y., Li, J., Huang, Y., Zhang, P., Zhao, B. and Chen, Y., 2010. PGC-1α regulates expression of myocardial mitochondrial antioxidants and myocardial oxidative stress after chronic systolic overload. *Antioxidants & redox signalling*, *13*(7), pp.1011-1022.

Madiraju, A.K., Erion, D.M., Rahimi, Y., Zhang, X.M., Braddock, D.T., Albright, R.A., Prigaro, B.J., Wood, J.L., Bhanot, S., MacDonald, M.J. and Jurczak, M.J., 2014. Metformin suppresses gluconeogenesis by inhibiting mitochondrial glycerophosphate dehydrogenase. *Nature*, *510*(7506), pp.542-546.

Mannowetz, N., Naidoo, N.M., Choo, S.A.S., Smith, J.F. and Lishko, P.V., 2013. Slo1 is the principal potassium channel of human spermatozoa. *elife*, *2*, p.e01009.

Marchant, J.S. and Patel, S., 2015. Two-pore channels at the intersection of endolysosomal membrane traffic. *Biochemical Society Transactions*, *43*(3), pp.434-441.

Marchetti, C., Obert, G., Deffosez, A., Formstecher, P. and Marchetti, P., 2002. Study of mitochondrial membrane potential, reactive oxygen species, DNA fragmentation and cell viability by flow cytometry in human sperm. *Human Reproduction*, *17*(5), pp.1257-1265.

Martin-Hidalgo, D., Hurtado de Llera, A., Calle-Guisado, V., Gonzalez-Fernandez, L., Garcia-Marin, L. and Bragado, M.J., 2018. AMPK function in mammalian spermatozoa. *International journal of molecular sciences*, *19*(11), pp.3293-3316.

Miki, K., Qu, W., Goulding, E.H., Willis, W.D., Bunch, D.O., Strader, L.F., Perreault, S.D., Eddy, E.M. and O'Brien, D.A., 2004. Glyceraldehyde 3-phosphate dehydrogenase-S, a sperm-specific glycolytic enzyme, is required for sperm motility and male fertility. *Proceedings of the National Academy of Sciences*, *101*(47), pp.16501-16506.

Montaigne, D., Butruille, L. and Staels, B., 2021. PPAR control of metabolism and cardiovascular functions. *Nature Reviews Cardiology*, *18*(12), pp.809-823.

Morgan, A. J., & Galione, A. (2007). NAADP induces pH changes in the lumen of acidic Ca^{2+} stores. *Biochemical Journal*, *402*(2), 301-310.

Morgan, A.J. and Galione, A., 2007. Fertilization and nicotinic acid adenine dinucleotide phosphate induce pH changes in acidic Ca^{2+} stores in sea urchin eggs. *Journal of Biological Chemistry*, *282*(52), pp.37730-37737.

Morgan, A.J., Martucci, L.L., Davis, L.C. and Galione, A., 2022. Two-pore channels: going with the flows. *Biochemical Society Transactions*, *50*(4), pp.1143-1155.

Mortimer, D., 2018. The functional anatomy of the human spermatozoon: relating ultrastructure and function. *MHR: Basic science of reproductive medicine*, *24*(12), pp.567-592.

Mousavi, M.S., Shahverdi, A., Drevet, J., Akbarinejad, V., Esmaeili, V., Sayahpour, F.A., Topraggaleh, T.R., Rahimizadeh, P. and Alizadeh, A., 2019. Peroxisome Proliferator-Activated Receptors (PPARs) levels in spermatozoa of normozoospermic and asthenozoospermic men. *Systems biology in reproductive medicine*, *65*(6), pp.409-419.

Müller, M., Gerndt, S., Chao, Y.K., Zisis, T., Nguyen, O.N.P., Gerwien, A., Urban, N., Müller, C., Gegenfurtner, F.A., Geisslinger, F. and Ortler, C., 2021. Gene editing and synthetically accessible inhibitors reveal role for TPC2 in HCC cell proliferation and tumor growth. *Cell chemical biology*, *28* (8), pp. 1119-1131.

Nassar, A., Mahony, M., Morshedi, M., Lin, M.H., Srisombut, C. and Oehninger, S., 1999. Modulation of sperm tail protein tyrosine phosphorylation by pentoxifylline and its correlation with hyperactivated motility. *Fertility and sterility*, *71*(5), pp.919-923.

Nayak, J., Jena, S.R. and Samanta, L., 2019. Oxidative stress and sperm dysfunction: An insight into dynamics of semen proteome. In *Oxidants, Antioxidants and Impact of the Oxidative Status in Male Reproduction* (pp. 261-275). Academic Press.

Nishigaki, T., José, O., González-Cota, A.L., Romero, F., Treviño, C.L. and Darszon, A., 2014. Intracellular pH in sperm physiology. *Biochemical and biophysical research communications*, *450* (3), pp. 1149-1158.

Notomi, T., Kise, C., Kobayashi, R., Otsuka, M., Momota, Y., Ezura, Y. and Kawazoe, T., 2021. TPC1 and TPC2 Promote Osteoclastogenesis. *Journal of Hard Tissue Biology*, *30*(4), pp.333-338.

Nowicka-Bauer, K. and Szymczak-Cendlak, M., 2021. Structure and function of ion channels regulating sperm motility—an overview. *International Journal of Molecular Sciences*, *22*(6), pp.3259-3282.

O'Flaherty, C., de Lamirande, E. and Gagnon, C., 2006. Positive role of reactive oxygen species in mammalian sperm capacitation: triggering and modulation of phosphorylation events. *Free Radical Biology and Medicine*, *41*(4), pp.528-540.

Oliver, E.I., Jabloñski, M., Buffone, M.G., Darszon, A., 2023. Two-pore channel 1 and Ca^{2+} release-activated Ca^{2+} channels contribute to the acrosomal pH-dependent intracellular Ca^{2+} increase in mouse sperm. *The Journal of Physiology,* 601, 2935-2958. https://doi.org10.1113/jp284247.

Ooi, E.H., Smith, D.J., Gadelha, H., Gaffney, E.A. and Kirkman-Brown, J., 2014. The mechanics of hyperactivation in adhered human sperm. *Royal Society open science*, *1*(2), pp.140230-140241.

Ota, K., Jaiswal, M.K., Ramu, S., Jeyendran, R., Kwak-Kim, J., Gilman-Sachs, A. and Beaman, K.D., 2013. Expression of a2 vacuolar ATPase in spermatozoa is associated with semen quality and chemokine-cytokine profiles in infertile men. *PloS one*, *8*(7), pp. e70470- e70476

Pacey, A. and Williams, K., 2018. The Human Spermatozoa. *Clinical Reproductive Science*, pp.65-73.

Pagel-Langenickel, I., Bao, J., Joseph, J.J., Schwartz, D.R., Mantell, B.S., Xu, X., Raghavachari, N. and Sack, M.N., 2008. PGC-1α integrates insulin signaling, mitochondrial regulation, and bioenergetic function in skeletal muscle. *Journal of Biological Chemistry*, *283*(33), pp.22464-22472.

Papas, M., Arroyo, L., Bassols, A., Catalán, J., Bonilla-Correal, S., Gacem, S., Yeste, M. and Miró, J., 2019. Activities of antioxidant seminal plasma enzymes (SOD, CAT, GPX and GSR) are higher in jackasses than in stallions and are correlated with sperm motility in jackasses. *Theriogenology*, *140*, pp.180-187.

Patsouris, D., Mandard, S., Voshol, P.J., Escher, P., Tan, N.S., Havekes, L.M., Koenig, W., März, W., Tafuri, S., Wahli, W. and Müller, M., 2004. PPARα governs glycerol metabolism. *The Journal of clinical investigation*, *114*(1), pp.94-103.

Peeker, R., Abramsson, L. and Marklund, S.L., 1997. Superoxide dismutase isoenzymes in human seminal plasma and spermatozoa. *Molecular human reproduction*, *3*(12), pp.1061-1066.

Perumal, P., 2014. Effect of superoxide dismutase on semen parameters and antioxidant enzyme activities of liquid stored (5 C) Mithun (Bos frontalis) semen. *Journal of Animals*, *2014*, pp.1-9

Picca, A. and Lezza, A.M.S., 2015. Regulation of mitochondrial biogenesis through TFAM–mitochondrial DNA interactions: useful insights from aging and calorie restriction studies. *Mitochondrion*, *25*, pp.67-75.

Piomboni, P., Focarelli, R., Stendardi, A., Ferramosca, A. and Zara, V., 2012. The role of mitochondria in energy production for human sperm motility. *International journal of andrology*, *35*(2), pp.109-124.

Pitt, S.J., Funnell, T.M., Sitsapesan, M., Venturi, E., Rietdorf, K., Ruas, M., Ganesan, A., Gosain, R., Churchill, G.C., Zhu, M.X. and Parrington, J., 2010. TPC2 is a novel NAADP-sensitive Ca^{2+} release channel, operating as a dual sensor of luminal pH and Ca^{2+}. *Journal of Biological Chemistry*, *285*(45), pp.35039-35046.

Pitt, S.J., Reilly-O'Donnell, B. and Sitsapesan, R., 2016. Exploring the biophysical evidence that mammalian two-pore channels are NAADP-activated calcium-permeable channels. *The Journal of Physiology*, *594* (15), pp. 4171-4179.

Pizzino, G., Irrera, N., Cucinotta, M., Pallio, G., Mannino, F., Arcoraci, V., Squadrito, F., Altavilla, D. and Bitto, A., 2017. Oxidative stress: harms and benefits for human health. *Oxidative medicine and cellular longevity*, *2017,* pp.1-13

Porta, C., Paglino, C. and Mosca, A., 2014. Targeting PI3K/Akt/mTOR signaling in cancer. *Frontiers in oncology*, *4*, pp.64-74.

Puigserver, P. and Spiegelman, B.M., 2003. Peroxisome proliferator-activated receptor-γ coactivator 1α (PGC-1α): transcriptional coactivator and metabolic regulator. *Endocrine reviews*, *24*(1), pp.78-90.

Ramalho-Santos, J., Schatten, G. and Moreno, R.D., 2002. Control of membrane fusion during spermiogenesis and the acrosome reaction. *Biology of reproduction*, *67*(4), pp.1043-1051.

Ren, D., Navarro, B., Perez, G., Jackson, A.C., Hsu, S., Shi, Q., Tilly, J.L. and Clapham, D.E., 2001. A sperm ion channel required for sperm motility and male fertility. *Nature*, *413*(6856), pp.603-609.

Rius-Pérez, S., Torres-Cuevas, I., Millán, I., Ortega, Á.L. and Pérez, S., 2020. PGC-1α, inflammation, and oxidative stress: an integrative view in metabolism. *Oxidative medicine and cellular longevity*, *2020*. pp.1-20

Roldan, E.R., Murase, T. and Shi, Q.X., 1994. Exocytosis in spermatozoa in response to progesterone and zona pellucida. *Science*, *266*(5190), pp.1578-1581.

Rossetti, T., Jackvony, S., Buck, J. and Levin, L.R., 2021. Bicarbonate, carbon dioxide and pH sensing via mammalian bicarbonate-regulated soluble adenylyl cyclase. *Interface Focus*, *11*(2), p.20200034.

Rowe, G.C., Jiang, A. and Arany, Z., 2010. PGC-1 coactivators in cardiac development and disease. *Circulation research*, *107*(7), pp.825-838.

Ruas, M., Davis, L.C., Chen, C.C., Morgan, A.J., Chuang, K.T., Walseth, T.F., Grimm, C., Garnham, C., Powell, T., Platt, N. and Platt, F.M., 2015. Expression of Ca^{2+}-permeable two-pore channels rescues NAADP signalling in TPC-deficient cells. *The EMBO journal*, *34*(13), pp.1743-1758.

Sánchez-Tusie, A.A., Vasudevan, S.R., Churchill, G.C., Nishigaki, T., Treviño, C.L., 2014. Characterization of NAADP-mediated calcium signaling in human spermatozoa. Biochem. Biophys. Res. Commun. 443, 531-536. https://doi.org10.1016/j.bbrc.2013.12.011.

Santi, C.M., Martínez-López, P., de la Vega-Beltrán, J.L., Butler, A., Alisio, A., Darszon, A. and Salkoff, L., 2010. The SLO3 sperm-specific potassium channel plays a vital role in male fertility. *FEBS letters*, *584*(5), pp.1041-1046.

Santi, C.M., Santos, T., Hernández-Cruz, A. and Darszon, A., 1998. Properties of a novel pH dependent Ca^{2+} permeation pathway present in male germ cells with possible roles in spermatogenesis and mature sperm function. *The Journal of general physiology*, *112*(1), pp.33-53.

Scientific Image and Illustration Software | BioRender https://www.biorender.com Accessed 16, Jan 2023.

Seksek, O., Henry-Toulmé, N., Sureau, F. and Bolard, J., 1991. SNARF-1 as an intracellular pH indicator in laser microspectrofluorometry: a critical assessment. *Analytical Biochemistry*, 193(1), pp.49-54.

Serrano, H. and Garcia-Suarez, D., 2001. Molecular aspects of mammalian fertilization. *Asian journal of andrology*, *3*(4), pp.243-249.

Shan, S., Xu, F., Hirschfeld, M. and Brenig, B., 2021. Sperm Lipid Markers of Male Fertility in Mammals. *International Journal of Molecular Sciences*, *22*(16), pp.8767-8787.

Si, Y. and Olds-Clarke, P., 2000. Evidence for the involvement of calmodulin in mouse sperm capacitation. *Biology of Reproduction*, *62*(5), pp.1231-1239.

Signorelli, J., Diaz, E.S. and Morales, P., 2012. Kinases, phosphatases, and proteases during sperm capacitation. *Cell and tissue research*, *349*(3), pp.765-782.

Sivandzade, F., Bhalerao, A. and Cucullo, L., 2019. Analysis of the mitochondrial membrane potential using the cationic JC-1 dye as a sensitive fluorescent probe. *Bio-protocol*, *9*(1), pp. e3128-e3128.

Soares, S., Thompson, M., White, T., Isbell, A., Yamasaki, M., Prakash, Y., Lund, F.E., Galione, A., and Chini, E.N., 2007. NAADP as a second messenger: neither CD38 nor base-exchange reaction are necessary for in vivo generation of NAADP in myometrial cells. *American Journal of Physiology-Cell Physiology*, *292*(1), pp.C227-C239.

Southgate, R.J., Bruce, C.R., Carey, A.L., Steinberg, G.R., Walder, K., Monks, R., Watt, M.J., Hawley, J.A., Birnbaum, M.J. and Febbraio, M.A., 2005. PGC-1α gene expression is down-regulated by Akt-mediated phosphorylation and nuclear exclusion of FoxO1 in insulin-stimulated skeletal muscle. *The FASEB journal*, *19*(14), pp.2072-2074.

Stocco, D.M. and McPhaul, M.J., 2006. Physiology of testicular steroidogenesis. In *Knobil and Neill's physiology of reproduction* (pp. 977-1016). Academic Press.

Suarez, S.S. and Dai, X., 1992. Hyperactivation enhances mouse sperm capacity for penetrating viscoelastic media. *Biology of reproduction*, *46*(4), pp.686-691.

Suarez, S.S., 2008. Control of hyperactivation in sperm. *Human reproduction update*, *14*(6), pp.647-657.

Sumigama S, Mansell S, Miller M, Lishko PV, Cherr GN, Meyers SA, Tollner T. Progesterone accelerates the completion of sperm capacitation and activates CatSper channel in spermatozoa from the rhesus macaque. Biology of reproduction. 2015 Dec 1;93(6):130-pp 1-11.

Sun, X.H., Zhu, Y.Y., Wang, L., Liu, H.L., Ling, Y., Li, Z.L. and Sun, L.B., 2017. The Catsper channel and its roles in male fertility: a systematic review. *Reproductive Biology and Endocrinology*, *15* (1), pp. 1-12.

Sutovsky, P. and Manandhar, G., 2006. Mammalian spermatogenesis and sperm structure: anatomical and compartmental analysis. *The sperm cell: Production, maturation, fertilization, regeneration*, pp.1-30.

Takei, G.L., Miyashiro, D., Mukai, C. and Okuno, M., 2014. Glycolysis plays an important role in energy transfer from the base to the distal end of the flagellum in mouse sperm. *Journal of Experimental Biology*, *217*(11), pp.1876-1886.

Tartarin, P., Guibert, E., Touré, A., Ouiste, C., Leclerc, J., Sanz, N., Brière, S., Dacheux, J.L., Delaleu, B., McNeilly, J.R. and McNeilly, A.S., 2012. Inactivation of AMPKα1 induces asthenozoospermia and alters spermatozoa morphology. *Endocrinology*, *153*(7), pp.3468-3481.

Tash, J.S., 1989. Protein phosphorylation: the second messenger signal transducer of flagellar motility. *Cell motility and the cytoskeleton*, *14*(3), pp.332-339.

Testai, L., Martelli, A., Marino, A., D'antongiovanni, V., Ciregia, F., Giusti, L., Lucacchini, A., Chericoni, S., Breschi, M.C. and Calderone, V., 2013. The activation of mitochondrial BK potassium channels contributes to the protective effects of naringenin against myocardial ischemia/reperfusion injury. *Biochemical pharmacology*, *85*(11), pp.1634-1643.

The Biology Notes, *Spermatogenesis- Definition, Stages and Process with figure* available at https://thebiologynotes.com/spermatogenesis/ published on 04 Feb 2023. Accessed on 10 Mar 2023.

Tourmente, M., Villar-Moya, P., Rial, E. and Roldan, E.R., 2015. Differences in ATP generation via glycolysis and oxidative phosphorylation and relationships with sperm motility in mouse species. *Journal of Biological Chemistry*, *290*(33), pp.20613-20626.

Travis, A.J. and Kopf, G.S., 2002. The role of cholesterol efflux in regulating the fertilization potential of mammalian spermatozoa. *The journal of clinical investigation*, *110* (6), pp. 731-736.

Tremellen, K., 2008. Oxidative stress and male infertility—a clinical perspective. *Human reproduction update*, *14*(3), pp.243-258.

Trufanov, S.K., Rybakova, E.Y., Avdonin, P.P., Tsitrina, A.A., Zharkikh, I.L., Goncharov, N.V., Jenkins, R.O. and Avdonin, P.V., 2019. The role of two-pore channels in norepinephrine-induced $[Ca^{2+}]_i$ rise in rat aortic smooth muscle cells and aorta contraction. *Cells*, *8*(10), pp.1144-1162.

Turner, R.M., 2005. Moving to the beat: a review of mammalian sperm motility regulation. *Reproduction, Fertility and Development*, *18*(2), pp.25-38.

Urra, F.A., Muñoz, F., Lovy, A. and Cárdenas, C., 2017. The mitochondrial complex (I) ty of cancer. *Frontiers in oncology*, *7*, pp.118-115.

Vasudevan, S.R., Lewis, A.M., Chan, J.W., Machin, C.L., Sinha, D., Galione, A. and Churchill, G.C., 2010. The calcium-mobilizing messenger nicotinic acid adenine dinucleotide phosphate

participates in sperm activation by mediating the acrosome reaction. *Journal of biological chemistry*, *285*(24), pp.18262-18269.

Vedel, F., Lalanne, É., Sabar, M., Chétrit, P. and De Paepe, R., 1999. The mitochondrial respiratory chain and ATP synthase complexes: composition, structure, and mutational studies. *Plant Physiology and Biochemistry*, *37*(9), pp.629-643.

Visconti PE, Moore GD, Bailey JL, Leclerc P, Connors SA, Pan D, Olds- Clarke P, Kopf GS. Capacitation of mouse spermatozoa. II. Protein tyrosine phosphorylation and capacitation are regulated by cAMP- dependent pathway. Development. 1995; 121:1139–1150.

Visconti, P.E., 2012. Sperm bioenergetics in a nutshell. *Biology of reproduction*, *87*(3), pp.72-75.

Visconti, P.E., and Kopf, G.S., 1998. Regulation of protein phosphorylation during sperm capacitation. *Biology of reproduction*, *59*(1), pp.1-6.

Vishwakarma, P., 1962. The pH and bicarbonate-ion content of the oviduct and uterine fluids. *Fertility and sterility*, *13*(5), pp.481-485.

Wagner, H., Cheng, J.W. and Ko, E.Y., 2018. Role of reactive oxygen species in male infertility: An updated review of literature. *Arab journal of urology*, *16*(1), pp.35-43.

Waheeb, R. and Hofmann, M.C., 2011. Human spermatogonial stem cells: a possible origin for spermatocytic seminoma. *International journal of andrology*, *34*(4pt2), pp.e296-e305.

Wang, D., King, S.M., Quill, T.A., Doolittle, L.K. and Garbers, D.L., 2003. A new sperm-specific Na^+/H^+ exchanger required for sperm motility and fertility. *Nature cell biology*, *5*(12), pp.1117-1122.

Wang, K., Chen, Z., Huang, L., Meng, B., Zhou, X., Wen, X. and Ren, D., 2017. Naringenin reduces oxidative stress and improves mitochondrial dysfunction via activation of the Nrf2/ARE signalling pathway in neurons. *International Journal of Molecular Medicine*, *40*(5), pp.1582-1590.

Wang, L., Li, Y., Fu, J., Zhen, L., Zhao, N., Yang, Q., Li, S. and Li, X., 2016. Cadmium inhibits mouse sperm motility through inducing tyrosine phosphorylation in a specific subset of proteins. *Reproductive toxicology*, *63*, pp.96-106.

Wang, X., Zhang, X., Dong, X.P., Samie, M., Li, X., Cheng, X., Goschka, A., Shen, D., Zhou, Y., Harlow, J. and Zhu, M.X., 2012. TPC proteins are phosphoinositide-activated sodium-selective ion channels in endosomes and lysosomes. *Cell*, *151* (2), pp. 372-383.

Wassarman, P.M., 1999. Mammalian fertilization: molecular aspects of gamete adhesion, exocytosis, and fusion. *Cell*, *96*(2), pp.175-183.

Wistuba, J., Stukenborg, J.B. and Luetjens, C.M., Mammalian spermatogenesis. *Functional Development and Embryology,* 2007; 1 (2): 99-117.

Wu, H., Deng, X., Shi, Y., Su, Y., Wei, J. and Duan, H., 2016. PGC-1α, glucose metabolism and type 2 diabetes mellitus. *Journal of Endocrinology*, *229*(3), pp. R99-R115.

Xu, J., Guo, Z., Yuan, S., & Li, H. (2022). BCL2L1 is identified as a target of naringenin in regulating ovarian cancer progression. *Molecular and Cellular Biochemistry*, *477*(5), pp. 1541-1553.

Yamashita, Y., Shimada, M., Okazaki, T., Maeda, T. and Terada, T., 2003. Production of progesterone from de novo-synthesized cholesterol in cumulus cells and its physiological role during meiotic resumption of porcine oocytes. *Biology of Reproduction*, *68*(4), pp.1193-1198.

Yanagimachi, R., 1994. Mammalian fertilization. *The physiology of reproduction*, *1*, pp.273-279.

Yang, Z., Pan, A., Zuo, W., Guo, J. and Zhou, W., 2014. Relaxant effect of flavonoid naringenin on contractile activity of rat colonic smooth muscle. *Journal of ethnopharmacology*, *155*(2), pp.1177-1183.

Yoshinaga, K. and Toshimori, K., 2003. Organization and modifications of sperm acrosomal molecules during spermatogenesis and epididymal maturation. *Microscopy Research and Technique*, *61*(1), pp.39-45.

Yusnita, Y., Norsiah, M.D. and Rahman, A.J., 2010. Mutations in mitochondrial NADH dehydrogenase subunit 1 (mtND1) gene in colorectal carcinoma. *The Malaysian journal of pathology*, *32*(2), pp.103-110.

Zabeo, D., Croft, J.T. and Höög, J.L., 2019. Axonemal doublet microtubules can split into two complete singlets in human sperm flagellum tips. *FEBS letters*, *593*(9), pp.892-902.

Zhang, J., Qiu, H., Huang, J., Ding, S., Huang, B., Zhou, P. and Jiang, Q., 2019. EETs/PPARs activation together mediates the preventive effect of naringenin in high glucose-induced cardiomyocyte hypertrophy. *Biomedicine & Pharmacotherapy*, *109*, pp.1498-1505.

Zhao, Y., Zhang, W.D., Liu, X.Q., Zhang, P.F., Hao, Y.N., Li, L., Chen, L., Shen, W., Tang, X.F., Min, L.J. and Meng, Q.S., 2016. Hydrogen sulfide and/or ammonia reduces spermatozoa motility through AMPK/AKT related pathways. *Scientific reports*, *6*(1), pp.1-11.

Zhu, Z., Li, R., Ma, G., Bai, W., Fan, X., Lv, Y., Luo, J. and Zeng, W., 2018. 5'-AMP-Activated protein kinase regulates goat sperm functions via energy metabolism in vitro. *Cellular Physiology and Biochemistry*, *47*(6), pp.2420-2431.

Zolezzi, J.M., Santos, M.J., Bastías-Candia, S., Pinto, C., Godoy, J.A. and Inestrosa, N.C., 2017. PPARs in the central nervous system: roles in neurodegeneration and neuroinflammation. *Biological Reviews*, *92*(4), pp.2046-2069.

Zong, X., Schieder, M., Cuny, H., Fenske, S., Gruner, C., Rötzer, K., Griesbeck, O., Harz, H., Biel, M. and Wahl-Schott, C., 2009. The two-pore channel TPCN2 mediates NAADP-dependent Ca^{2+}-release from lysosomal stores. *Pflügers Archiv-European Journal of Physiology*, *458*, pp.891-899.

Zorova, L.D., Popkov, V.A., Plotnikov, E.Y., Silachev, D.N., Pevzner, I.B., Jankauskas, S.S., Babenko, V.A., Zorov, S.D., Balakireva, A.V., Juhaszova, M. and Sollott, S.J., 2018. Mitochondrial membrane potential. *Analytical biochemistry*, *552*, pp.50-59.